ISBN 978-82-326-2122-4 (printed version)
ISBN 978-82-326-2123-1 (electronic version)
ISSN 1503-8181

Doctoral theses at NTNU, 2017:20

Alessia Colombo

The interaction between calcium lignosulfonate and cement

NTNU
Norwegian University of
Science and Technology
Faculty of Engineering
Science and Technology
Department of StructuralEngineering

NTNU
Norwegian University of
Science and Technology

Doctoral theses at NTNU, 2017:20

NTNU

NTNU
Norwegian University of
Science and Technology

Alessia Colombo

The interaction between calcium lignosulfonate and cement

Thesis for the degree of Philosophiae Doctor

Trondheim, January 2017

Norwegian University of Science and Technology
Faculty of Engineering
Science and Technology
Department of StructuralEngineering

NTNU
Norwegian University of
Science and Technology

NTNU
Norwegian University of Science and Technology

Thesis for the degree of Philosophiae Doctor

Faculty of Engineering
Science and Technology
Department of StructuralEngineering

ISBN 978-82-326-2122-4 (printed version)
ISBN 978-82-326-2123-1 (electronic version)
ISSN 1503-8181

Doctoral theses at NTNU, 2017:20

Printed by Skipnes Kommunikasjon as

Preface

This doctoral thesis is submitted to the Norwegian University of Science and Technology (NTNU) for the degree of Philosophiae Doctor (PhD). The research was carried out at the Department of Structural Engineering at NTNU in Trondheim, Norway.

The PhD project was part of a larger project called “Lignosulfonate for future concrete” (NFR 225358/O30), funded by the Norwegian Research Council and Borregaard AS, Norway. The PhD project started in August 2013 and the thesis was submitted in September 2016.

The main supervisor of the PhD project was Associate Professor Dr Klaartje De Weerdt (NTNU, Norway). The co-supervisors were Professor Dr Mette Geiker (NTNU, Norway), and Professor II Dr Harald Justnes (SINTEF Building and Infrastructure/NTNU, Norway).

The thesis consists of an introduction and three appended papers.

Trondheim, 25.01.2017

Alessia Colombo

Acknowledgements

The research project presented in this thesis was carried out at the Norwegian University of Science and Technology (NTNU) in Trondheim and it is part of a wider research plan funded by Borregaard AS (Norway) and by the Norwegian Research Council (NFR 225358/O30). I acknowledge Borregaard and the Norwegian Research Council for financially supporting my PhD studies and for facilitating the cooperation between partner universities and industry.

I would like to acknowledge my Supervisors, Klaartje De Weerdt, Mette Geiker and Harald Justnes, and the Project Manager from Borregaard, Rolf Andreas Lauten, for giving me the opportunity of taking this PhD. Thank you for guiding me through my PhD project and helping me with your expertise, for always aiming to keep the level of our research high, and for supporting me with your enthusiasm and passion for the work. You have taught me a lot under both professional and human level.

I would like to acknowledge Gwenn Le Saoût and Nathalie Azema (Ecole des Mines d'Alès, France) for giving me the opportunity of visiting their laboratories and working with them for one week, for the interesting discussions and for their availability in performing, amongst other analyses, the characterization of the materials used in my PhD. Gunnar Westman (Chalmers University of Technology, Sweden) and Serina Ng (SINTEF Building and Infrastructure) are also acknowledged for the helpful discussions. Thanks also to Tobias Danner for always being available to discuss my results and help me in the laboratory when I needed it.

I would like to acknowledge all the employees of the laboratories and the administration of the Department of Structural Engineering at NTNU that helped me during my PhD. Thanks go to Ove Loraas and Steinar Seehuus for helping the concrete group in getting a real chemical laboratory and for always being available. I would also like to thank Tone Anita Østnor (SINTEF Building and Infrastructure / NTNU) for giving me training and support for the many machines present in the laboratory in the green building. Appreciated was also the help of Irene Bragstad (SINTEF Sustainable Energy Technology) for performing the BET measurements, Syverin Lierhagen (NTNU) for performing the ICP-MS analysis, Verner Håkonsen for helping me with the SEM-EDS analysis, Kevin Roque (Ecole des Mines d'Alès, France) for performing, amongst other analyses, the TOC analysis. Thanks to the students Marius Ekanger Aasheim and Massimiliano Salvemini for helping me in the laboratory with my experiments.

Many thanks go to my colleagues in the Department of Structural Engineering at NTNU for creating a friendly and fun working environment, for always being available to talk and support each other inside and outside the work place. My PhD time would not have been the same without you.

Last but not least, special thanks go to my dearest ones for their love and tireless support.

Abstract

Modern concrete applications intensify the need for highly-flowable concretes, which are at the same time durable and possess good mechanical properties. The addition of plasticizers to the concrete mix allows obtaining highly workable concretes maintaining low water-to-binder ratios, which is beneficial for compressive strength and durability.

However, the addition of plasticizer can cause retardation in the setting time of concrete, which limits the dosage of plasticizer usable in practice. In addition, incompatibility issues can exist between plasticizer and cement, possibly leading to higher LSs dosage needed to reach a given workability, severe setting retardation, rapid set, and sudden slump loss.

In this PhD thesis, a sugar-reduced softwood calcium lignosulfonate (LSs) was used as plasticizer. The LSs was used in pastes of two Portland cements with different chemical composition and specific surface area: a CEM I 52.5 N (ANL) and a CEM I 52.5 R (CX), as defined by the European Standard EN197-1:2011.

The first objective of this PhD thesis is to understand the mechanisms behind the interaction between lignosulfonate and cement. This is important to foresee the effects of the plasticizer on workability and setting time of cement, avoiding any possible incompatibility issue.

In light of the mechanisms of consumption of LSs by the cement paste, the impact of the LSs on the rheology and setting time of the cement paste was studied. This represented the second objective of this PhD thesis.

The investigations in this first phase of the PhD project brought in light that the amount and morphology of the ettringite formed in the cement paste played a major role in the rheological and setting behaviour of the cement pastes investigated. For this reason, the third objective of this PhD thesis was to investigate more deeply the impact of the LSs on ettringite.

The investigations undertaken in this PhD thesis highlighted that, when added immediately with the mixing water (immediate addition, IA), the LSs led to an increased formation of ettringite after 30 minutes of hydration, especially for the high-C_3A cement (CX). No increase in the ettringite formed was detected when the LSs was added after 10 minutes of hydration (delayed addition, DA). The ettringite had cubic or rectangular prism shape and length between 0.1 and 0.4 μm. The ettringite morphology appeared unaltered when observed after 6 hours of hydration. Therefore, the LSs was found not to change the morphology of ettringite in the systems analysed in this PhD thesis.

The large amount of ettringite formed provided additional surface area, which increased the LSs consumption for monolayer surface adsorption. This was found to be the main mechanism of LSs consumption for CX cement both for IA and for DA. Monolayer surface adsorption was also found to be the main mechanism of LSs adsorption for ANL cement for DA, while other mechanisms, still to be determined, appeared to play a role for ANL cement for IA. For both cements, calcium complexation, multilayer adsorption and intercalation in AFm were considered unlikely.

The large amount of ettringite formed appeared to decrease the workability of cement paste, leading to early stiffening and, in some cases, to rapid set. The workability of cement paste with LSs also seemed directly correlated to the degree of LSs coverage of the available surface for adsorption. A sudden drop in yield stress and viscosity was measured for the cement pastes that reached an adsorption plateau (DA). Samples which did not reach surface saturation (IA) showed a more gradual increase in workability, requiring higher LSs dosages when compared to those needed for DA. However, for DA, both cement pastes were found to be very sensitive to variations in LSs dosage: even a small increase from the optimal LSs dosage could lead to sudden slump loss.

As to the impact of LSs on setting time, the setting retardation was found to be directly correlated to the amount of free LSs in the pore solution. The DA of LSs was found to lead to higher setting retardation, because of the lower LSs consumption by the cement paste compared to when the LSs was added with IA. This led to a higher amount of free LSs available to retard C_3S hydration. In the samples where the highest amount of ettringite was formed, the increased LSs adsorption caused by the additional surface area reduced the amount of free LSs in the pores solution. This was reflected in lower setting retardation, which was measured with isothermal calorimetry. In addition, increasing LSs dosages led to larger retardation of the silicate peak compared to the aluminate one, causing the two peaks to merge. This can potentially lead to poisoning of C_3S hydration and severe delay of setting, causing incompatibility between plasticizer and cement.

In conclusion, the use of the LSs studied in this PhD thesis in combination with cement characterized by high C_3A content and fineness appears critical, as possibly leading to incompatibility issues such as higher LSs dosage needed to reach a given workability, severe setting retardation, rapid set, and sudden slump loss. Therefore, before using LSs in the concrete practice, special attention should be paid to the combination between the LSs and the cement chosen.

Table of contents

List of appended papers

The thesis includes the following appended papers:

I **On the mechanisms of consumption of calcium lignosulfonate by cement paste**
Colombo, Alessia; Geiker, Mette R.; Justnes, Harald; Lauten, Rolf. A.; De Weerdt, Klaartje
Submitted to Cement and Concrete Research (January 2016)

II **On the effect of calcium lignosulfonate on the rheology and setting time of cement paste**
Colombo, Alessia; Geiker, Mette R.; Justnes, Harald; Lauten, Rolf. A.; De Weerdt, Klaartje
Submitted to Cement and Concrete Research (December 2016)

III **On the effect of calcium lignosulfonate on ettringite in cement paste**
Colombo, Alessia; Geiker, Mette R.; Justnes, Harald; Lauten, Rolf. A.; De Weerdt, Klaartje
Submitted to Cement and Concrete Research (September 2016)

Other publications

In addition to the appended papers, the author of this thesis has written to the following publications, which are not included in the doctoral thesis:

Conference proceedings

Effect of fly ash on the consumption of lignosulfonate by cement paste
Colombo, Alessia; Geiker, Mette R.; Justnes, Harald; De Weerdt, Klaartje
Proceedings of 11th International Conference on Superplasticizers and other chemical Admixtures in Concrete (Supplementary papers), Ottawa (Canada), July 12th-15th 2015

Impact of mixing in the early hydration of cement paste with lignosulfonate (extended paper)
Colombo, Alessia; Geiker, Mette R.; Justnes, Harald; Danner, Tobias; De Weerdt, Klaartje
Proceeding of 34th Cement and Concrete Science Conference, Sheffield (UK), September 14th-17th 2014

Impact of mixing in the early hydration of cement paste with lignosulfonate (long abstract)
Colombo, Alessia; Geiker, Mette R.; Justnes, Harald; Danner, Tobias; De Weerdt, Klaartje
Proceeding of XXII Nordic Concrete Research Symposium, Reykjavik (Iceland), August 13th-15th 2014

Articles in popular science magazines

Plastiserende stoffer til betong på nanonivå
Colombo, Alessia; Geiker, Mette R.; De Weerdt, Klaartje
Byggeindustrien 2016 (12), page 78

Declaration of authorship

Alessia Colombo conducted most of the experiments, evaluated the results and wrote the appended papers and every other part of this thesis. The co-authors contributed in planning the experiments, discussing the results and helping in writing the papers. Kevin Roque, Ecole des Mines d'Alès, France, performed the measurement of the total organic carbon content (TOC). Irene Bragstad, SINTEF, Norway, performed the BET specific surface area measurements. Syverin Lierhagen, NTNU, Norway, performed the inductively coupled plasma mass spectrometry (ICP-MS). Verner Håkonsen, NTNU, Norway, assisted performing the scanning electron microscopy and the energy dispersive X-ray spectroscopy (SEM-EDS).

List of symbols and abbreviations

Latin letters

ANL	*Anlegg Portland cement (CEM I 52.5 N*)*
apw	*artificial pore water*
BET	*Brunauer-Emmett-Teller surface area analysis*
-COOH	*carboxyl group*
$C\underline{S}H_x$	*calcium sulfate hydrates*
CX	*Cemex Portland cement (CEM I 52.5 R*)*
$\underline{C}$	*CO_2 (released during TG analysis by $CaCO_3$ and LSs)*
DA	*delayed addition of plasticizer*
EDS	*energy-dispersive X-ray spectroscopy*
IA	*immediate addition of plasticizer*
ICP-MS	*inductively coupled plasma mass spectroscopy*
LDH	*layered double hydroxide*
LSs	*softwood low-sugar Ca-lignosulfonate*
OPC	*ordinary Portland cement*
TGA	*thermogravimetric analysis*
TOC	*total organic carbon*
SCM	*supplementary cementitious material*
SEM	*scanning electron microscopy*
XRD	*X-Ray powder diffraction*
w/b	*water-to-binder ratio*

Greek letters

$\dot{\gamma}$	*shear rate*	*[s^{-1}]*
φ-OH	*phenolic OH-group*	
μ	*viscosity*	*[Pa·s]*
τ	*shear stress*	*[Pa]*
τ_0	*yield stress*	*[Pa]*

* As defined in the European standard EN197-1

Part 1 – Introduction to the doctoral thesis

1. Introduction

The strict regulations in matter of structural design have led to reinforced concrete elements with high density of steel rebars. Moreover, the increase in complexity of modern concrete structures requires for example casting concrete in formworks with complicated geometry, or pumping concrete at tens of meters height. Such concrete applications, amongst others, intensify the need for a highly-flowable concrete, which is able to flow easily between the reinforcement bars, reaching every corner of complex casting formworks. Moreover, the need for concretes which are durable and possess high mechanical properties require a decrease in their liquid content (lower water-binder ratios). An increase in the solid fraction of concrete equals in turn to a decrease in workability, which increase the difficulty degree in operations like casting, vibrating and surface-finishing.

In modern concrete technology, this issue has been solved by adding plasticizers to the concrete mix. Plasticizers, or water-reducers, are chemical admixtures which allow obtaining highly flowable and workable materials, even with low water-solid ratios. They are known to reduce both the yield stress and the viscosity of concrete, by changing its flocculation state (Hot et al., 2014). In this thesis, the plasticizer used is lignosulfonate, a classic water-reducer produced by the pulping industry. The main shortcoming of adding this chemical admixture is the retardation it causes to concrete hydration, which limits the maximum dosage usable in practice (Collepardi et al., 1973, Young, 1972). Additionally, incompatibility issues sometimes exist between plasticizer and cement, which can lead, for example, to high consumption of plasticizer by the cement paste, reducing the amount of admixture effective in dispersing the cement paste (Agarwal et al., 2000, Nkinamubanzi et al., 2004). A high dosage of plasticizer might in turn lead to incompatibility phenomena such as severe setting retardation or sudden slump loss. For these reasons, a thorough understanding of the mechanisms of interaction between plasticizers and cement paste is needed to optimize the use of plasticizers in concrete technology, avoiding any incompatibility issue. In light of the results contained in the present thesis, it appears that the use of cements with high C_3A content and the addition of the plasticizer after some minutes of hydration require special attention in order to avoid incompatibility phenomena such as severe delay of setting and sudden slump loss.

2. Objectives and limitations

2.1 Objectives

The PhD project aimed to obtain a deeper understanding of the mechanisms of consumption of lignosulfonate (LSs) by Portland cement paste, and the factors behind the cement-lignosulfonate interactions. This is important to foresee the effects of lignosulfonate on workability and setting time of cement paste, avoiding any possible incompatibility issue.

The following main objectives were defined:

1. To identify the consumption mechanisms of lignosulfonate by Portland cement paste;
2. To link the lignosulfonate consumption to its effect on the rheological properties and setting time of Portland cement paste;
3. To understand the effect of lignosulfonate on the amount of ettringite formed and on its morphology;

2.2 Limitations

In this PhD thesis, materials which are commonly available on the Norwegian market were used. The study was limited to one type of lignosulfonate and two Portland cements. Cement pastes were investigated; i.e. the study did not include any testing on concrete or mortar. Only one water-to-binder ratio was investigated for the cement pastes. The cement pastes were analysed mainly at the fresh state after 30 minutes of hydration. Two procedures of lignosulfonate addition to the cement paste were used: immediate addition of the lignosulfonate with the mixing water (IA), or addition of the lignosulfonate after 10 minutes of hydration (DA). The study did not include any in-depth analysis of the polymer properties influencing or determining its interactions with cementitious materials.

3. Background

3.1 Portland cement

Concrete is one of the most commonly used building materials. Concrete is a mixture of water, cement, and fine and coarse aggregates. Additionally, supplementary cementitious materials (SCMs) can replace part of the cement. Through the hydration reaction, the paste hardens gaining strength, forming the rock-like mass known as concrete.

Portland cement is one of the most used hydraulic binders worldwide. The cement production starts with burning a raw meal composed by mainly limestone, in addition to for example clays, sands and pyrite ashes, in a rotary kiln at the temperature of 1300-1450 °C, e.g. (Coppola, 2007). The material obtained after burning is called clinker. After burning, the clinker is cooled rapidly, and subsequently ground to a fine powder together with a small fraction of gypsum to regulate setting. SCMs, such as fly ash, ground granulated blast furnace slag or limestone, can be added either before or after grinding to the gypsum-clinker blend, e.g. (Bensted and Barnes, 2002). According to the European Standard EN 197-1:2011, cements can be divided in five main categories (CEM I, II, III, IV, V) based on the type and amount of SCM replacing part of the Portland cement.

In this thesis, a CEM I 52.5 N ("ANL"), and a CEM I 52.5 R ("CX") are used. As defined in the European Standard EN 197-1:2011, CEM I cements contain at least 95% of Portland clinker.

3.2 Plasticizing admixtures

In order to achieve both low water-binder ratio and high workability, plasticizers or superplasticizers (or water-reducers) are commonly added to the concrete mix. The only difference between the two is the reduction in water-cement ratio they can achieve. The maximum water reduction achievable by plasticizers like lignosulfonate is about 10 %, while it is about 30 % for superplasticizers like PNS and PMS, and about 40 % for superplasticizers like PCEs (Nkinamubanzi et al., 2016).

Three main families of water-reducers are currently used:

- Natural polymers (mainly lignosulfonate);
- Linear synthetic polymers (mainly polycondensates like polynaphtalene sulfonates and polymelamine sulfonates);
- Comb-shaped copolymers or polycarboxylic ethers.

Lignosulfonate (LS) is a plasticizer which was introduced in concrete technology in the 1930s and still widely used nowadays. LS is obtained as a by-product from wood pulping industry. Its molecules are characterized by a mainly hydrophobic hydrocarbon core with numerous functional groups on its surface (e.g. carboxylic acids, phenolic hydroxyl, sulphonic acid), as displayed in Figure 1 (Rezanowich and Goring, 1960).

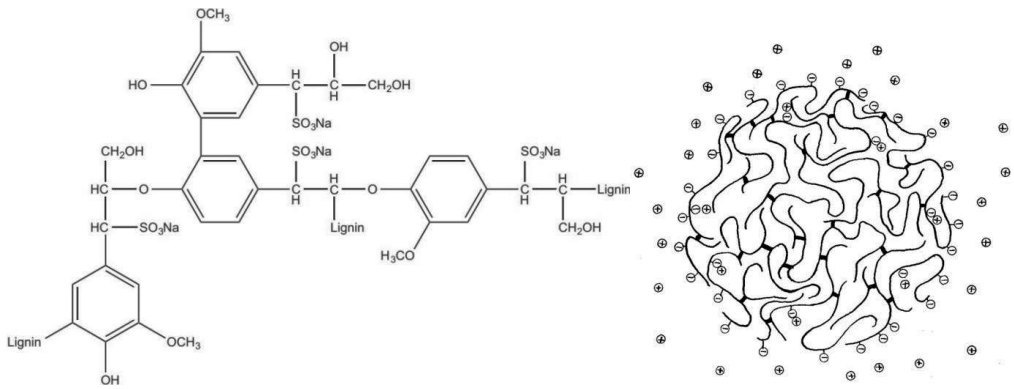

Figure 1 – Left) chemical structure of a lignosulfonate molecule, after (Gelardi et al., 2016), and right) lignosulfonate macromolecule, after (Rezanowich and Goring, 1960)

Lignosulfonates are broadly polydispersed natural polymers, with average molecular weight (M_w) between 5000 and 30000 g/mol. LS can be derived from different sources of biomass, giving molecules with different M_w, and type and amount of functional groups. LS produced from hardwood lignin has remarkably lower M_w than softwood LS. Different cations can be used in LS production, mainly calcium and sodium. LS naturally contains sugars, which can strongly retard the setting time of concrete. The sugars can be almost completely removed, however also sugar-reduced LS can cause retardation (Reknes and Gustafsson, 2000). LS can disperse cement particles by both electrostatic repulsion and steric hindrance, as reported by Vikan, amongst others (Vikan, 2005). The bulk of the LS molecule is constituted of cross-linked, poly-aromatic chains, which are randomly coiled. The negatively charged sulfonic groups are mainly positioned on the surface of the molecule, and a double layer of counter-ions is present in the solvent (Rezanowich and Goring, 1960).

Polycondensates can be divided in polynaphtalene sulfonates (PNS), also known as sulfonated naphthalene formaldehyde condensates, and polymelamine sulfonates (PMS), also known as sulfonated melamine formaldehyde condensates. They are superplasticizers first used as concrete admixture in the 1960s. They have broad M_w distributions and their molecule can have several structures (linear, branched, cross-linked). They disperse cement particles mainly by electrostatic repulsion.

Comb-shaped copolymers, or polycarboxylic ethers (PCEs), were introduced in the 1980s. Their structure consists of a main chain bearing carboxyl groups, or backbone, to which non-ionic polyethers side chains are attached (Gelardi et al., 2016). The negatively-charged backbone adsorbs on the surface of positively-charged cement particles, while the non-adsorbing side chains will disperse through steric hindrance (Flatt et al., 2009). This type of admixture became quickly very popular because of the possibility to synthesize polymers with the most suitable molecular structure based on the aimed performance and application.

In this thesis, a sugar-reduced softwood calcium lignosulfonate was used.

3.3 Plasticizer-cement interactions

When plasticizers are added to cement paste, several types of interactions can take place:

- Adsorption of the plasticizer on the surface of cement grains and hydrates in one or multiple layers (Flatt and Houst, 2001, Hot, 2013, Jolicoeur and Simard, 1998);
- Intercalation of the plasticizer into the structure of layer-like hydrates (mainly AFm) (Flatt and Houst, 2001, Hot, 2013, Jolicoeur and Simard, 1998);
- Complexation between functional groups of the plasticizer and calcium ions dissolved in the pore solution (Collins et al., 1977, Plank and Sachsenhauser, 2009, Sowoidnich et al., 2015);
- Excess plasticizer dissolved in the pore solution (Flatt and Houst, 2001, Hot, 2013, Jolicoeur and Simard, 1998).

The different types of interaction will be discussed separately in the following paragraphs.

3.3.1 The adsorption of plasticizers in cement paste

The dispersive action of plasticizers is mainly caused by the adsorption of superplasticizer molecules on the anhydrous cement grains as well as on the cement hydrates. The mechanisms of adsorption of plasticizers on cement particles are based on the particles interactions caused by their surface charge. Any fractured mineral particle is characterized both by areas with positive and negative charge. Positive Ca^{2+} ions dissolved in the pore solution will be attracted by the negatively charged areas, turning them into positively-charged (Chatterji and Kawamura, 1992). The head groups of plasticizing polymers' surface are commonly negatively charged. They will then be electrostatically attracted by the positively-charged sheath around the cement particles and will adsorb. Therefore, the surfaces of the cement particles will achieve the same negative electrical charge, electrostatically repulsing each other, increasing their dispersion (Uchikawa et al., 1992). Additionally, when two surfaces approach enough for their adsorbed layers to overlap, a steric force develops. This will contribute in hindering particles to get close enough to form agglomerates. The key parameters that govern the steric repulsion are the adsorption layer thickness and its conformation at the solid liquid interface (Houst et al., 2008).

Polymers do not seem to be adsorbed equally on the four main cement phases. According to Yoshioka et al. (Yoshioka et al., 2002), much higher adsorption occurs on aluminate and ferrite than on the silicate phases. The plasticizer might also be adsorbed on the surface of cement hydrates, between which ettringite was found to be one with highest adsorption by Zingg et al. (Zingg et al., 2008). It must be noted that, in both the cited references, the results were reported by unit of mass and not by unit of specific surface.

Polymer adsorption by a solid is usually described through isotherms, in which the amount of polymer adsorbed is plotted against the total amount of polymer added to the system (Hiemenz and Rajagopalan, 1997). The shape of an isotherm is largely determined by the adsorption mechanisms. When monolayer adsorption is reached, the adsorption isotherm generally displays a plateau. In this thesis, the adsorption isotherms were obtained by fitting the experimental data to the non-linear Langmuir model, typically used for describing monolayer adsorption (Hiemenz and Rajagopalan, 1997).

3.3.2 Intercalation

Adsorption onto the surface of cement particles and hydrates is not the only potential consumption mechanism taking place when a plasticizer is added to a cementitious system. According to, among others, Flatt and Houst (Flatt and Houst, 2001), Planck and Sachsenhauser (Plank and Sachsenhauser, 2009), Girardeau et al. (Giraudeau et al., 2009), Jolicoeur and Simard (Jolicoeur and Simard, 1998), part of the water-reducing admixture might also be intercalated in the hydration products, mainly in the layered structure of AFm. When tricalcium aluminate (C_3A) enters in contact with water, it reacts immediately forming, in absence of gypsum, the metastable layered phases C_4AH_{19} and C_2AH_8. In presence of gypsum, C_3A will react with water forming $C_6A\bar{S}_3H_{32}$ (ettringite) and $C_4A\bar{S}H_{12}$ (monosulphate). C_4AH_{19}, C_2AH_8 and $C_4A\bar{S}H_{12}$ belong to the group of layered double hydroxides (LDHs). Several anions and polyelectrolytes can intercalate in between the cationic layers of LDH compounds by replacing their hydroxyl ions. According to Plank et al. (Plank et al., 2006), intercalation was found to be possible for polymers with different structure, namely, linear, comb-like and polymer brushes with very long side chains. The polymer intercalated in LDHs will no longer be available for dispersing cement particles; therefore a higher dosage of polymer will be necessary to reach the desired workability.

3.3.3 Multilayer adsorption and calcium complexation

Polymer adsorption can also take place in multiple layers on cement particles and hydrates. After ideal monolayer coverage, the cement particles will have a negative surface charge. Ca^{2+} ions will then be electrostatically attracted to the negatively charged groups of the polymer, compensating for the charge. This Ca^{2+} outer layer will allow the adsorption of an additional layer of negatively-charged polymer (Zhang and Kong, 2015, Mollah et al., 2000), facilitating additional consumption of polymers.

Another possible mechanism of polymer consumption is complexation between functional groups of the plasticizer and calcium ions dissolved in the pore solution, as observed by Collins et al. (Collins et al., 1977), Planck and Sachsenhauser (Plank and Sachsenhauser, 2009), Sowoidnich et al. (Sowoidnich et al., 2015) amongst others. Collins et al. (Collins et al., 1977) found that calcium ions dissolved in a calcium lignosulfonate solution with pH over 10-11 can hold together a matrix of lignosulfonate molecules, forming a gel. Other polycharged cations, e.g. aluminium and iron, could also tightly bind to the functional groups of the LS molecule, especially to the sulfonic and carboxyl groups. The polymer molecules captured in the complexes with calcium ions might still have some free anionic functional groups on their outer regions. These anionic functional groups might as well be attracted to the positive charged calcium ions adsorbed on the polymer layer over cement particles and hydrates. The calcium-polymer complexes might then bind to the cement particles already covered with polymer, decreasing the amount of free LSs in the pore solution and forming multiple layers of polymer adsorbed. For this reason the mechanisms of calcium complexation and multilayer adsorption can be considered interrelated and, sometimes, undistinguishable from each other. This additional layer of polymer is considered to be limitedly beneficial to the dispersion of cement particles. However, such layer could have an effect on the hydration kinetics of fresh cement paste, slowing down the diffusion of the anhydrous phases covered

by the polymer (Marchon et al., 2016). The complexes of calcium and polymer might also stay dissolved in the pore solution, thus reducing the concentration in solution of calcium ions. A lower Ca-to-Si ratio of the pore solution could possibly modify the hydration reactions and the resulting hydrates, as stated by Yousuf et al. (Yousuf et al., 1995). Additionally, a mechanisms that takes out calcium ions from the pore solution slows down the build-up of calcium supersaturation, which is needed for the nucleation of cement hydrates, hence it slows down cement hydration (Marchon et al., 2016).

3.4 Rheology of cement paste

Rheology is defined as the science of deformation and flow of matter. The fundamental parameters studied by this science are the yield stress, τ_0, and the viscosity, μ, of a material when a shear rate $\dot{\gamma}$ is applied, causing a certain shear stress τ in the material, where $\dot{\gamma} = \frac{d\gamma}{dt}$, γ: deformation.

If the fluid has a Newtonian behavior, viscosity can be expressed as: $\mu = \frac{\tau}{\dot{\gamma}} = \text{const.}$

The viscosity of Newtonian fluids is independent of the shear rate applied and there is a direct proportion between the shear stress and the shear rate applied.

Many materials display a flow behavior that differs from the simple Newtonian model: the shear stress might increase or decrease with the increase of the shear rate applied. These fluids are called non-Newtonian with shear-thickening or shear-thinning behavior, respectively.

Finally some materials behave like a solid if the shear stress applied is below a certain value and like a liquid if, on the contrary, the shear stress applied exceeds this value. They are defined as non-Newtonian materials with a yield value, and the threshold value is called yield stress (τ_0). When the shear stress applied exceeds the yield stress, they can exhibit shear-thinning or shear-thickening behavior. Cement paste belongs to this type of fluids.

The behavior of this type of materials can be, as a simplification, described by the Bingham model: $\tau = \tau_0 + \mu \cdot \dot{\gamma}$

If $\tau \geq \tau_0$, the material will flow.

The different yield stress-shear rate correlations are displayed in Figure 2.

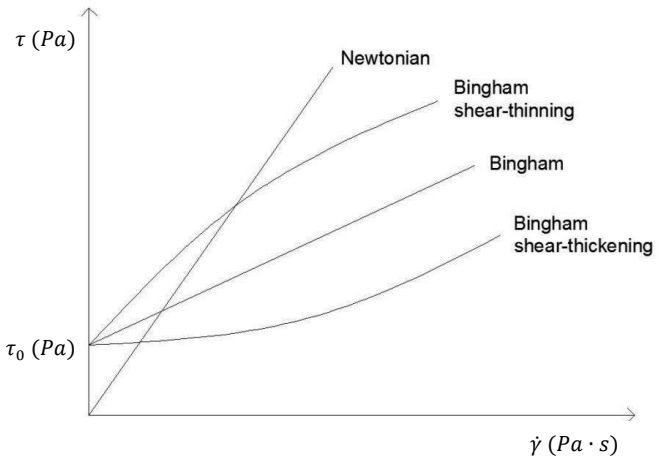

Figure 2 – Correlations between shear stress and shear rate for different types of fluids

Cement paste generally displays a shear-thinning behavior. However, a shear-thickening behavior can be exhibited under some conditions, i.e. the addition of a plasticizer, depending on the dosage (Jayasree et al., 2011).

As described by e.g. Roussel et al. (Roussel et al., 2010), in a cementitious system the yield stress corresponds to the energy needed to break down a network of interaction between particles. Its origin lays in colloidal and contact interactions between particles. Viscosity results from hydrodynamic, colloidal and contact forces involved in the motion of the suspended cement grains. The yield stress is often considered as the most relevant parameter to describe workability and the ability of a material to properly fill a mold under its own weight (Roussel, 2007). However, the viscosity is also a very relevant parameter to describe cement or concrete workability, especially for systems with low water-binder ratio (Hot et al., 2014, Roussel, 2007). Plasticizing admixtures can change both yield stress and viscosity by adsorbing on cement particles and changing the flocculation state of cement paste (Hot et al., 2014).

3.5 Effect of plasticizers on setting time

In addition to dispersion, the interaction between cement and plasticizer can potentially lead to retardation of the setting time of the cement paste. Several mechanisms of retardation are hypothesized in the literature, the main ones being: calcium complexation, nucleation poisoning of hydrates, surface adsorption on unhydrated cement grains, and presence of sugars in the plasticizer (Hot et al., 2014, Bishop et al., 2003, Cheung et al., 2011, Marchon and Flatt, 2016).

Calcium complexation involves the interaction between plasticizing polymers and calcium ions in the pore solution. This would slow down the build-up of calcium supersaturation needed for the nucleation of hydration products. However, according to Bishop et al. (Bishop et al., 2003), and Marchon and Flatt (Marchon and Flatt, 2016), amongst others, the low dosages of plasticizers generally used limit the amount of calcium potentially complexed.

Thus, calcium complexation does not appear likely as a main mechanism of setting retardation of cement.

As stated by Thomas and Birchall (Thomas and Birchall, 1983) and Marchon and Flatt (Marchon and Flatt, 2016) amongst others, retardation by nucleation poisoning of hydrates is where the plasticizer adsorbs on the nuclei of CH, preventing its growth. By suppressing CH precipitation, C_3S dissolution is delayed, as the degree of calcium saturation of the pore solution is unaltered. Hence, C-S-H precipitation is hindered, which leads to prolongation of the induction period of the cement paste (Marchon and Flatt, 2016). Moreover, plasticizers could increase cement solubility, thus allowing ions to coexist in solution at much higher concentrations without causing precipitation, thus prolonging the cement induction period (Thomas and Birchall, 1983).

Retardation due to surface adsorption on unhydrated cement grains is due to the adsorption of the plasticizer on the anhydrous cement phases, which reduces their dissolution. This, in turn, retards the formation of hydrates, prolonging the induction period of the cement paste (Marchon and Flatt, 2016).

Finally, the sugars contained in the plasticizer generally delay the onset of the acceleration period, by adsorbing on anhydrous phases like C_3S, but also on cement hydrates, especially CH. However, the rate in this period was found to be higher than in the reference (Young, 1972).

In conclusion, the mechanisms that most likely retard the cement setting appears to be related to the plasticizers poisoning the nuclei of CH, retarding C_3S dissolution and C-S-H precipitation, the reduced dissolution of cement anhydrous phases, and the possible presence of sugars in the plasticizer.

As other plasticizers, lignosulfonate is known to have a retarding effect on cement hydration (Collepardi, 1982, Ramachandran and Feldman, 1971, Lorprayoon and Rossington, 1981). The sugars naturally contained in lignin contribute to longer setting times of cement, in particular the hexoses, which, however, can be removed by fermentation in low-sugar lignosulfonates. However, also sugar-reduced LS can cause retardation of cement paste hydration (Reknes and Gustafsson, 2000). Several studies concluded that the addition of calcium lignosulfonate changes the hydration of C_3S and C_3A (Ramachandran, 1972, Monosi et al., 1982, Collepardi et al., 1973, Ramachandran, 1994, Lorprayoon and Rossington, 1981, Young, 1962). According to Ramachandran (Ramachandran, 1994), a strongly surface-bound calcium lignosulfonate complex could be detected for both C_3A and C_3S, which could cause retardation of C_3A and C_3S hydration. In another paper (Ramachandran, 1972), Ramachandran stated that the retardation effect of calcium lignosulfonate depends on its concentration in solution and not on its proportion with respect to C_3S. The C_3S hydration was delayed in proportion to the concentration, and it practically stopped for concentrations above 3 g/l of water. On the contrary, C_3S hydration was found to speed up for lignosulfonate concentrations under 1 g/l of water. Monosi et al. (Monosi et al., 1982) found that, in a C_3A-C_3S system, the addition of calcium lignosulfonate led to a strong retardation in C_3S hydration, while C_3A hydration was slightly accelerated. The C_3S retardation in the C_3A-C_3S

system was lower than that in pure C_3S systems. In fact, the lignosulfonate adsorption by C_3A decreases the concentration of polymer available to retard the C_3S hydration. Moreover, the arrest in C_3S hydration is partially counterbalanced by the increase in rate of hydration of C_3A, as stated by Collepardi et al. (Collepardi et al., 1973). In conclusion, lignosulfonate was found to retard or accelerate C_3S hydration (Ramachandran, 1994, Lorprayoon and Rossington, 1981) depending on its concentration in the pore solution (Ramachandran, 1972). C_3A hydration was found to be retarded by lignosulfonate by some authors (Ramachandran, 1994, Young, 1962, Lorprayoon and Rossington, 1981), while not retarded (Monosi et al., 1983) or slightly accelerated (Monosi et al., 1982, Collepardi et al., 1973) by other authors.

3.6 Effect of the addition time of the plasticizer

As described by e.g. Flatt and Houst (Flatt and Houst, 2001), the addition time of the plasticizer to the cement paste greatly affects the amount of plasticizer consumed by the cement paste and the extent of retardation. Several studies, amongst others Uchikawa et al. (Uchikawa et al., 1992), Chiocchio and Paolini (Chiocchio and Paolini, 1985), Aiad et al. (Aiad et al., 2002), Vikan (Vikan, 2005), found that, at equal plasticizer dosage, the flow of cement paste prepared by delayed addition is higher than that of cement paste prepared by immediate addition. Moreover, the setting is further retarded in case of DA. Chiocchio and Paolini (Chiocchio and Paolini, 1985) found that the optimum addition time of plasticizer to achieve the maximum workability corresponds to the beginning of the dormant period of the cement hydration without admixture. Hot (Hot, 2013), Hsu et al. (Hsu et al., 1999), and Aiad (Aiad, 2003) found that the optimum addition time was between 10 and 15 minutes after water addition.

4. Summary of conducted experiments, materials, and methods

Three main objectives of investigation were defined for the PhD project (see paragraph 2.1). Three papers were written based on the findings from the investigations undertaken. An overview is given in Table 1.

Table 1 – Overview of experimental work conducted during the PhD project and related papers and appendices

Paper	Topic	Experimental technique	Objective
I	Consumption mechanisms of LSs by two cement pastes	UV-spectroscopy, TOC, TGA, BET surface area measurement	1, 2
II	Effect of LSs on rheology, setting time, and hydrates amount of two Portland cements	Rheological measurements, isothermal calorimetry, UV-spectroscopy, BET surface area measurement, ICP-MS	1, 2, 3
III	Effect of LSs on ettringite in cement paste	UV-spectroscopy, TGA, XRD, BET surface area measurement, SEM-EDS, ICP-MS	1, 3

The experiments were performed on two different cements: a CEM I 52.5 N (ANL) and a CEM I 52.5 R (CX), as defined by the European Standard EN197-1. The composition and physical properties of the two cements are listed in every paper appended to this thesis. During the project, the materials were stored in sealed plastic bags of about 3 kg each. For shorter periods they were stored in plastic zipper bags of about 1 kg each, stored in desiccators over silica gel and soda lime. The unhydrated cements were analysed with XRD and TGA in the beginning of the project and about 2 years after. The results showed no sign of pre-hydration.

A sugar-reduced softwood calcium lignosulfonate (LSs) was used as plasticizer. Its mass weighted molecular weight (M_w), as measured with gel permeation chromatography (GPC), was 29000 g/mol and the number weighted molecular weight (M_n) was 2100 g/mol, giving broad molar-mass dispersity ($Đ_M$) equal to 13.8. The molar-mass dispersity, also called polydispersity index, is defined as the ratio between M_w and M_n (Gilbert et al., 2009). Additional physical and chemical properties of the lignosulfonate are listed in every paper appended to this thesis. For the lignosulfonate used in the present investigation, the sugars were removed by fermentation and the resulting alcohol by distillation. The LSs was dissolved in deionised water to concentrations varying from 1 to 45 % to ease dosing, and the water content was included in the calculation of the water-to-binder ratio (w/b).

In paper I, $CaCO_3$ and $Ca(OH)_2$ were used as reference materials to be compared with cement paste, since they share some properties with cement, as specified more in detail in paragraph 2.2.2 and 2.2.3 in Paper I, but do not hydrate with water. The characteristics of the two materials can be found in Paper I. The high fineness of the $Ca(OH)_2$ powder required a water-

solid ratio by mass of 8.0. For $CaCO_3$, the water-to-solid ratio by mass was 0.3. Both the materials were mixed with artificial pore water. The artificial pore water was a solution of 5.9 g/l NaOH and 2.1 g/l KOH with K/Na molar ratio equal to 2 and pH of about 13.

In paper III, in order to study the effect of LSs on the solubility of calcium sulfates, anhydrite ($CaSO_4$), hemihydrate ($CaSO_4 \cdot 0.5H_2O$) and dihydrate ($CaSO_4 \cdot 2H_2O$) were used. The anhydrite and the dihydrate were analytical grade, while the hemihydrate was technical grade. The characteristics of the two materials can be found in Paper III. They were mixed with artificial pore water obtaining a water-to-solid ratio by mass of 1.0.

The amount of polymer consumed by two cement pastes was determined on filtrated pore solution by **UV-spectrometry** (see method description in Paper I), which allowed the calculation of adsorption isotherms. The samples were analysed both by adding the lignosulfonate immediately with the mixing water (immediate addition, IA), and by adding it after 10 minutes of hydration (delayed addition, DA). Some of the samples were also measured with total organic carbon (**TOC)** in order to confirm the results obtained with UV-spectroscopy (see method description in Paper I).

Changes in the surface area of the hydrated cement particles were measured by **BET** both on hydrated and unhydrated samples (see method description in Paper I). The results allowed normalizing the adsorption isotherms of the cement pastes to the actual surface area of the hydrated cement particles after 30 minutes of hydration.

The changes in type and amount of cement hydrates caused by the addition of lignosulfonate were investigated with thermogravimetric analysis (**TGA**) and X-ray powder diffraction (**XRD**) (see methods description in Paper I and III, respectively). The morphology of the hydrates was observed with scanning electron microscopy in secondary-electron mode (**SEM-SE**), while their composition was analysed with energy-dispersive X-ray spectroscopy (**EDS**) (see method description in Paper III).

The elemental composition of the pore solution extracted from the two cement paste samples was determined by inductively coupled plasma mass spectroscopy (**ICP-MS**) (see method description in Paper III).

Once the LSs consumption mechanisms by cement paste were investigated, the amount of polymer consumed by the two cement pastes was correlated to the changes in rheological properties of the two cement pastes. The rheological properties of the cement pastes were measured with a **parallel plates rheometer** (see method description in Paper II). The effect of LSs addition on the setting time of the two cement pastes was measured with **isothermal calorimetry** (see method description in Paper II).

An overview of the experiments undertaken is reported in Table 2:

Table 2 – Overview of the experiments conducted in the PhD project

Analysis	**Material**	**Addition method**	**LSs dosage**	**Analysis time**	
			mass % of binder	minutes	days
UV spectroscopy	ANL cement	IA	0.1; 0.2; 0.4; 0.6; 0.8; 1.2; 1.5	30	
		DA	0.05; 0.1; 0.25; 0.4; 0.8; 1.2; 1.5		
	CX cement	IA	0.1; 0.2; 0.4; 0.6; 0.8; 1.0		
		DA	0.05; 0.1; 0.25; 0.4; 0.8; 1.2; 1.5		
	$CaCO_3$	IA	0.05; 0.1; 0.2; 0.4; 0.8; 1.0; 1.2; 1.5		
	$Ca(OH)_2$	IA	1.0; 2.0; 5.0; 8.0; 12.0; 22.0		
	Gypsum	IA	0.2; 0.4; 0.8; 1.5; 2.0; 3.0		
	Hemihydrate	IA	0.2; 0.4; 0.8; 1.5; 2.0; 3.0		
	Anhydrite	IA	0.2; 0.4; 0.8; 1.5; 2.0; 3.0		
TOC	ANL cement	IA	0.2; 0.4; 1.0; 1.5	30	
BET	ANL cement		0	Unhydrated	
	CX cement		0	Unhydrated	
	$CaCO_3$		0	Unhydrated	
	$Ca(OH)_2$		0	Unhydrated	
	Gypsum		0	Unhydrated	
	Hemihydrate		0	Unhydrated	
	Anhydrite		0	Unhydrated	
	ANL cement		0	30	
		IA	0.2; 0.4; 0.8; 1.5		
		DA	0.05; 0.2; 0.4; 0.8; 1.5		
	CX cement		0		
		IA	0.8; 1.5		
		DA	0.8; 1.5		
TGA	ANL cement		0	30	
		IA	0.8; 1.5; 2.0; 3.0		
		DA	0.8; 1.5		
			0		28
		IA	0.8; 1.5		
		DA	0.8; 1.5		
	CX cement		0	30	
		IA	0.8; 1.5; 2.0; 3.0		
		DA	0.8; 1.5		
			0		28
		IA	0.8; 1.5		
		DA	0.8; 1.5		
XRD	ANL cement		0	30	
		IA	0.8; 1.5		

Analysis	Material	Addition method	LSs dosage	Analysis time	
			mass % of binder	minutes	days
	CX cement		0		
		IA	0.8; 1.5		
Rheological measurement	ANL cement		0	10; 20; 30	
		IA	0.1; 0.4; 0.8; 1.2; 1.5		
		DA	0.1; 0.25; 0.4	12; 20; 30	
	CX cement		0	10; 20; 30	
		IA	0.4; 0.8; 1.5		
		DA	0.25; 0.4	12; 20; 30	
Isothermal calorimetry	ANL cement		0		
		IA	0.1; 0.2; 0.4; 0.6; 0.8		
		DA	0.05; 0.1; 0.2; 0.4		
Isothermal calorimetry	CX cement		0		
		IA	0.1; 0.2; 0.4; 0.6; 0.8		
		DA	0.05; 0.1; 0.2; 0.4		
ICP-MS	ANL cement		0		
		IA	0.8; 1.5		
		DA	0.8; 1.5		
	CX cement		0		
		IA	0.8; 1.5	30	
		DA	0.8; 1.5		
	Gypsum	IA	0.8; 1.5		
	Hemihydrate	IA	0.8; 1.5		
	Anhydrite	IA	0.8; 1.5		
SEM-EDS	ANL cement		0		
		IA	1.5	30	
		DA	1.5		
			0	360	
	CX cement		0		
		IA	1.5	30	
		DA	1.5		
			0	360	

5. Findings

In this chapter, the main findings of the PhD study will be summarized. They are presented according to the four main objectives of the PhD project.

Paper I: On the mechanisms of consumption of calcium lignosulfonate by cement paste

The first objective of the PhD project was to investigate the mechanisms of consumption of lignosulfonate by the Portland cement paste. The experimental work and the findings related to Objective 1 were mainly reported in Paper I, even though some findings included in the following appended papers also contributed to a more complete understanding of Objective 1.

First a literature review was done, which highlighted that the main mechanisms behind the consumption of plasticizers by cement paste could potentially be: polymer intercalation into early cement hydrates, surface multilayer adsorption / complexation between functional groups of the plasticizer and calcium ions dissolved in cement pore solution, and monolayer surface adsorption of LSs on cement particles and hydrates.

Consequently, the experimental work followed. A softwood sugar-reduced calcium lignosulfonate (LSs) and two Portland cements (a CEM I 52.5 N, ANL, and a CEM 1 52.5 R, CX) were used. $CaCO_3$ and $Ca(OH)_2$ mixed in artificial pore solution were also used as comparison to the cements. All the samples were analyzed after 30 minutes of hydration, when the LSs adsorption by the cement paste was measured to be approximately constant in time. Adsorption isotherms were calculated for each cement paste based on the measurements from UV-spectroscopy (Figure 2 a, b). The effect of two LSs addition methods (immediate addition of the LSs with the mixing water, IA, vs. delayed addition of the LSs after 10 minutes of hydration, DA) was also compared.

For both cement pastes the following was observed:

- The adsorption isotherms obtained for IA showed a continuous increase in LSs consumption with increasing LSs added to the cement paste;
- The adsorption isotherms obtained for DA reached an adsorption plateau;
- A noticeable difference in LSs consumption was displayed between IA and DA.

The difference in plasticizer consumption between IA and DA is commonly attributed to the mechanism of intercalation of plasticizer molecules into the structure of AFm, e.g. (Flatt and Houst, 2001). In the present thesis, no AFm was found in pastes of the same cements without LSs or with 1.5 mass % LSs added with IA or with DA, since no peak corresponding to AFm could be detected with TGA after 30 minutes of hydration (Figure 4 a, b). Therefore, for the materials investigated in this paper, intercalation in AFm did not appear as a possible LSs consumption mechanism and could not explain the difference in LSs consumption between the samples mixed with IA and those mixed with DA.

The possibilities of calcium complexation and multilayer adsorption were examined. The LSs consumption on $CaCO_3$ and $Ca(OH)_2$ were measured, as reference of comparison with LSs consumption by cement paste (Figure 2 a, b). Calcium carbonate is known to be a suitable model system for investigating stability and rheology of cement paste (N. Mikanovic et al.),

and it is characterized by a very low solubility, also at high pH. $Ca(OH)_2$ is one of the main cement hydrates and its solubility is about 100 times higher than the one of $CaCO_3$. The adsorption isotherms of both these materials displayed an adsorption plateau. The plateau of $Ca(OH)_2$ was more than 10 times higher than the one of $CaCO_3$ because of the very high specific surface area of $Ca(OH)_2$. Therefore, their main mechanism of LSs consumption appeared to be monolayer surface adsorption. Since calcium complexation or multilayer adsorption appeared as a minor or non-existing mechanism for both $CaCO_3$ and $Ca(OH)_2$ (IA), and for the cements for DA, these mechanisms of LSs consumption were considered unlikely also for the cements for IA.

It is known from literature that adsorption isotherms generally display a plateau when monolayer adsorption is reached, e.g. (Hiemenz and Rajagopalan, 1997). Therefore, it was concluded that monolayer surface adsorption was the main mechanism of LSs consumption for both cements when the LSs was added with DA.

Considering the average molecular weight of the LSs molecule (29000 g/mol) and the specific surface area of the hydrated cement pastes as measured with BET, and knowing the LSs consumed at monolayer surface saturation, the LSs "molecular footprint" was calculated. It resulted to be about 25 nm^2 for ANL cement and about 30 nm^2 for CX cement. It should be noted that the LSs is characterized by a high polydispersity index, so only an approximate calculation of the molecular footprint is possible.

As to the mechanisms of LSs consumption for IA, more possible mechanisms had to be evaluated.

An increasing amount of ettringite had formed in the samples containing 1.5 mass % LSs added with IA compared to the reference sample without LSs, as shown by the TGA results (Figure 4 a, b). No increase in the ettringite amount was measured when the LSs was added with DA. The amount of ettringite formed was noticeably larger for CX cement than for ANL cement.

Additionally, the BET surface analysis showed that, when the LSs was added with IA, the surface area of the hydrated cement samples remarkably increased with increasing LSs amount (Figure 5). On the contrary, nearly no increase was found when the LSs was added with DA. The increase was larger for CX cement paste, which also contained a larger amount of ettringite. Therefore, the increase in particle surface area was considered to be possibly correlated to the increased amount of ettringite.

In conclusion, for IA, it appeared likely that, for CX cement paste, the observed increase in LSs consumption occurred solely because of the increase in particle surface area available for adsorption due to the increase in ettringite amount. In this case, the only mechanism of LSs consumption would have been monolayer surface adsorption. On the other hand, for ANL cement paste where the LSs was added with IA, the increase in ettringite amount, hence in specific surface area, was not large enough to explain the high LSs consumption observed. Therefore, other consumption mechanisms, still to be determined, were acting in addition to surface monolayer adsorption.

Paper II: On the effect of calcium lignosulfonate on the rheology and setting time of cement paste

The second objective of the PhD project was to investigate the changes in rheology and setting time of the cement paste due to the addition of the LSs, and to relate them to the mechanisms of LSs consumption found in Paper I. The experimental work and the findings were mainly reported in Paper II.

The cements and lignosulfonate used were the same as those used in Paper I. The LSs was added either immediately with the mixing water (IA), or delayed after 10 minutes of hydration (DA).

First, the rheological properties of the cement pastes were measured with a serrated parallel plate rheometer after 10 (12 for DA), 20 and 30 minutes of hydration with varying LSs dosage. The results showed that in general the LSs was able to reduce both the yield stress and the viscosity of the two cement pastes at the times considered (Figure 1 a, b and Figure 2 a, b). The only exception was CX cement paste after 30 minutes of hydration, which displayed a nearly constant yield stress and a remarkable increase in viscosity when increasing LSs dosages had been added with IA. For all the other samples mixed with IA, the reduction in yield stress and viscosity appeared to be gradual. On the contrary, the samples mixed with DA showed a sudden drop in yield stress and viscosity for lower LSs dosages than for IA.

The rheological data was also presented as the area under the flow curve, or flow resistance (Figure 3 a, b). These results tendentially agreed with those calculated as yield stress and viscosity.

When compared to the adsorption isotherms obtained in Paper I (Figure 7), the rheological results led to the conclusion that the rheological behavior related to the degree of LSs coverage of the available surface for adsorption. Indeed, a clear drop in yield stress and viscosity was measured for the cement pastes that reached an adsorption plateau, as observed for DA. On the contrary, the samples which did not reach surface saturation showed a more gradual increase in workability, as observed for IA. The very sudden drop in yield stress and viscosity observed for the samples mixed with DA makes the system less robust and very vulnerable to dosing.

The rheology also appeared to be influenced by the larger amount of ettringite observed for IA with elevated LSs dosages already observed in Paper I, and later confirmed in the present paper with XRD. The increased formation of ettringite led to early stiffening of the cement paste, as also found by Hanehara and Yamada (Hanehara and Yamada, 1999), and hence to lower workability. In extreme cases, such as with CX cement with 1.5 mass % of binder LSs added with IA, the amount of ettringite was so large that it caused early hardening of the cement paste after 30 minutes of hydration. This represents an example of incompatibility between cement and the investigated plasticizer dosage.

The effect of LSs on the hydration development of the two cement pastes was investigated with isothermal calorimetry, which allowed the calculation of the setting time (Figure 4 a, b and Figure 5 a, b). The hydration curves obtained from calorimetry displayed that both the

silicate and the aluminate peak were delayed by LSs addition in both cement pastes, and, between the two peaks, the silicates peak was the most retarded. The two peaks even merged in most samples at higher LSs dosages. This is a known compatibility issue between plasticizer and cement (Sandberg and Roberts, 2003, Marchon et al., 2014, Tuthill et al., 1961, Roberts and Taylor, 2007): in some cases, the aluminate peak can occur earlier than the silicate one, leading to poisoning of C_3S hydration and severe delay of setting. For the same LSs dosage, DA resulted in a larger retardation than IA, and ANL cement paste showed a larger delay than CX cement paste. This can be understood by lower LSs consumption

When compared to the adsorption isotherms obtained in Paper I (Figure 7), the results from calorimetry indicated correlations between the setting retardation and the amount of free LSs in the pore solution. Indeed, over a certain threshold LSs dosage, any increase in free LSs corresponded to a large increase in setting retardation, especially for samples mixed with DA. The threshold also corresponded to a drop in yield stress. The larger setting retardation observed with DA might thus be explained with the higher amount of free LSs in the pore solution, hence higher amount of LSs available to retard C_3S hydration.

Finally, the elemental concentration of Al, Ca, Fe, Si and S in the pore solution extracted from ANL and CX cement pastes after 30 minutes of hydration was determined with ICP-MS (Figure 6). The results showed that only for the samples mixed with DA an increase in Al, Fe and Si concentration was measured in the pore solution as the LSs dosage increased. The increase was considerably larger for ANL cement than for CX cement. Aluminum ions dissolved in the pore solution were found to negatively impact the C_3S hydration, both by increasing its induction period (Odler and Schüppstuhl, 1981, Valenti et al., 1978), and by reducing the extent of its hydration. This appears to be one of the feasible explanations for the increased setting retardation measured for DA compared to IA.

In conclusion, the rheological behavior appeared to relate to the degree of LSs coverage of the available surface for adsorption, while the setting time was found to relate to the amount of free LSs in the pore solution. Additionally, the amount of ettringite formed upon IA appeared to influence both the rheology and the setting time of cement paste. Indeed, the ettringite supplied additional surface area, increasing the LSs consumption by adsorption, with consequent reduction of free LSs in the pore solution and lower setting retardation. Enhanced ettringite formation resulted in less free LSs dissolved in the pore solution and available to retard C_3S hydration. The increased ettringite precipitation also led to faster sulfates depletion.

Paper III: On the effect of calcium lignosulfonate on ettringite formation in cement paste

Ettringite formation was found to have a key role in the interactions between cement and lignosulfonate. For this reason, Paper III focused on the effect of varying dosages of LSs on the amount and morphology of the ettringite formed in Portland cement.

The cements and lignosulfonate used were the same as those used in Paper I and in Paper II. The LSs was either added immediately with the mixing water (IA), or delayed after 10 minutes of hydration (DA).

The hydrates formed in pastes of the two cements with increasing LSs dosages, both for IA and DA, after 30 minutes of hydration were identified using TGA and XRD. The amount of hydrates was estimated by TGA. The results showed that the amount of ettringite formed for IA increased with the LSs dosage up to a threshold value, over which the increase was noticeably smaller (Figure 1 to Figure 7). The presence of a large amount of small ettringite crystals indicates that the LSs enhanced ettringite formation when added with IA. For DA, on the other hand, a constant amount of ettringite was observed with increasing LSs dosages.

Since the amount of ettringite formed, especially in CX cement paste for IA, was large, the authors investigated whether other factors could have enhanced ettringite formation. The maximum amount of ettringite that could have theoretically formed based on the amount of aluminates and sulfates available, as defined in paper III, paragraph 4.1.1, was calculated. The paste of CX cement with 1.5 mass % LSs added with IA formed the highest amount of ettringite. For this sample, no considerable difference was found between the amount of ettringite that could theoretically have formed and the one measured with TGA. Therefore, other mechanisms that could have increased the amount of ettringite formed, such as the intercalation of sulfonate groups from the LSs molecule, appeared to be minor, if present at all.

Another mechanism that could have enhanced ettringite formation is the possible increase in dissolution of the calcium sulfates. This concerns especially anhydrite, since it is only contained in CX cement, which formed the largest amount of ettringite. The content in Ca and S of the pore solution extracted after 30 minutes of hydration from samples of gypsum, hemihydrate and anhydrite containing increasing LSs dosages was measured. The results showed that both for gypsum, anhydrite and hemihydrate, the LSs appeared to even suppress their dissolution (Figure 21). Therefore, it was concluded that the large increase in ettringite formed in CX cement paste was not due to an increased dissolution of the calcium sulfates.

The hydrates formed in the pastes of the two cements after 30 minutes of hydration were observed with SEM and their chemical composition was analyzed with EDS (Figure 8 to Figure 14). The ettringite crystals were visually observed in a real cement system and not as a pure synthesized phase. The pastes of ANL and CX cements looked noticeably different depending on the addition time of the LSs. For IA, the particles of both cement pastes presented large portions of surface covered with ettringite crystals, while, for DA, the crystals observed were noticeably fewer. The crystals observed for the two cements appeared of different size and shape: cubic with size between 0.1 and 0.2 μm for ANL cement, and cuboidal with length between 0.2 and 0.4 μm for CX cement (aspect-ratio varying between 1.5:1 and 4:1).

In addition to the amount, several studies in literature also found that plasticizers can change the morphology of ettringite, from the typical needle-like structure, to a more round or cubic one (Prince et al., 2002, Kerui et al., 2002, Hekal and Kishar, 1999, Cody et al., 2004, Danner

et al., 2016, Stöber and Pöllmann, 1998). In the present study, after 30 minutes of hydration, no major difference in ettringite morphology could be observed between pastes of ANL and CX cements without LSs or with 1.5 mass % of binder LSs added with IA or with DA (Figure 8 to Figure 12). It can be therefore concluded that, after 30 minutes of hydration, the addition of LSs did not lead to changes in ettringite shape for the cements analysed in this study.

No major difference in ettringite morphology was found between samples of ANL and CX cement pastes with 1.5 mass % of binder LSs added with IA hydrated for 30 minutes and those of the same pastes without LSs hydrated for 6 hours, and between the two cements (Figure 15 and Figure 16). Indeed, in both systems the ettringite crystals appeared with a compact and cuboidal shape instead of the expected needle-like shape.

In light of the differences in amount of ettringite in fresh cement paste caused by the addition of LSs, the effect of LSs on the hydrates of 28 days-old cement was also investigated with TGA (Figure 22 and Figure 23). No major differences in hydrates type or amount were observed between IA and DA and between the samples containing different LSs dosages. Therefore, the addition of LSs and its addition time seemed not to play a major role in type and amount of hydrates formed in ANL and CX cement pastes after 28 days of hydration. For DA, the addition of a high LSs dosage (compared to the dosages normally used in practice), was found to cause lack of hardening in ANL cement even after 28 days of hydration.

In conclusion, the IA of the LSs appeared to promote ettringite formation after 30 minutes of hydration, especially for CX cement. On the contrary, ettringite morphology was found not to be influenced by the LSs addition. The formation of a large amount of ettringite for IA after 30 minutes of hydration might lead to several consequences concerning the LSs consumption, rheology and setting time of cement paste:

The large specific surface area due to the additional ettringite formed led to higher LSs consumption by surface adsorption by the cement paste. This led to the need of a higher LSs dosage in order to reach a given workability. This also led to less free LSs in the pore solution available to delay C_3S hydration, thus a more limited setting retardation, when compared to DA. In addition, the retardation appeared to be less sensitive to small variations in dosing for IA than for DA, i.e. the system was more robust for IA. For DA, a small increase in LSs dosage led to large increase in setting retardation, which can be a source of incompatibility between cement and plasticizer.

The presence of numerous ettringite crystals on the surface of unhydrated cement grains could also change the workability of the cement paste. Indeed, the increased formation of ettringite measured for IA led to early stiffening of the cement paste, reduced workability until potential rapid set. This is a form of incompatibility between cement and plasticizer.

6. Conclusions

The experiments included in this PhD thesis were conducted on a sugar-reduced softwood calcium lignosulfonate (LSs), and on pastes of two Portland cements: a CEM I 52.5 N (ANL) and a CEM I 52.5 R (CX), as defined by the European Standard EN197-1:2011. Between the two cements studied, CX cement had the highest C_3A content and fineness. The conclusions drawn from the conducted experiments are hereby reported according to the objective they answer to.

Objective 1: To identify the consumption mechanisms of lignosulfonate by Portland cement paste

Neither AFm nor intercalated AFm were observed. Therefore, intercalation could not explain the differences in LSs consumption observed between IA and DA.

Calcium complexation and multilayer adsorption were considered as minor mechanisms of LSs consumption in the cements for IA, since they appeared minor or not existing for both $CaCO_3$ and $Ca(OH)_2$, and for the cements in case of DA.

Immediate addition (IA) of LSs to the cement pastes led, up to a threshold LSs dosage, to increased formation of ettringite, and subsequent surface area, compared to the same pastes of the cements without LSs or to those mixed with delayed addition (DA).

The mechanism of LSs consumption appeared to be mainly monolayer surface adsorption for CX cement (both for IA and for DA), and for ANL cement when DA was applied. For ANL, other mechanisms in addition to monolayer surface adsorption appeared to play a role in LSs consumption when IA was applied.

For high surface area and high C_3A cement (as CX cement), the difference in LSs consumption between IA and DA was most likely due to the increased ettringite amount and subsequent surface area. For ANL cement, other mechanisms contributed to LSs consumption additionally to surface adsorption in case of IA.

Objective 2: To link the lignosulfonate consumption to its effect on the rheological properties and setting time of Portland cement paste

The rheological behavior of cement paste with LSs related to the degree of LSs coverage of the available surface for adsorption. A drop in yield stress and viscosity was measured for the cement pastes that reached an adsorption plateau, as observed for DA. Samples which did not reach surface saturation, as observed for IA, showed a more gradual increase in workability requiring higher LSs dosages when compared to those needed for DA.

The setting behavior of cement paste with LSs appeared to relate to the amount of free LSs in the pore solution. For IA, the large amount of ettringite formed provided additional surface area. This caused higher LSs adsorption, reducing the amount of free LSs in the pore solution and, in turn, the setting retardation.

Increased ettringite precipitation was observed to lead to earlier sulfate depletion, accelerating the aluminates reaction, possibly altering the balance between silicates and aluminates.

Objective 3: To understand the effect of lignosulfonate on the amount of ettringite formed and on its morphology

Immediate addition (IA) of LSs to the cement pastes led to a considerable increase in the amount of ettringite formed compared to pastes of the same cements without LSs. Delayed addition (DA) of LSs did not affect the amount of ettringite formed.

For the systems analyzed in this paper, no changes in the morphology of the ettringite crystals appeared to be caused by LSs addition.

SEM imaging allowed observing the finely dispersed ettringite crystals in the cement paste. In case of immediate addition (IA) of LSs, the ettringite shape was cubic with size between 0.1 and 0.2 µm for ANL cement, and cuboidal with length between 0.2 and 0.4 µm for CX cement (aspect-ratio varying between 1.5:1 and 4:1).

The study of pure calcium sulfate systems indicated that the large amount of ettringite formed upon LSs addition with IA was not due to an increased dissolution of the calcium sulfates.

The presence of numerous small ettringite crystals on the surface of unhydrated cement grains upon LSs addition with IA led to an increase in plasticizer adsorption. This renders the system more robust, i.e. less sensitive to variations in dosing, regarding retardation and slump loss compared to DA. However, the large amount of crystals might potentially cause incompatibility problems due to early stiffening.

After 28 days of hydration, no noticeable effect of LSs addition and of its addition time on the amount of hydrates formed was observed, despite the large differences in the amount of ettringite formed after 30 minutes.

Final remarks

In conclusion, the use of the LSs studied in this PhD thesis in combination with cements characterized by high C_3A content and fineness appears critical, as possibly leading to incompatibility issues such as higher LSs dosage needed to reach a given workability, severe setting retardation, rapid set, and sudden slump loss. Therefore, before using LSs in the concrete practice, special attention should be paid on the compatibility between the LSs and the cement chosen.

As to the LSs addition method, the DA of LSs after 10 minutes of hydration was found to reach a given workability increase with lower LSs dosages than for IA. However, for DA, pastes of both cements were found to be very sensitive to variations in LSs dosage: even a small increase from the optimal LSs dosage could lead to sudden drop in yield stress and viscosity. Therefore, a special attention has to be paid when the LSs is added with DA.

7. Future research

Consumption mechanisms of LSs by the cement paste

For immediate addition, the mechanism of LSs consumption was found to be mainly monolayer surface adsorption for CX cement paste. However, for ANL cement paste, monolayer surface adsorption could not fully explain the amount of LSs consumed. Therefore, further investigations are needed to identify other possible mechanisms of LSs consumption.

Influence of the plasticizer addition time on ettringite development

The results reported in Paper 3 showed that the hydrates formed after 30 minutes of hydration by the two cement pastes were different depending on the presence of LSs and its addition time. Further investigations are necessary to understand what are the mechanisms behind the increase in ettringite formed for IA, but not for DA.

Effect of LSs on the physical and mechanical properties of hardened cement

The great majority of the experiments contained in this PhD thesis were conducted on fresh cement paste after 30 minutes of hydration. The results from TGA displayed that the addition of increasing LSs dosages did not lead to remarkable differences in hydrates type and amount in hardened cement paste. However, the way the crystals are formed will influence the microstructure of the hardened cement, which can impact the compressive strength (Papadakis and Tsimas, 2002). Therefore, it appears a matter of interest to further investigate the impact of lignosulfonate on the morphology and microstructure of hydrates of hardened cement paste.

Polydispersity of lignosulfonate

The lignosulfonate used in this PhD thesis is characterized by a weighted molecular weight (M_w) of 29000 g/mol and a number weighted molecular weight (M_n) of 2100 g/mol, giving a broad molar-mass dispersity equal to 13.8. The molar-mass dispersity ($Đ_M$), also called polydispersity index, is defined as the ratio between M_w and M_n. Since the molecular mass of a plasticizer is known to influence its adsorption (Ramachandran, 1996), deeper investigations of the mechanisms of adsorption of lignosulfonate molecules based on their size seems of great interest.

References

AGARWAL, S. K., MASOOD, I. & MALHOTRA, S. K. 2000. Compatibility of superplasticizers with different cements. *Construction and Building Materials,* 14**,** 253-259.

AIAD, I. 2003. Influence of time addition of superplasticizers on the rheological properties of fresh cement pastes. *Cement and Concrete Research,* 33**,** 1229-1234.

AIAD, I., ABD EL-ALEEM, S. & EL-DIDAMONY, H. 2002. Effect of delaying addition of some concrete admixtures on the rheological properties of cement pastes. *Cement and Concrete Research,* 32**,** 1839-1843.

BENSTED, J. & BARNES, P. 2002. *Structure and performance of cements*, Taylor & Francis.

BISHOP, M., BOTT, S. G. & BARRON, A. R. 2003. A New Mechanism for Cement Hydration Inhibition: Solid-State Chemistry of Calcium Nitrilotris(methylene)triphosphonate. *Chemistry of Materials,* 15**,** 3074-3088.

CHATTERJI, S. & KAWAMURA, M. 1992. Electrical double layer, ion transport and reactions in hardened cement paste. *Cement and Concrete Research,* 22**,** 774-782.

CHEUNG, J., JEKNAVORIAN, A., ROBERTS, L. & SILVA, D. 2011. Impact of admixtures on the hydration kinetics of Portland cement. *Cement and Concrete Research,* 41**,** 1289-1309.

CHIOCCHIO, G. & PAOLINI, A. E. 1985. Optimum time for adding superplasticizer to Portland cement pastes. *Cement and Concrete Research,* 15**,** 901-908.

CODY, A. M., LEE, H., CODY, R. D. & SPRY, P. G. 2004. The effects of chemical environment on the nucleation, growth, and stability of ettringite [Ca3Al(OH)6]2(SO4)3·26H2O. *Cement and Concrete Research,* 34**,** 869-881.

COLLEPARDI, M. 1982. The influence of admixtures on concrete rheological properties. *Il cemento.*

COLLEPARDI, M., MARCIALIS, A. & SOLINAS, V. 1973. The influence of calcium lignosulfonate on the hydration of cements. *Il cemento.*

COLLINS, J. W., TORKELSON, J. M. & WEBB, A. A. 1977. Some viscosity properties of lignosulfonates isolated by ultrafiltration. *Journal of Agricultural and Food Chemistry,* 25**,** 743-746.

COPPOLA, L. 2007. *Concretum*, McGraw-Hill.

DANNER, T., JUSTNES, H., GEIKER, M. & LAUTEN, R. A. 2016. Early hydration of C3A–gypsum pastes with Ca- and Na-lignosulfonate. *Cement and Concrete Research,* 79**,** 333-343.

FLATT, R. J. & HOUST, Y. F. 2001. A simplified view on chemical effects perturbing the action of superplasticizers. *Cement and Concrete Research,* 31**,** 1169-1176.

FLATT, R. J., SCHOBER, I., RAPHAEL, E., PLASSARD, C. & LESNIEWSKA, E. 2009. Conformation of Adsorbed Comb Copolymer Dispersants. *Langmuir,* 25**,** 845-855.

GELARDI, G., MANTELLATO, S., MARCHON, D., PALACIOS, M., EBERHARDT, A. B. & FLATT, R. J. 2016. 9 - Chemistry of chemical admixtures. *Science and Technology of Concrete Admixtures.* Woodhead Publishing.

GILBERT, R. G., HESS, M., JENKINS, A. D., JONES, R. G., KRATOCHVIL, P. & STEPTO, R. F. T. 2009. Dispesity in polymer science. *Pure applied chemistry,* 81**,** 351-353.

GIRAUDEAU, C., D'ESPINOSE DE LACAILLERIE, J.-B., SOUGUIR, Z., NONAT, A. & FLATT, R. J. 2009. Surface and intercalation chemistry of polycarboxylates copolymers in cementitious systems. *Journal of the American Ceramic Society,* 92**,** 2471-2488.

HANEHARA, S. & YAMADA, K. 1999. Interaction between cement and chemical admixture from the point of cement hydration, absorption behaviour of admixture, and paste rheology. *Cement and Concrete Research,* 29**,** 1159-1165.

HEKAL, E. E. & KISHAR, E. A. 1999. Effect of sodium salt of naphthalene-formaldehyde polycondensate on ettringite formation. *Cement and Concrete Research,* 29**,** 1535-1540.

HIEMENZ, P. C. & RAJAGOPALAN, R. 1997. *Principles of colloid and surface chemistry*, Taylor & Francis Group.

HOT, J. 2013. *Influence des polymères de type superplastifiants et agents entraineurs d'air sur la viscosité macroscopique des matériaux cimentaires.* Doctoral degree, Université Paris-Est.

HOT, J., BESSAIES-BEY, H., BRAMAUD, C., DUC, M., CHARLENE & ROUSSEL, N. 2014. Adsorbing polymers and viscosity of cement pastes. *Cement and Concrete Research,* 63**,** 12-19.

HOUST, Y. F., BOWEN, P., PERCHE, F., KAUPPI, A., BORGET, P., GALMICHE, L., LE MEINS, J.-F., LAFUMA, F., FLATT, R. J., SCHOBER, I., BANFILL, P. F. G., SWIFT, D. S., MYRVOLD, B. O., PETERSEN, B. G. & REKNES, K. 2008. Design and function of novel superplasticizers for more durable high performance concrete (superplast project). *Cement and Concrete Research,* 38**,** 1197-1209.

HSU, K.-C., CHIU, J.-J., CHEN, S.-D. & TSENG, Y.-C. 1999. Effect of addition time of a superplasticizer on cement adsorption and on concrete workability. *Cement and Concrete Composites,* 21**,** 425-430.

JAYASREE, C., MURALI KRISHNAN, J. & GETTU, R. 2011. Influence of superplasticizer on the non-Newtonian characteristics of cement paste. *Materials and Structures,* 44**,** 929-942.

JOLICOEUR, C. & SIMARD, M.-A. 1998. Chemical admixture-cement interactions: Phenomenology and physico-chemical concepts. *Cement and Concrete Composites,* 20**,** 87-101.

KERUI, Y., CAIWEN, Z. & ZHIGANG, L. 2002. The influence of calcium lignosulphonate–sodium bicarbonate on the status of ettringite crystallization in fly ash cement paste. *Cement and Concrete Research,* 32**,** 51-56.

LORPRAYOON, V. & ROSSINGTON, D. R. 1981. Early hydration of cement constituents with organic admixtures. *Cement and Concrete Research,* 11**,** 267-277.

MARCHON, D. & FLATT, R. J. 2016. 12 - Impact of chemical admixtures on cement hydration. *Science and Technology of Concrete Admixtures.* Woodhead Publishing.

MARCHON, D., JACHIET, M., FLATT, R. J. & JUILLAND, P. Impact of polycarboxylate superplasticizers on polyphased clinker hydration. 34th cement and concrete science conference, 2014 Sheffield, UK. 79-82.

MARCHON, D., MANTELLATO, S., EBERHARDT, A. B. & FLATT, R. J. 2016. 10 - Adsorption of chemical admixtures. *Science and Technology of Concrete Admixtures.* Woodhead Publishing.

MOLLAH, M. Y. A., ADAMS, W. J., SCHENNACH, R. & COCKE, D. L. 2000. A review of cement–superplasticizer interactions and their models. *Advances in Cement Research* [Online], 12. Available: http://www.icevirtuallibrary.com/content/article/10.1680/adcr.2000.12.4.153.

MONOSI, S., MORICONI, G. & COLLEPARDI, M. 1982. Combined effect of lignosulfonate and carbonate on pure portland clinker compounds hydration. III. Hydration of tricalcium silicate alone and in the presence of tricalcium aluminate. *Cement and Concrete Research,* 12**,** 425-435.

MONOSI, S., MORICONI, G., PAURI, M. & COLLEPARDI, M. 1983. Influence of lignosulphonate, glucose and gluconate on the C3A hydration. *Cement and Concrete Research,* 13**,** 568-574.

N. MIKANOVIC, C. JOLICOEUR & PAGE, M. Influence of Surfactant Chemical Admixtures on the Stability and Rheological Properties of Calcium Carbonate and Cement Pastes. *Special Publication,* 239.

NKINAMUBANZI, P., IUML & TCIN, P. 2004. Cement and Superplasticizer Combinations: Compatibility and Robustness.

NKINAMUBANZI, P. C., MANTELLATO, S. & FLATT, R. J. 2016. 16 - Superplasticizers in practice. *Science and Technology of Concrete Admixtures.* Woodhead Publishing.

ODLER, I. & SCHÜPPSTUHL, J. 1981. Early hydration of tricalcium silicate III. Control of the induction period. *Cement and Concrete Research,* 11**,** 765-774.

PAPADAKIS, V. G. & TSIMAS, S. 2002. Supplementary cementing materials in concrete: Part I: efficiency and design. *Cement and Concrete Research,* 32**,** 1525-1532.

PLANK, J., KELLER, H., ANDRES, P. R. & DAI, Z. 2006. Novel organo-mineral phases obtained by intercalation of maleic anhydride–allyl ether copolymers into layered calcium aluminum hydrates. *Inorganica Chimica Acta,* 359**,** 4901-4908.

PLANK, J. & SACHSENHAUSER, B. 2009. Experimental determination of the effective anionic charge density of polycarboxylate superplasticizers in cement pore solution. *Cement and Concrete Research,* 39**,** 1-5.

PRINCE, W., EDWARDS-LAJNEF, M. & AïTCIN, P. C. 2002. Interaction between ettringite and a polynaphthalene sulfonate superplasticizer in a cementitious paste. *Cement and Concrete Research,* 32**,** 79-85.

RAMACHANDRAN, V. S. 1972. Interaction of calcium lignosulfonate with tricalcium silicate, hydrated tricalcium silicate, and calcium hydroxide. *Cement and Concrete Research,* 2**,** 179-194.

RAMACHANDRAN, V. S. 1994. Interaction of admixtures in the cement-water system. *Application of admixtures in concrete.* CRC Press.

RAMACHANDRAN, V. S. 1996. *Concrete Admixtures Handbook, 2nd Ed.: Properties, Science and Technology*.

RAMACHANDRAN, V. S. & FELDMAN, R. F. 1971. Adsorption of calcium lignosulfonate on tricalcium aluminate and its hydrates in a non-aqueous medium. *Cement technology.*

REKNES, K. & GUSTAFSSON, J. Effect of modifications of lignosulfonate on adsorption on cement and fresh concrete properties. 7th International Conference on Superplasticizers and Other Chemical Admixtures in Concrete, 2000. 127-142.

REZANOWICH, A. & GORING, D. A. I. 1960. Polyelectrolyte expansion of a lignin sulfonate microgel. *Journal of Colloid Science,* 15**,** 452-471.

ROBERTS, L. R. & TAYLOR, P. C. 2007. Understanding cement-SCM-admixture interaction issues. *Concrete international***,** 33-41.

ROUSSEL, N. 2007. Rheology of fresh concrete: from measurements to predictions of casting processes. *Materials and Structures,* 40**,** 1001-1012.

ROUSSEL, N., LEMAÎTRE, A., FLATT, R. J. & COUSSOT, P. 2010. Steady state flow of cement suspensions: A micromechanical state of the art. *Cement and Concrete Research,* 40**,** 77-84.

SANDBERG, P. & ROBERTS, L. R. Studies of cement-admixture interactions related to use of chemical admixtures. 7th CANMET/ACI International Conference on Superplasticizers and other chemical Admixtures in concrete, 2003. 529-542.

SOWOIDNICH, T., RACHOWSKI, T., RÖßLER, C., VÖLKEL, A. & LUDWIG, H.-M. 2015. Calcium complexation and cluster formation as principal modes of action of polymers used as superplasticizer in cement systems. *Cement and Concrete Research,* 73**,** 42-50.

STÖBER, S. & PÖLLMANN, H. 1998. Crystalchemistry of organic sulfonates used as cement additives. *Materials Science Forum,* 278-281**,** 904-908.

THOMAS, N. L. & BIRCHALL, J. D. 1983. The retarding action of sugars on cement hydration. *Cement and Concrete Research,* 13**,** 830-842.

TUTHILL, L. H., ADAMS, R. F., BAILEY, S. N. & SMITH, R. W. 1961. A case of abnormally slow hardening concrete for tunnel lining. *ACI Journal,* 57**,** 1091-1109.

UCHIKAWA, H., HANEHARA, S., SHIRASAKA, T. & SAWAKI, D. 1992. Effect of admixture on hydration of cement, adsorptive behaviour of admixture and fluidity and setting of fresh cement paste. *Cement and Concrete Research,* 22**,** 1115-1129.

VALENTI, G. L., SABATELLI, V. & MARCHESE, B. 1978. Hydration kinetics of tricalcium silicate solid solutions at early ages. *Cement and Concrete Research,* 8**,** 61-72.

VIKAN, H. 2005. *Rheology and reactivity of cementitious binders with plasticizers.* NTNU Trondheim.

YOSHIOKA, K., TAZAWA, E.-I., KAWAI, K. & ENOHATA, T. 2002. Adsorption characteristics of superplasticizers on cement component minerals. *Cement and Concrete Research,* 32**,** 1507-1513.

YOUNG, J. F. 1962. Hydration of tricalcium aluminate with lignosulphonate additives. *Magazine of Concrete Research,* 14**,** 137-142.

YOUNG, J. F. 1972. A review of the mechanisms of set-retardation in portland cement pastes containing organic admixtures. *Cement and Concrete Research,* 2**,** 415-433.

YOUSUF, M., MOLLAH, A., PALTA, P., HESS, T. R., VEMPATI, R. K. & COCKE, D. L. 1995. Chemical and physical effects of sodium lignosulfonate superplasticizer on the hydration of portland cement and solidification/stabilization consequences. *Cement and Concrete Research,* 25**,** 671-682.

ZHANG, Y. & KONG, X. 2015. Correlations of the dispersing capability of NSF and PCE types of superplasticizer and their impacts on cement hydration with the adsorption in fresh cement pastes. *Cement and Concrete Research,* 69**,** 1-9.

ZINGG, A., WINNEFELD, F., HOLZER, L., PAKUSH, J., BECKER, S. & GAUCKLER, L. 2008. Adsorption of polyelectrolytes and its influence on the rheology, zeta potential, and microstructure of various cement and hydrate phases. *Journal of Colloid and Interface Science,* 323**,** 301-312.

Part II – Appended papers

Paper I

On the mechanisms of consumption of calcium lignosulfonate by cement paste

Revised version submitted to Cement and Concrete Research (September 2016)

Colombo, A.; Geiker, M.R.; Justnes, H.; Lauten, R.A.; De Weerdt, K.

ON THE MECHANISMS OF CONSUMPTION OF CALCIUM LIGNOSULFONATE BY CEMENT PASTE

A. Colombo (1), M. Geiker (1), H. Justnes (1,2), R. A. Lauten (4), K. De Weerdt (1)

(1) Department of Structural Engineering, Norwegian University of Science and Technology, Norway

(2) SINTEF Building and Infrastructure, Trondheim, Norway

(3) Borregaard, Sarpsborg, Norway

ABSTRACT

The aim of this paper is to assess the mechanisms of consumption of softwood calcium lignosulfonate (LSs) by cement paste. The LSs consumption by two different cements (CX and ANL) and two reference materials ($CaCO_3$ and $Ca(OH)_2$) was investigated, either by adding the LSs immediately with the mixing water (IA) or after 10 minutes of hydration (DA). For IA, the increase in LSs dosage caused additional ettringite formation and an increase in particle surface area. This was not observed for DA. Since no AFm phase could be detected, intercalation in AFm seemed not to occur for the investigated materials. The main mechanism of LSs consumption for CX cement (both for IA and DA) and for ANL cement (only for DA) appeared to be monolayer adsorption. For IA, the amount of consumed LSs could not be ascribed exclusively to monolayer surface adsorption and other LSs consumption mechanisms might play a role.

1. INTRODUCTION

Water-reducers, or plasticizers, are commonly used as admixture for concrete. Their addition to fresh concrete allows obtaining highly fluid concrete at low water-binder ratios, improving the mechanical properties of the hardened concrete. To optimize the polymer-cement combination and the amount of admixture needed to achieve the desired workability, it is important to understand the mechanisms of consumption of plasticizer by cement paste.

The plasticizer investigated in this paper is a low-sugar softwood calcium lignosulfonate (LSs), commonly used in concrete in the dosage of 0.25-0.40 mass % of binder. Lignosulfonates are polyelectrolytes derived from lignins from pulping industry. The lignins are fragmented and sulfonated, thereby becoming water-soluble. Lignin can be derived both from softwood and hardwood trees, which results in lignosulfonates with different molecular weight and amount of molecular functional groups (carboxyl groups, phenolic-OH, sulfonic groups). Lignosulfonate is known to have medium retarding effect on cement hydration. The sugars naturally contained in lignin remain in lignosulfonate after its production. These sugars contribute to longer setting times of cement, in particular the hexoses, which can be removed by fermentation in low-sugar lignosulfonates. However, studies in literature found that also sugar-free lignosulfonates exhibited pronounced retardation of cement paste hydration, e.g. [1, 2].

Plasticizers interact with unhydrated and hydrated cement grains, as summarized in a recent literature review by Marchon and Flatt [3]. In this paper, the amount of polymer uptaken by the cement paste is defined as "consumed" as opposed to the free one dissolved in the pore solution. The mechanisms of polymer consumption will be separately discussed in this paragraph.

The dispersing effectiveness of a superplasticizer on cementitious materials is, amongst others, a function of its degree of adsorption on the surface of cement grains and hydrates. The adsorbed plasticizer layer renders the total particle surface negatively charged, i.e. with a negative zeta potential. As negatively charged particles approach each other there will be an electrostatic repulsion preventing them from forming agglomerates. Additionally, when two surfaces approach enough for their adsorbed layers to overlap, a steric force develops. This will contribute in hindering particles to get close enough to form agglomerates. The key parameters that govern the steric repulsion are the adsorption layer thickness and its conformation at the solid liquid interface [4].

The polymer will not be adsorbed equally on the four main cement phases. According to Yoshioka et al. [5], much higher adsorption occurs on aluminate and ferrite than on the silicate phases. The amount of adsorbed polymer on ettringite was found to be the largest amongst the cement hydrates by Zingg et al. [6]. It must be noted that, in both the cited references, the results were reported by unit of mass and not by unit of specific surface.

Polymer adsorption can also take place in multiple layers on cement particles and hydrates. After ideal monolayer coverage, the cement particles will have a negative surface charge. Ca^{2+} ions will then be electrostatically attracted to the negatively charged groups of the polymer and they will bond with them. This Ca^{2+} outer layer will allow the adsorption of a further layer of negatively charged polymer [7, 8], facilitating additional consumption of polymers.

Adsorption onto the surface of cement particles and hydrates is not the only potential consumption mechanism taking place when a plasticizer is added to a cementitious system. Part of the water-reducing admixture might also be intercalated in the hydration products, mainly in the layered structure of AFm, and part of the admixture will remain dissolved in the aqueous phase, according to, amongst others, [9-12]. When tricalcium aluminate (C_3A) enters in contact with water, it reacts immediately forming, in absence of gypsum, the metastable layered phases C_4AH_{19} and C_2AH_8. In presence of gypsum, C_3A will react with water forming $C_6A\bar{S}_3H_{32}$ (ettringite) and $C_4A\bar{S}H_{12}$ (monosulphate). C_4AH_{19}, C_2AH_8 and $C_4A\bar{S}H_{12}$ belong to the group of layered double hydroxides (LDHs). Several anions and polyelectrolytes can intercalate in between the cationic layers of LDH compounds by replacing their hydroxyl ions. According to Plank et al. [10], intercalation was found to be possible for polymers with different structure, namely, linear, comb-like and polymer brushes with very long side chains. The polymer intercalated in LDHs will no longer be available for dispersing cement particles; therefore a higher dosage of polymer will be necessary to reach the desired workability.

Another possible mechanism of polymer-cement interaction is complexation between functional groups of the plasticizer and calcium ions dissolved in the pore solution, as observed in several studies [13-16]. Collins et al. [13] found that calcium ions dissolved in a calcium lignosulfonate solution with pH over 10-11 can hold together a matrix of lignosulfonate molecules, forming a gel. Other cations, e.g. aluminium and iron, could also tightly bind to LS molecules. As mentioned by Sowoidnich et al. [15], the interaction between calcium ions and polymer functional groups (mainly sulfonic and carboxyl groups) can be divided into complexation of calcium ions in aqueous solution, complexation of calcium ions on particles surface (adsorption) and formation of polymer-containing clusters. Formation of Ca-polymer complexes will increase the amount of consumed polymer if they are precipitated or form colloids that are filtered away when collecting pore solution, and decrease the amount of free Ca^{2+} ions in the pore solution, lowering the Ca-Si ratio of the pore solution, hence possibly modifying the hydration reactions and the resulting hydrates, as stated by Yousuf et al. [17]. The polymer molecules captured in the complexes with calcium ions might still have some free anionic functional groups on their outer regions. These anionic functional groups might as well be attracted to the positive charged calcium ions adsorbed on the polymer layer over cement particles and hydrates. The calcium-polymer complexes might then bind to the cement particles already covered with polymer, decreasing the amount of free LSs in the pore solution and forming multiple layers of polymer adsorbed. For this reason the mechanisms of calcium complexation and multilayer adsorption can be considered interrelated and, sometimes, undistinguishable from each other.

The subject of this paper is to investigate the mechanisms consuming a low-sugar softwood calcium lignosulfonate (LSs) in paste of two Portland cements with different surface area and C_3A content. The effects were studied both by adding the lignosulfonate immediately with the mixing water (IA) and by adding it after 10 minutes of hydration (DA). The amount of polymer consumed by the cement paste was determined by UV-spectrometry and adsorption isotherms were calculated. Comparison of adsorption isotherms onto cement and reference materials representative of cement but which do not hydrate ($CaCO_3$ and $Ca(OH)_2$), allow a better elucidation of the LSs consumption mechanisms in simpler systems than cement. Changes in the surface area of the hydrated cement particles were investigated by BET. The changes in composition and amount of cement hydrates caused by the addition of lignosulfonate were investigated with thermogravimetric analysis (TGA).

2. EXPERIMENTAL

2.1 Materials

The mechanisms of plasticizer consumption by cement paste were studied adding a low-sugar softwood calcium lignosulfonate (LSs) to two Portland cements: a CEM I 52.5 N (ANL) and a CEM I 52.5 R (CX). The two cements were chosen because of their different surface area and C_3A content. The content of the main clinker phases of the cements quantified by XRD Rietveld are given in Table 1. The chemical composition of the cements and the loss of ignition at 950 ºC determined by XRF are reported in Table 2. The particle size distribution (d_{10}, d_{50}, d_{90}), Blaine surface area and density, BET surface area are given in Table 3.

A sugar-reduced softwood calcium lignosulfonate (LSs) was used as plasticizer. Its mass weighted molecular weight (M_w), as measured with gel permeation chromatography (GPC), was 29000 g/mol and the number weighted molecular weight (M_n) was 2100 g/mol, giving broad molar-mass dispersity ($Đ_M$) equal to 13.8. The molar-mass dispersity, also called polydispersity index, is defined as the ratio between M_w and M_n [18]. Additional physical and chemical properties of the lignosulfonate are listed in Table 4. For the lignosulfonate used in the present investigation, the sugars were removed from the polymer molecule by fermentation and resulting alcohol by distillation. The LSs was dissolved in deionised water to concentrations varying from 1 to 45 % to ease dosing, and the water content was included in the calculation of the water-to-binder ratio (w/b).

$CaCO_3$ and technical-grade precipitated $Ca(OH)_2$ were also mixed with lignosulfonate in order to study some simplified model systems. Their specific surface areas determined by BET are reported in Table 5. In order to mimic the basic pH of cement paste, these samples were mixed with LSs solution diluted in artificial pore water. The artificial pore water was a solution of NaOH and KOH with K/Na molar ratio equal to 2 and measured pH of 12.9.

2.2 Sample preparation

2.2.1 Portland cements

Cement was mixed with distilled water and/or lignosulfonate solution in a high-shear mixer MR530 by Braun at intensity 6 obtaining pastes with w/b = 0.4. About 200 ml of cement paste was mixed per batch. In order to investigate the effect of the time of addition of lignosulfonate, two different mixing procedures were compared: immediate addition of LSs with the mixing water (IA) and delayed addition of LSs at 10 minutes of hydration (DA).

For IA, the binder was mixed with distilled water (and/or lignosulfonate diluted in distilled water or artificial pore water) according to the procedure used by Vikan [19]: 30 seconds mixing and scraping the walls of the mixer to homogenize the mix, 5 minutes resting and 1 minute mixing.

For DA, the binder and 85% of the needed water were mixed according to the following mixing procedure: 30 seconds mixing and scraping the mixer walls to homogenize the mix, 10 min resting (delay time chosen according several studies in literature [20-23]). LSs and the remaining 15% of the needed water were then added to the mix which was mixed for 1 minute.

After mixing, about 35 ml of paste was poured in 50 ml sealed plastic centrifuge tubes and let rest until the chosen analysis time.

2.2.2 Calcium carbonate

Calcium carbonate has been shown to be a suitable model system for investigating stability and rheology of cement paste. Mikanovic et al. [24] showed that calcium carbonate exhibits colloidal properties very similar to those of cement paste at early ages (hydration < 1 hour). $CaCO_3$ exhibit surface properties and flocculation behavior similar to that of cement paste, namely, an irregular spheroid shape, and a low surface charge in water. In addition it has a

very low solubility, also at high pH. In addition, this material was expected not to noticeably react with water.

About 300 g of $CaCO_3$ was mixed with about 90 g of LSs solution dissolved in artificial pore water in a high-shear mixer MR530 by Braun at intensity 6. The mixing procedure was identical to the one used for neat cement with IA. The water-solid ratio by mass was 0.3. Several LSs dosages were analysed, as reported in Table 6. The samples were let to rest for 30 minutes prior to being analysed.

2.2.3 Calcium hydroxide

$Ca(OH)_2$ is one of the main cement hydrates and its solubility is about 100 times higher than the one of $CaCO_3$, so it appears to be useful to investigate the possible interaction between the LSs and calcium ions. About 5 g of $Ca(OH)_2$ was mixed with about 40 g of LSs solution dissolved in artificial pore water in plastic centrifuge tubes and mixed by hand for 1 minute. The high fineness of the $Ca(OH)_2$ powder required a water-solid ratio by mass of 8.0. The mixing solution contained increasing amounts of LSs, as reported in Table 6. All the samples were let to rest for 30 minutes prior to being analysed.

2.3 Methods

2.3.1 Adsorption isotherms

Polymer adsorption by a solid is usually described through isotherms, in which the amount of polymer adsorbed is plotted against the total amount of polymer added to the system [25]. The shape of an isotherm is largely determined by the adsorption mechanism. In this study, the isotherms were drawn relating the amount of LSs consumed by the cement paste to the amount of total LSs added to the sample.

With the help of a calibration curve, achieved by measuring the UV absorbance of pure LSs solutions in artificial pore water at different concentrations, the amount of free plasticizer (g LS/100 g solution) was calculated. This amount was related to the amount of binder in the sample (g LS/100 g binder). The LSs consumed by the investigated systems was then calculated by subtracting the amount of free LSs from the total amount of LSs initially added to the sample, as displayed in the following equation:

$$\text{consumed LSs} = \text{total LSs} - \text{free LSs} \quad (1)$$

The absorbance of the pore solution was measured with UV-spectroscopy. In order to confirm the results obtained with UV-spectroscopy, the adsorption isotherm of ANL cement for IA was measured also with total organic carbon analysis (TOC). Potential removal of polymer aggregates by filtration was eliminated as error source, by comparing TOC analysis of filtered and un-filtered samples which were found to be very similar

2.3.1.1 UV-spectroscopy

UV-spectrometry allowed measuring the absorbance of the pore solution at increasing LSs dosage. The LSs dosages tested are summarized in Table 6.

The pore solution was extracted from the cement paste by centrifuging the samples in a Heraeus Megafuge 8 centrifuge by Thermo Scientific for 3 minutes at the speed of 4500 rpm. The supernatant pore solution was extracted and filtered with 0.45 µm cellulose acetate syringe filters by VWR. The amount of free LSs in the pore water was measured with UV-spectrometry with a Genesys 10S UV-spectrophotometer by Thermo Scientific. Several wavelengths have been reported in literature to study the amount of lignosulfonate in pore solution: Perche [26] and Ratinac [27] used 280 nm, Uchikawa et al. [28] and Houst at al. [4] used 284 nm, Vikan [19] used 283 nm. Samples diluted 1:100 with distilled water were scanned with different wavelengths from 190 to 300 nm using distilled water as blank reference sample. For the plasticizer used in this study, 281 nm was chosen as the best wavelength to measure the absorbance value.

The amount of plasticizer consumed by cement paste as a function of increasing hydration time was determined by centrifugation of pastes aged for different times (5-120 minutes). As displayed in Figure 1, it was found that at 10 minutes of hydration the LSs uptake reached an equilibrium value. All the samples were then analysed aftert 30 minutes of hydration.

2.3.1.2 Total organic carbon (TOC)

The concentration of free polymer in the pore solution extracted by ANL cement (0.2; 0.4; 0.8; 1.0; 1.5 mass % of binder LSs IA) was measured with the total organic carbon analysis (TOC). The TOC analysis was performed using a Vario TOC Cube by Elementar. The extracted pore solution was filtered with 0.20 µm cellulose acetate filters. Part of the sample was acidified with 2 drops of concentrated HCl to prevent any formation of precipitates in the solution. The amount of consumed LSs was measured by TOC on the same sample before and after acidification. Acidification did not lead to any variation in the results. No notable difference in the results obtained with UV-spectroscopy and with TOC was displayed up to a LSs dosage of 0.6 mass % of binder. Over this dosage, the consumed LSs from TOC measurements was from 3 to 15 % higher than the one measured with UV-spectroscopy. The difference might be due to the differences in sample preparation (different sample dilution, different filter used) and the measurement techniques. However, the results obtained with the two different techniques showed similar trends.

2.3.2 Solvent exchange

A solvent exchange procedure with isopropanol was used to stop the hydration of the cement paste after 30 minutes of hydration. The samples were then analysed with thermogravimetric analysis (TGA) and BET.

About 5 ml of cement paste was transferred in a 50 ml centrifuge tube and centrifuged for 1 minute at 2000 rpm. The supernatant water was removed. About 40 ml of isopropanol was poured in the centrifuge tube. The tube was shaken for 30 seconds and let to rest for 5 minutes. The sample was centrifuged again for 1 minute at 2000 rpm and the supernatant liquid was removed. The solvent exchange procedure with isopropanol was repeated once, followed by a final solvent exchange with 10 ml of petroleum ether. The resulting paste was let to dry for 2 days in a desiccator over silica gel, and soda lime to minimize carbonation.

After drying, the samples were homogenized in a porcelain mortar and stored in sealed containers in a desiccator over silica gel and soda lime until analysis.

2.3.3 Thermogravimetric analysis (TGA)

The thermogravimetric analysis (TGA) was performed with a Mettler Toledo TGA DSC3+ on hydrated cement paste after stopping the hydration using solvent exchange. Approximately 200 mg of cement paste powder was loaded in 600 µl alumina crucibles. The samples were heated from 40 to 900°C at a rate of 10°C/min while purging with 50 ml/min N_2.

2.3.4 Characterization of surface area of hydrated cement pastes by BET

The BET measurements were performed using a Tristar II Plus by Micromeritics on samples of which the hydration was stopped with the solvent exchange procedure. Before the measurement, the samples were degassed for about 5 minutes at room temperature. The measurement was performed purging the samples with nitrogen at room temperature, which took about 10 minutes. The sample mass was about 2 g. The samples did not undergo any thermal treatment before the measurement to avoid any possible destruction of ettringite, as recommended by Mantellato et al. [29, 30].

3 RESULTS

3.1 Adsorption isotherms

The adsorption isotherms of ANL and CX cement pastes, $CaCO_3$, and $Ca(OH)_2$ were obtained by measuring the amount of consumed polymer for an increasing dosage of polymer in the mix as described in Table 6. Higher LSs dosages were used for $Ca(OH)_2$ due to its very small particle size, and thus larger specific surface. For CX cement it was not possible to extract pore water at LSs dosages over 1.0 mass % of binder due to paste hardening after 30 minutes of hydration. The LSs was added to the cement paste either immediately with the mixing water (IA), or after 10 minutes of hydration (DA). The results are presented as consumed LS per mass % of binder in Figure 2a, and per m^2 of unhydrated substrate surface area available for adsorption in Figure 2b. The isotherms were obtained by fitting the experimental data to the non-linear Langmuir model [25]. As reported in [31], the Langmuir model is not ideal for a system like cement paste, which surface area changes with hydration and where the polymer is not adsorbed equally on all cement phases. The Langmuir model was however used to fit the adsorption measurements collected in the present paper, keeping in mind the limitations connected to it. The adsorption isotherm of $Ca(OH)_2$ is omitted in Figure 2 a because of the higher LSs dosages used. It must be noted that the water-solid ratio by mass was 0.3 for $CaCO_3$ and 8.0 for $Ca(OH)_2$, while it was 0.4 for the neat cements.

The results were also presented in Figure 3 as consumed LSs amount (% of the LSs amount added) versus the LSs amount added. Figure 3 shows that all the adsorption isotherms for the cements displayed similar LSs consumption at low LSs dosage (up to about 0.25 mass % of binder LSs). At these low LSs dosages, about 75 % of the LSs added was consumed both for IA and for DA. At LSs dosages higher than about 0.25 mass % of binder, the curves obtained for IA showed a LSs consumption of about 70 % of the LSs added. The consumption kept constant with increasing LSs dosages. For DA, the amount of LSs consumed decreased from

about 75 % to about 30 % of the LSs added when the LSs dosage increased from 0.25 to 1.5 mass % of binder.

As displayed in Figure 2, for IA, no adsorption plateau could be detected within the tested range, neither for ANL nor for CX cement. This has also been observed by others, e.g. by Vikan [19] and Ratinac et el. [27]. The isotherms' shape indicated a continuous LSs uptake when more LSs was added to the mix.

For DA, an adsorption plateau was found for both cements. The isotherms that reached an adsorption plateau also displayed a considerably lower amount of LSs consumed by the cement pastes compared to those that did not reach any plateau.

3.2 Surface area of hydrated cement particles

The BET surface area was measured for ANL and CX cement pastes with increasing LSs amounts hydrated for 30 minutes. The hydration was stopped by solvent exchange after 30 minutes. The results are shown in Figure 5.

For both cements the surface area after 30 minutes of hydration was found to increase as the dosage of plasticizer added to the cement paste increased. The increase in surface area was remarkably larger for CX than for ANL cement, and for IA compared to DA.

New adsorption isotherms were calculated dividing the amount of consumed LSs by the actual surface area of ANL and CX cements after 30 minutes of hydration as measured with BET for both IA and DA. The results are displayed in Figure 6. For CX cement, the isotherms obtained with IA and DA nearly coincide, both reaching an adsorption plateau. On the contrary, for ANL cement, even when expressed relative to the hydrated surface area, the adsorption isotherms remain qualitatively similar to those obtained considering the unhydrated surface area.

3.3 LSs molecular footprint

As displayed in Figure 6, for ANL cement, the adsorption plateau was reached for a total LSs amount between 0.8 and 1.2 mass % of binder, which the authors assume to be due to the achievement of monolayer surface coverage. Knowing the molecular weight of the LSs molecule (29000 g/mol) and the specific surface area of hydrated ANL cement as measured with BET (174 m^2/100g cement with 0.8 mass % of binder LSs, and 184 m^2/100g cement with 1.2 mass % of binder LSs), it is possible to calculate the LSs "molecular footprint". The LSs molecular footprint resulted to be about 25 nm^2 for ANL cement for both LSs dosages, which agrees to the data given by the producer (50 ± 30 nm^2). The producer calculated this value from the plateau values of the adsorption isotherms of LSs on MgO at alkaline pH.

For CX cement, the adsorption plateau was reached for a total LSs amount between 1.2 and 1.5 mass % of binder. Knowing the specific surface area of hydrated CX cement as measured with BET (286 m^2/100g cement with 1.2 mass % of binder LSs, and 301 m^2/100g cement with 1.5 mass % of binder LSs), the LSs molecular footprint was calculated as about 30 nm^2 for both LSs dosages. This value also agrees to the data given by the producer (50 ± 30 nm^2).

In order to get a deeper understanding of the actual plasticizer consumption mechanisms by cement paste, the adsorption isotherms determined with ANL or CX cements were compared to those obtained for simplified model systems, $CaCO_3$ and $Ca(OH)_2$.

The $CaCO_3$ isotherm is displayed in Figure 2 a per mass % of dry powder. The $CaCO_3$ isotherm reached an adsorption plateau for a total LSs amount between 0.2 and 0.4 mass % of binder. At surface saturation, about 0.06 g of admixture was adsorbed on 100 g of $CaCO_3$. Since the specific surface area of the unhydrated $CaCO_3$ was measured with BET as 57 $m^2/100g$, the surface coverage can be calculated as about 920 m^2/g_{LS}. Hence, the molecular "footprint" (coverage) of LSs was calculated as about 45 nm^2 for both LSs dosages. This result agrees with the data given by the producer (50 ± 30 nm^2).

The $Ca(OH)_2$ isotherm, omitted in the figures due to the high LSs dosages used, reached an adsorption plateau for a total LSs amount between 8.0 and 12.0 mass % of binder. The high LSs dosages at which the plateau is reached is most likely due to the high specific surface area of the $Ca(OH)_2$ particles. At surface saturation, about 0.06 g of admixture was adsorbed on 100 g of $Ca(OH)_2$. Since the specific surface area of the unhydrated $Ca(OH)_2$ was measured with BET as 1666 $m^2/100g$, the molecular "footprint" of LSs was calculated as about 70 nm^2 for both LSs dosages. This value resulted higher than the one obtained for $CaCO_3$, even though still included in the range given by the producer (50 ± 30 nm^2).

The consumed LSs at plateau achievement and the molecular footprint calculated for the different materials can be found in Table 7. It has to be kept in mind that the LSs has a broad polydispersity index, which leads to a wide error in the molecular footprint given by the producer. The results reported in Table 7 showed that a relatively similar footprint was obtained for the model materials, i.e. $CaCO_3$ and $Ca(OH)_2$, and the real cements.

3.4 Hydrates characterization

In order to investigate the effects of LSs on hydrates formation, thermogravimetric curves were measured on ANL and CX cement pastes with 1.5 mass % of binder LSs added with IA and DA. A reference sample of ANL and CX pastes without LSs was also measured. The hydration of the tested samples was stopped after 30 minutes with the solvent exchange procedure using isopropanol and petroleum ether, as described in paragraph 2.3.2. The results are displayed in Figure 4 a, b.

Several peaks could be observed: the peak at about 120 ºC and the smaller one at 240 ºC indicate the presence of ettringite (ettr.). The peak around 160 ºC represents the decomposition of sulfates. The sulfates will be most likely gypsum (x = 2) for ANL cement. CX cement originally contains anhydrite (x = 0), which will not show any peak in the TGA curve, since it does not contain water, and hemihydrate (x = 0.5). After 30 minutes of hydration, hemihydrate will be partly or completely converted to gypsum. The peak around 160 ºC in CX cement will then be due to the decomposition of gypsum and/or hemihydrate. The peak around 420 ºC shows the presence of portlandite (CH); the ones around 610 ºC and 780 ºC represent the decomposition of carbonates (CO_2). The peaks over 500 ºC can be attributed both to the decomposition of limestone included in the used cements and, for the

samples containing LSs, to the decomposition of LSs. No peak ascribable to AFm phases was detected.

The results show that, for IA, the addition of LSs led to additional formation of ettringite and reduced amount of gypsum. For DA, in presence of LSs, no remarkable changes in the ettringite or gypsum amounts were observed. The LSs addition caused an increase in the weight loss in the carbonate region both for IA and DA. Similar trends were observed for both cements, even though remarkably more ettringite and fewer sulfates were measured for CX cement, which might be linked to the larger amount of C_3A in CX cement than in ANL cement.

4 DISCUSSION

The subject of this paper is to investigate the mechanisms consuming LSs in paste for two Portland cements, both for immediate and delayed addition of plasticizer. From literature the potential main mechanisms are: polymer intercalation into early cement hydrates; surface multilayer adsorption / complexation between functional groups of the plasticizer and calcium ions dissolved in cement pore solution; and monolayer surface adsorption of LSs on cement particles and hydrates. Each mechanism will be discussed separately in the following section.

4.1 Mechanisms of polymer consumption by the cement paste

4.1.1 Intercalation

According to, amongst others, Flatt and Houst [9] and Flatt and Ferraris [32], intercalation in AFm is generally considered to be the main cause of the difference between the adsorption isotherms obtained for IA or for DA. According to the theory, from the moment cement enters in contact with water, calcium aluminates start being consumed in AFt formation. In order for polymer intercalation to take place, calcium aluminates and polymer must be simultaneously available in solution. In case of DA, most hydrated aluminates have already been consumed in AFt formation at the time the polymer is added, hence the aluminates will no longer be available to form intercalated AFm.

Zingg et al. [6] formulated an alternative explanation for the difference in polymer consumption between IA and DA, which does not include intercalation. They hypothesized that, for IA, due to the dispersive effect of the plasticizer, numerous fine ettringite particles are floating in the pore solution, providing additional particle surface area for adsorption. On the contrary, with DA, the ettringite particles have already precipitated on the C_3S surface and cannot be redispersed. Hence, there will be no increase in surface area and, consequently, in polymer adsorption. However, it must be kept in mind that Zingg et al. did not investigate the amount of surface of ettringite which is made available through a change of the initial hydration reactions by the addition of the polymer.

The adsorption isotherms presented in Figure 2a,b displayed a remarkable difference in LSs consumption between the isotherm obtained for IA and the one obtained for DA. However, no peak corresponding to AFm phase could be detected with TGA, as shown in Figure 4a,b. For the materials investigated in this paper, intercalation in AFm seems less likely as a LSs

consumption mechanism for the investigated materials and dosages, while the theory of Zingg et al. [6] appears more feasible.

4.1.2 Calcium complexation / multilayer surface adsorption

In the case that LSs would be consumed in calcium complexes, either in solution or as multilayer surface adsorption, the adsorption isotherms would display an increase in LSs consumption with the amount of total LSs added, even for LSs dosages over the surface saturation value, as calcium is buffered by the cement hydration.

In this study, the adsorption isotherms of both $CaCO_3$ and $Ca(OH)_2$ reached an adsorption plateau, as shown in Figure 2 b. According to Lide [33], $CaCO_3$ has a solubility of 0.0014 g/100g in cold water, while $Ca(OH)_2$ of 0.185 g/100g. Because of the negligible release of calcium ions by $CaCO_3$, calcium complexation or multilayer adsorption with LSs molecules would be limited. The solubility of $Ca(OH)_2$ is about 100 times higher than the one of $CaCO_3$. However, also for $Ca(OH)_2$ no calcium complexation or multilayer adsorption with LSs molecules seemed to take place. Therefore, the LSs consumed by both $CaCO_3$ and $Ca(OH)_2$ was most likely entirely due to monolayer adsorption of LSs molecules on the particles surface.

Concerning the two cements, as shown in Figure 2a,b, the isotherm for both ANL and CX cement reached an adsorption plateau for DA. As for $CaCO_3$, the main LSs consumption seems to be monolayer surface adsorption. For IA, on the contrary, the isotherm of both the cements did not reach an adsorption plateau, indicating a continuous polymer uptake by the cement paste the more polymer is added. However, the authors assume that, as calcium complexation/multilayer adsorption was minor or not existing for both $CaCO_3$ and $Ca(OH)_2$, and for the cements in case of DA, also for the cements in case of IA calcium complexation/multilayer adsorption should not be a major mechanism behind the LSs consumption.

4.1.3 Monolayer surface adsorption

In the case that LSs would adsorb as a monolayer onto the cement particles, the adsorption isotherms would display a plateau when the entire surface is covered by the polymer, as displayed in several studies [5, 19, 34, 35]. This mechanism, monolayer adsorption, can be described by the Langmuir model [25]. Since such a plateau is reached by both ANL and CX cements when the polymer was added with DA, and considering the above conjectures, it is likely that monolayer surface adsorption is the main mechanism of LSs consumption for DA.

No adsorption plateau was reached when the polymer was added with IA. This might be due to different reasons. First, it is possible that the increase in LSs consumption solely occurs due to the increase in particle surface area available for adsorption due to cement hydration, as displayed in Figure 5. In this case, the only mechanism of LSs consumption would be monolayer surface adsorption. Another possibility is that other consumption mechanisms were acting in addition to surface adsorption. In order to examine these possibilities, it is first necessary to further investigate the effect of the increase of particle surface area with hydration on LSs consumption by the cement paste.

Finally, as shown in Figure 2a,b, for IA, ANL cement surprisingly consumed more LSs than CX cement, even though CX cement contains about three times more C_3A than ANL cement and has a higher particle surface area. However, several plasticizers were found to adsorb nearly to the same extent on C_3A and C_4AF by Yoshioka et al. [5]. In the materials used in the present paper, the total content of aluminate and ferrite phases (cubic and orthorhombic C_3A, and C_4AF) is equal to 16.2 % in ANL and 13.6 % in CX. Based on these facts, it is difficult to conclude about the reasons behind the difference in LSs consumption by the two cements with IA. As for DA, CX cement, which has a higher particle surface area, consumed more plasticizer, as displayed in Figure 2a,b. This might indicate that the amount of surface area available for plasticizer interaction is the main parameter governing the LSs consumption for DA.

4.2 The effect of LSs on the increase in particle surface area with hydration

As displayed in Figure 5, the BET measurements showed an increase in particle surface area with hydration, which was influenced both by the plasticizer dosage and by its addition time. The increase in surface area was larger for CX than for ANL cement, and greatly larger for IA than for DA for both cements. As shown in Figure 6, the influence of the different surface area of the two hydrated cements could be eliminated by expressing the results relative to the surface area of the hydrated substrate as measured with BET.

For CX cement, the isotherms obtained with IA and DA nearly coincide, both reaching an adsorption plateau. This indicates that the higher LSs consumption by CX cement paste measured with IA is mainly due to the larger increase in particle surface area that takes place with IA, which, on the contrary, does not take place with DA. Hence, for CX cement, the main mechanism for LSs consumption seems to be monolayer surface adsorption for both IA and DA.

Regarding ANL cement, even when expressed relative to the hydrated surface area, the adsorption isotherms remain qualitatively similar to those obtained considering the unhydrated surface area. Therefore, for ANL cement, monolayer surface adsorption does not seem to be the only LSs consumption mechanism for IA.

Finally, as displayed in Figure 4, when LSs was added to the cement pastes with IA, a higher amount of ettringite was formed by both cements compared to the sample without LSs. Moreover, as shown in Figure 5, the LSs addition led to an increase in particle surface area. The increase was larger for CX cement, which also presented a larger amount of ettringite. Therefore, the increase in particle surface area seems to be directly correlated to the increased amount of ettringite produced by the cements in presence of LSs.

5 SUMMARY AND CONCLUSIONS

The aim of this paper is to obtain a better understanding of the mechanisms for lignosulfonate (LSs) consumption by cement paste. This is considered to be crucial to maximize the efficiency of the plasticizer. According to literature, the mechanisms behind the consumption of a softwood low-sugar calcium lignosulfonate can potentially be: monolayer adsorption, intercalation, and calcium complexation/multilayer adsorption. The LSs consumption by two

different cements at immediate (IA) and delayed (DA) addition was investigated using UV-spectroscopy and adsorption isotherms were calculated. The changes in particle surface area with hydration were measured with BET. The changes in hydrates due to the addition of LSs were examined with TGA. The results obtained for cement pastes were compared to those obtained for reference materials (i.e. calcium carbonate, calcium hydroxide). The following conclusions were drawn:

- The presence of LSs in the cement paste led to an additional formation of ettringite for IA, while an increase was not detected for DA;
- An increase in LSs dosage led to an increase in particle surface area after 30 minutes of hydration. This increase was considerably higher for IA rather than for DA.
- Neither AFm nor intercalated AFm were observed. Therefore, intercalation cannot explain the differences in LSs consumption observed between IA and DA.
- The mechanism of LSs consumption seems to be mainly monolayer surface adsorption for CX cement (both for IA and for DA), and for ANL cement when DA was applied. For ANL, other mechanisms in addition to monolayer surface adsorption appear to play a role in LSs consumption when IA is applied.

6 FUTURE RESEARCH

In a follow-up study, the effect of LSs on the amount and morphology of ettringite produced both for IA and DA will be investigated. A deeper investigation on the mechanisms behind LSs consumption in ANL cement for IA will also be considered for future research.

7 ACKNOWLEDGEMENTS

The authors wish to acknowledge the Norwegian Research Council (NFR 225358/O30) and Borregaard AS, Norway, for financing this research work. Gwenn Le Saout and Nathalie Azema, Ecole des Mines d'Ales, France, Gunnar Westman, Chalmers University of Technology, Sweden, and Serina Ng, SINTEF, are also acknowledged for the helpful discussions. Kevin Roque, Ecole des Mines d'Ales, is acknowledged for performing the TOC analysis and the BET measurements. Irene Bragstad, SINTEF, is acknowledged for performing the BET measurements.

8 REFERENCES

[1] V.S. Ramachandran, M.S. Lowery, Conduction calorimetric investigation of the effect of retarders on the hydration of Portland cement, Thermochimica Acta, 195 (1992) 373-387.
[2] K. Reknes, J. Gustafsson, Effect of modifications of lignosulfonate on adsorption on cement and fresh concrete properties, 7th International Conference on Superplasticizers and Other Chemical Admixtures in Concrete, 2000, pp. 127-142.
[3] D. Marchon, R.J. Flatt, 12 - Impact of chemical admixtures on cement hydration, Science and Technology of Concrete Admixtures, Woodhead Publishing2016, pp. 279-304.

[4] Y.F. Houst, P. Bowen, F. Perche, A. Kauppi, P. Borget, L. Galmiche, J.-F. Le Meins, F. Lafuma, R.J. Flatt, I. Schober, P.F.G. Banfill, D.S. Swift, B.O. Myrvold, B.G. Petersen, K. Reknes, Design and function of novel superplasticizers for more durable high performance concrete (superplast project), Cement and Concrete Research, 38 (2008) 1197-1209.
[5] K. Yoshioka, E.-i. Tazawa, K. Kawai, T. Enohata, Adsorption characteristics of superplasticizers on cement component minerals, Cement and Concrete Research, 32 (2002) 1507-1513.
[6] A. Zingg, F. Winnefeld, L. Holzer, J. Pakush, S. Becker, L. Gauckler, Adsorption of polyelectrolytes and its influence on the rheology, zeta potential, and microstructure of various cement and hydrate phases, Journal of Colloid and Interface Science, 323 (2008) 301-312.
[7] Y. Zhang, X. Kong, Correlations of the dispersing capability of NSF and PCE types of superplasticizer and their impacts on cement hydration with the adsorption in fresh cement pastes, Cement and Concrete Research, 69 (2015) 1-9.
[8] M.Y.A. Mollah, W.J. Adams, R. Schennach, D.L. Cocke, A review of cement–superplasticizer interactions and their models, Advances in Cement Research, 2000, pp. 153-161.
[9] R.J. Flatt, Y.F. Houst, A simplified view on chemical effects perturbing the action of superplasticizers, Cement and Concrete Research, 31 (2001) 1169-1176.
[10] J. Plank, H. Keller, P.R. Andres, Z. Dai, Novel organo-mineral phases obtained by intercalation of maleic anhydride–allyl ether copolymers into layered calcium aluminum hydrates, Inorganica Chimica Acta, 359 (2006) 4901-4908.
[11] C. Jolicoeur, M.-A. Simard, Chemical admixture-cement interactions: Phenomenology and physico-chemical concepts, Cement and Concrete Composites, 20 (1998) 87-101.
[12] C. Giraudeau, J.-B. D'Espinose De Lacaillerie, Z. Souguir, A. Nonat, R.J. Flatt, Surface and intercalation chemistry of polycarboxylates copolymers in cementitious systems, Journal of the American Ceramic Society, 92 (2009) 2471-2488.
[13] J.W. Collins, J.M. Torkelson, A.A. Webb, Some viscosity properties of lignosulfonates isolated by ultrafiltration, Journal of Agricultural and Food Chemistry, 25 (1977) 743-746.
[14] J. Plank, B. Sachsenhauser, Experimental determination of the effective anionic charge density of polycarboxylate superplasticizers in cement pore solution, Cement and Concrete Research, 39 (2009) 1-5.
[15] T. Sowoidnich, T. Rachowski, C. Rößler, A. Völkel, H.-M. Ludwig, Calcium complexation and cluster formation as principal modes of action of polymers used as superplasticizer in cement systems, Cement and Concrete Research, 73 (2015) 42-50.
[16] F. Caruso, S. Mantellato, M. Palacios, R.J. Flatt, ICP-OES method for the characterization of cement pore solutions and their modification by polycarboxylate-based superplasticizers, Cement and Concrete Research, (In review).
[17] M. Yousuf, A. Mollah, P. Palta, T.R. Hess, R.K. Vempati, D.L. Cocke, Chemical and physical effects of sodium lignosulfonate superplasticizer on the hydration of portland cement and solidification/stabilization consequences, Cement and Concrete Research, 25 (1995) 671-682.
[18] R.G. Gilbert, M. Hess, A.D. Jenkins, R.G. Jones, P. Kratochvil, R.F.T. Stepto, Dispesity in polymer science, Pure applied chemistry, 81 (2009) 351-353.

[19] H. Vikan, Rheology and reactivity of cementitious binders with plasticizers, Department of Materials Science and Engineering, NTNU Trondheim, 2005.
[20] J. Hot, Influence des polymères de type superplastifiants et agents entraineurs d'air sur la viscosité macroscopique des matériaux cimentaires, Université Paris-Est, Paris, 2013.
[21] I. Aiad, Influence of time addition of superplasticizers on the rheological properties of fresh cement pastes, Cement and Concrete Research, 33 (2003) 1229-1234.
[22] G. Chiocchio, A.E. Paolini, Optimum time for adding superplasticizer to Portland cement pastes, Cement and Concrete Research, 15 (1985) 901-908.
[23] K.-C. Hsu, J.-J. Chiu, S.-D. Chen, Y.-C. Tseng, Effect of addition time of a superplasticizer on cement adsorption and on concrete workability, Cement and Concrete Composites, 21 (1999) 425-430.
[24] N. Mikanovic, K. Khayat, M. Pagé, C. Jolicoeur, Aqueous CaCO3 dispersions as reference systems for early-age cementitious materials, Colloids and Surfaces A: Physicochemical and Engineering Aspects, 291 (2006) 202-211.
[25] P.C. Hiemenz, R. Rajagopalan, Principles of colloid and surface chemistry, Taylor & Francis Group1997.
[26] F. Perche, Adsorption de Polycarboxylates et de Lignosulfonates sur Poudre modele et Ciments, École Polytechnique Federale de Lausanne, 2004.
[27] K.R. Ratinac, O.C. Standard, P.J. Bryant, Lignosulfonate adsorption and stabilization of lead zirconate titanate in aqueous suspension, Journal of Colloid and Interface Science, 273 (2004) 442-454.
[28] H. Uchikawa, S. Hanehara, T. Shirasaka, D. Sawaki, Effect of admixture on hydration of cement, adsorptive behaviour of admixture and fluidity and setting of fresh cement paste, Cement and Concrete Research, 22 (1992) 1115-1129.
[29] S. Mantellato, M. Palacios, R.J. Flatt, Reliable specific surface area measurements on anhydrous cements, Cement and Concrete Research, 67 (2015) 286-291.
[30] S. Mantellato, M. Palacios, R.J. Flatt, Impact of sample preparation on the specific surface area of synthetic ettringite, Cement and Concrete Research, 86 (2016) 20-28.
[31] D. Marchon, S. Mantellato, A.B. Eberhardt, R.J. Flatt, 10 - Adsorption of chemical admixtures, Science and Technology of Concrete Admixtures, Woodhead Publishing2016, pp. 219-256.
[32] R.J. Flatt, C.F. Ferraris, Acoustophoretic characterization of cement suspensions, Materials and Structures, 35 (2002) 541-549.
[33] D.R. Lide, Handbook of chemistry and physics, 72nd ed., CRC Press1991-1992.
[34] H. Bessaies-Bey, J. Hot, R. Baumann, N. Roussel, Consequeces of competitive adsorption between polymers on the rheological bahaviour of cement pastes, Cement and Concrete Research, (2014).
[35] R.J. Flatt, Interparticle forces and Superplasticizers in Cement Suspensions, École Polythechnique Fédérale de Lausanne, 1999.

Notation

apw	artificial pore water
ANL	Anlegg cement
CX	Cemex cement
IA	immediate addition of plasticizer
DA	delayed addition of plasticizer
LSs	softwood low-sugar Ca-lignosulfonate
OPC	ordinary Portland cement
w/b	water-binder ratio
LDHs	layered double hydroxides

List of tables

List of figures

Table 1 – *Main phases in cement ANL and CX from XRD-Rietveld analysis performed at École des Mines d'Alès, France.* [a]*: results obtained with TGA analysis*

Phase composition (%wt)	**ANL**	**CX**
Alite	60.5	54.3
Belite	14.2	18.8
Aluminate cubic	1.3	4.7
Aluminate ortho.	0.9	2.4
Ferrite	14.0	6.5
periclase	0.4	1.1
quartz	0.3	-
calcite	3.2/ 3.8 [a]	3.6/ 3.7 [a]
portlandite	1.1/ 1.4 [a]	2.6/ 2.5 [a]
anhydrite	-	2.1
hemihydrate	2.6	1.8
gypsum	1.0	-
arcanite		0.6
aphthitalite	0.4	0.7
thenardite	-	0.8

Table 2 – *Chemical composition of the raw materials given by the producers*

Chemical compound (%wt)	**ANL**	**CX**
Fe_2O_3	3.50	2.60
TiO_2	0.22	0.25
CaO	62.70	64.00

K_2O	0.40	1.00
P_2O_5	0.15	0.23
SiO_2	20.60	20.00
Al_2O_3	4.40	4.60
MgO	1.60	2.40
Na_2O	0.30	0.20
SO_3	3.30	3.60
LOI (%) 1000 °C	1.6	1.7
Sum	97.17	98.88

Table 3 - *Physical properties of ANL and CX cements performed at École des Mines d'Alès, France, or given by the producer (*).*

	ANL	**CX**
Surface area (BET) (m^2/kg)	890	1326
Blaine surface (m^2/kg) *	360	540
Density (g/cm^3) *	3.13	3.09
d_{10} (µm)	2.0	2.0
d_{50}	12.0	10.0
d_{90}	34.0	26.0

Table 4 - *Chemical and physical properties of the lignosulfonate plasticizer used*

Plasticizer type	**Mw**	**Org S (∝ SO_3)**	**SO_4^{2-} (mass %)**	**Ca^{2+}**	**Na**	**COOH**	**φ-OH**	**Total sugar (%)**
LSs	29000	4.6	0.9	4.6	0.9	7.1	1.4	8.3

Table 5 – *Surface area (from BET) of $CaCO_3$ and $Ca(OH)_2$*

	$CaCO_3$	**$Ca(OH)_2$**
Surface area (BET) (m^2/kg)	570	16661

Table 6 – *Tested samples to obtain adsorption isotherms*

Material	LSs addition procedure	LSs dosage tested (mass % solid)
ANL cement	IA	0.1; 0.2; 0.4; 0.6; 0.8; 1.2; 1.5
	DA	0.05; 0.1; 0.25; 0.4; 0.8; 1.2; 1.5
CX cement	IA	0.1; 0.2; 0.4; 0.6; 0.8; 1.0
	DA	0.05; 0.1; 0.2; 0.4; 0.8; 1.2; 1.5
$CaCO_3$	IA	0.05; 0.1; 0.2; 0.4; 0.8; 1.0; 1.2; 1.5
$Ca(OH)_2$	IA	1.0; 2.0; 5.0; 8.0; 12.0; 22.0

Table 7 – *Molecular footprints calculated for the different materials*

Material	Added LSs at plateau (mass % of binder)	Consumed LSs at plateau (mg/m^2)	Molecular footprint (nm^2)
ANL cement	0.8 – 1.2	0.17 – 0.18	25
CX cement	1.2 – 1.5	0.15 – 0.16	30
$CaCO_3$	0.2 – 0.4	0.06 – 0.07	45
$Ca(OH)_2$	8.0 – 12.0	1.16 – 1.19	70

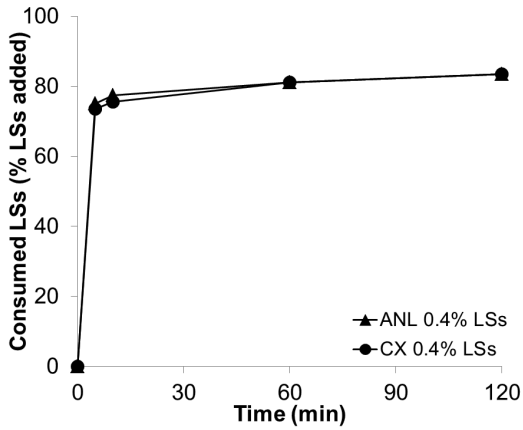

Figure 1 - *Amount of consumed LSs as % of added LSs vs. hydration time of ANL and CX cement pastes with 0.40 mass % of binder LSs*

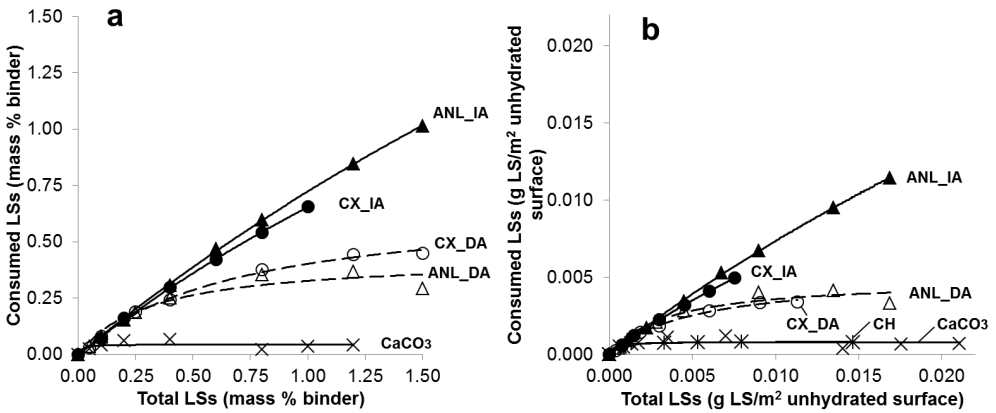

Figure 2a, b – *Amount of consumed LSs after 30 min. of hydration vs. amount of LSs added to neat ANL and CX cements (IA and DA), and to $CaCO_3$*. The results are calculated per mass % of binder in fig. 2 a and per unit of surface area available for adsorption of unhydrated particles in fig. 2 b. * In* Figure 2*a, the isotherms of CH is omitted due to the higher LSs dosage used for this sample.*

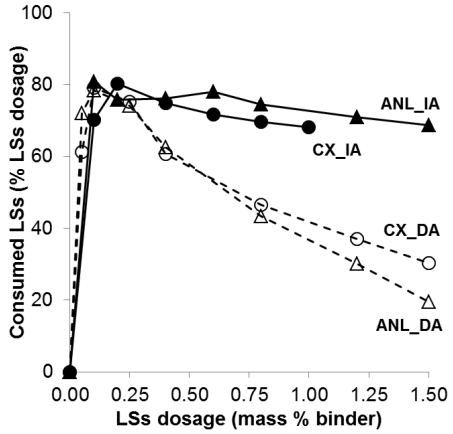

Figure 3 – *Consumed LSs (% LSs dosage) vs. LSs dosage (mass % of binder) for pastes of ANL and CX cements where LSs was added both with IA and DA*

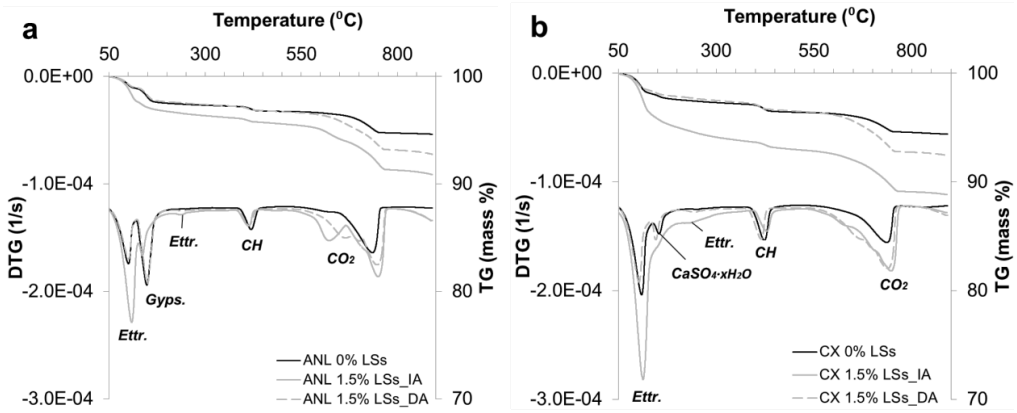

Figure 4 a, b - *Thermogravimetric curves and their derivatives for ANL (a) and CX (b) cement paste without LSs (black) and with 1.5 mass % of binder LSs (gray)(full line for IA and dotted line for DA) for which hydration was stopped after 30 minutes. The peaks corresponding to the decomposition of ettringite (ettr.), hemihydrate ($CaSO_4 \cdot 0.5H_2O$) or gypsum ($CaSO_4 \cdot 2H_2O$), portlandite (CH) and carbonates (CO_2)*

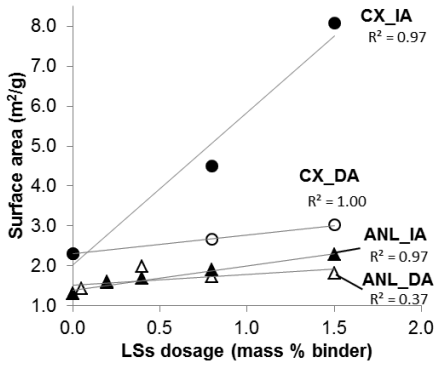

Figure 5 – *Surface area of ANL and CX cement particles hydrated for 30 min. both for IA and DA vs. the total dosage of LSs added (mass % of binder)*

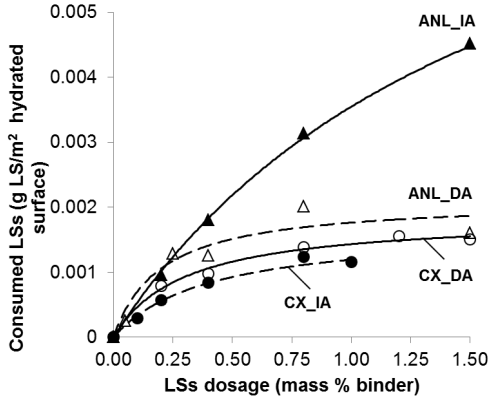

Figure 6 - A*mount of consumed LSs at 30 min. hydration (calculated as unit of surface area of hydrated substrate) vs. amount of LSs added to neat ANL and CX cement (IA and DA) (calculated as mass % of binder). For CX cement, the data points for 0.2; 0.4; 1.2 mass % of binder LSs (IA/DA) were calculated with interpolation and were not experimentally measured*

Paper II

On the effect of calcium lignosulfonate on the rheology and setting time of cement paste

Submitted to Cement and Concrete Research (December 2016)

Colombo, A.; Geiker, M.R.; Justnes, H.; Lauten, R.A.; De Weerdt, K.

ON THE EFFECT OF CALCIUM LIGNOSULFONATE ON THE RHEOLOGY AND SETTING TIME OF CEMENT PASTE

A. Colombo (1), M. R. Geiker (1), H. Justnes (2,3), R. A. Lauten (4), K. De Weerdt (1)

(1) Department of Structural Engineering, Norwegian University of Science and Technology, Trondheim, Norway

(2) SINTEF Building and Infrastructure, Trondheim, Norway

(3) Department of Materials Science and Engineering, Norwegian University of Science and Technology, Trondheim, Norway

(4) Borregaard, Sarpsborg, Norway

ABSTRACT

The effect of softwood calcium lignosulfonate, LSs, on the rheology and setting time of cement paste has been investigated. Two Portland cements with different surface area and C_3A content were used. The lignosulfonate was added either immediately with the mixing water or delayed after 10 minutes of hydration. The cement pastes were characterized in terms of specific surface, rheology and heat of hydration. Extracted pore solutions were analysed for free lignosulfonate concentration and for changes in elemental composition. Immediate addition of LSs increased the specific surface, but not delayed addition. Correlations were found between rheology and surface coverage by LSs, as determined by adsorption isotherms, and between the setting time and the amount of free LSs in the pore solution. An increased setting retardation upon delayed addition related to an increased concentration of Al in the pore solution.

KEYWORDS

Lignosulfonate; admixture; rheology; setting retardation; adsorption

INTRODUCTION

Water-reducers, or plasticizers, are commonly used admixtures for concrete. Their addition to fresh concrete allows obtaining highly fluid concrete at low water-binder ratios, improving the mechanical properties and the durability of the hardened concrete. The plasticizer used in this paper is a low-sugar softwood calcium lignosulfonate (LSs), commonly used in concrete in dosages 0.25-0.40 mass % of binder. Lignosulfonates are polyelectrolytes derived from lignins in the pulping industry. Lignin can be derived from various sources of biomass, and lignosulfonates of different molecular weight and amount of functional groups (carboxyl groups, phenolic-OH, sulfonic groups) can be produced.

The dispersing effectiveness of plasticizers on cementitious materials is, amongst others, a function of the degree of adsorption on the surface of the cement grains and hydrates. The adsorbed plasticizer layer renders the particle surface negatively charged, i.e. with a negative zeta potential. As negatively charged particles approach each other, electrostatic repulsion

prevents them from forming agglomerates. Additionally, in the case of synthetic polycarboxylic ethers, or simply branched molecules as in the case of lignosulphonate, side chains stretching out from the polymer backbone hinder particles to get close enough to form agglomerates (steric hindrance) [1].

In addition to dispersion, the interaction between cement and plasticizer can potentially lead to retardation of the setting time of the cement paste. Several mechanisms of retardation are hypothesized in the literature, the main ones being: calcium complexation, nucleation poisoning of hydrates, surface adsorption on anhydrates, and semipermeable layer [2-5]. Calcium complexation involves the interaction between plasticizing polymers and calcium ions in the pore solution. This would slow down the build-up of calcium supersaturation needed for hydrates nucleation. However, according to Bishop et al. [2], and Marchon and Flatt [4], amongst others, the low dosages of plasticizers generally used limit the amount of calcium potentially complexed. Thus, calcium complexation does not appear likely as a main mechanism of setting retardation of cement. As stated by Thomas and Birchall [6] amongst others, retardation by nucleation poisoning of hydrates is where the plasticizer poisons the nuclei of CH and C-S-H and prevents their growth by adsorbing onto nuclei or particles. Moreover, plasticizers could increase cement solubility, thus allowing ions to coexist in solution at much higher concentrations without causing precipitation, thus prolonging the cement induction period [6]. In a related manner, the direct adsorption of plasticizers on the surface of both anhydrous and hydrated phases could hinder further reactions with water [2]. Plasticizer adsorbed at the surface of partially hydrated cement grains could also form a semipermeable layer slowing down the migration of water and lengthening the induction period. Eventually, water penetrating by osmosis to the unhydrated cement surface could create a high pressure inside the coating, making it burst and allow hydration to continue [2]. Juilland et al. [7], amongst others, considered the latter theory to be unlikely, since no experimental evidence has been found to support it. In conclusion, the mechanisms that most likely retard the cement setting appear to be related to the plasticizers poisoning the nuclei of CH and C-S-H, modifying hydrates growth, or adsorbing on the surface of hydrated and unhydrated cement particles, thus hindering further contact with water.

As other plasticizers, lignosulfonate is known to have a retarding effect on cement hydration [8-10]. The sugars naturally contained in lignin contribute to longer setting times of cement, in particular the hexoses, which, however, can be removed by fermentation in low-sugar lignosulfonates. Several studies concluded that the addition of calcium lignosulfonate changes the hydration of C_3S and C_3A [10-15]. According to Ramachandran [14], a strongly surface-bound calcium lignosulfonate complex could be detected for both C_3A and C_3S, which could cause retardation of C_3A and C_3S hydration. In another paper [11], Ramachandran stated that the retardation effect of calcium lignosulfonate depends on its concentration in solution and not on its proportion with respect to C_3S. C_3S hydration was delayed in proportion to the concentration, and it practically stopped for concentrations above 3 g/l of water. On the contrary, C_3S hydration was found to speed up for lignosulfonate concentrations under 1 g/l of water. Monosi et al. [12] found that, in a C_3A-C_3S system, the addition of calcium lignosulfonate led to a strong retardation in C_3S hydration, while C_3A hydration was slightly accelerated. The retardation in the C_3A-C_3S system was lower than that in pure C_3S systems.

In fact, the lignosulfonate adsorption by C_3A decreases the concentration of polymer available to retard the C_3S hydration. Moreover, the arrest in C_3S hydration is partially counterbalanced by the increase in rate of hydration of C_3A, as stated by Collepardi et al. [13]. In conclusion, lignosulfonate was found to retard C_3S hydration [10, 14] depending on its concentration in the pore solution [11]. C_3A hydration was found to be retarded by lignosulfonate by some authors [10, 14, 15], while not retarded [16] or slightly accelerated [12, 13] by other authors.

As described by e.g. Flatt and Houst [17], the addition time of the plasticizer to the cement paste greatly affects the amount of plasticizer consumed by the cement paste and the extent of retardation. Several studies, amongst others Uchikawa et al. [18], Chiocchio and Paolini [19], Aiad et al. [20], found that, at equal plasticizer dosage, the flow of cement paste prepared by delayed addition is higher than that of cement paste prepared by immediate addition. Moreover, the setting is further retarded in case of DA. Chiocchio and Paolini [19] found that the optimum addition time of plasticizer to achieve the maximum workability corresponds to the beginning of the dormant period of the cement hydration without admixture. Hot [21], Hsu et al. [22], and Aiad [23] found that the optimum addition time was between 10 and 15 minutes after water addition.

The rheological behavior of fresh cementitious materials is generally characterized by yield stress (τ) and viscosity (μ). As described by e.g. Roussel et al. [24], the yield stress corresponds to the energy needed to break down a network of interaction between particles in a cementitious system. Its origin lays in colloidal and contact interactions between particles. Viscosity results from hydrodynamic, colloidal and contact forces involved in the motion of the suspended cement grains. The yield stress is often considered as the most relevant parameter to describe workability and the ability of a material to properly fill a mold under its own weight. However, the viscosity also seems to be a very relevant parameter to describe cement or concrete workability, especially for systems with low water-binder ratio [25, 26]. Plasticizing admixtures can change both yield stress and viscosity by adsorbing on cement particles and changing the flocculation state of cement paste [26].

The subject of this paper is to investigate the effect of LSs on the rheological properties and setting time of two Portland cements with different physical and chemical properties (e.g. surface area, C_3A content). The samples were studied both by adding the lignosulfonate immediately with the mixing water (IA) and by adding it after 10 minutes hydration (DA). The results were compared to the adsorption isotherms presented in a previous paper by the same authors [27]. The amount of polymer consumed by the cement paste was related to the changes in rheological properties and hydration kinetics of the cement pastes due to LSs addition. Changes in the surface area of the hydrated cement particles were investigated by BET. The elemental composition of the pore solution extracted from the cement paste samples was analysed with ICP-MS. The results of this paper will contribute to a deeper understanding on the physical and chemical mechanisms behind the changes in rheological properties and setting time of cement paste with lignosulfonate.

1. EXPERIMENTAL

2.1 Materials

The experiments were performed on two different cements: a CEM I 52.5 N (ANL) and a CEM I 52.5 R (CX), as defined in the European standard EN197-1. The content of the main clinker phases of the cements quantified by XRD Rietveld, according to the technique described in [28], are given in Table 1. The chemical composition of the cements determined by XRF and the loss of ignition at 950 ºC are reported in Table 2. The particle size distribution (d_{10}, d_{50}, d_{90}), Blaine and BET surface area, and density are given in Table 3.

A sugar-reduced softwood calcium lignosulfonate (LSs) was used as plasticizer. Its mass weighted molecular weight (M_w), as measured with gel permeation chromatography (GPC), was 29000 g/mol and the number weighted molecular weight (M_n) was 2100 g/mol, giving broad molar-mass dispersity ($Đ_M$) equal to 13.8. The molar-mass dispersity, also called polydispersity index, is defined as the ratio between M_w and M_n [29]. Additional physical and chemical properties of the lignosulfonate are listed in Table 4. For the lignosulfonate used in the present investigation, the sugars were removed from the polymer molecule by fermentation and resulting alcohol by distillation. The LSs was dissolved in deionised water to concentrations varying from 1 to 45 % to ease dosing, and the water content was included in the calculation of the water-to-binder ratio (w/b).

2.2 Sample preparation

About 300 g cement was mixed with deionised water and/or lignosulfonate solution in a high-shear MR530 by Braun mixer at intensity 6 obtaining a paste with w/b = 0.4. A cement paste volume of about 200 ml was mixed for all the cement pastes. In order to investigate the effect of the time of addition of lignosulfonate, two different mixing procedures were applied: immediate addition of LSs with the mixing water (IA) and delayed addition of LSs after 10 minutes of hydration (DA).

For IA, the binder was mixed with deionised water (and/or lignosulfonate diluted in deionised water) according to the procedure used by Vikan [30]: 30 seconds mixing, scraping the mixer walls to homogenize the mix, 5 minutes resting and 1 minute mixing.

For DA, the binder and 85% of the water were mixed according to the following mixing procedure: 30 seconds mixing, scraping the mixer walls to homogenize the mix, 10 minutes resting (delay time chosen according to several studies in literature [19, 21-23]). LSs diluted in the remaining 15% of the needed water were then added to the mix, which was mixed for 1 minute.

2.3 Methods

2.3.1 Rheological measurements

The rheological properties were measured with a Physica MCR 300 rheometer using parallel plates with serrated surfaces of 150 µm depth. The radius of the plates was 30 mm and the gap between the plates was set to 1 mm. The bottom plate or stator was kept at a constant temperature of 20 ºC. Some drops of deionized water were put in the water trap located on the

upper plate or rotor and an enclosure was used to limit evaporation of water from the paste sample during the measurement.

After the mixing sequence (as described in paragraph 2.2), about 2.5 ml of cement paste was placed on the bottom plate of the rheometer, and the rheological measurement was started 10 minutes after water addition. Up-down flow curves were measured at 10, 20 and 30 minutes of hydration. For the samples to which the plasticizer was added at 10 minutes hydration (DA), the first flow curve was measured at 12 minutes of hydration instead of 10 minutes. Before every measuring cycle, the paste was stirred for 30 seconds at the constant shear rate of 60 s^{-1}. The measuring sequence, described in Table 5, allowed measuring the shear stress of cement paste as the shear rate increased from 0 to 60 s^{-1} (up flow curve) or decreased from 60 to 0 s^{-1} (down flow curve).

The flow curves generally showed a pronounced shear-thinning behavior. The Bingham model was applied to the second part of the down flow curve, obtained for shear rate between 26 and 60 s^{-1}. The linear fitting of this flow-curve segment allowed the calculation of the static yield stress, τ_0, as the extrapolated intercept with the ordinate, and of the plastic viscosity, μ_p, as the slope of the linear fit.

2.3.1 Isothermal calorimetry

Isothermal calorimetry was carried out at 20˚C in a TAM Air eight-channel isothermal calorimeter produced by Thermometric AB. The evolution in time of the heat of hydration of ANL and CX cements was measured for different dosages of LSs and both for IA and DA of plasticizer. The samples were prepared as described in paragraph 2.2. After mixing, about 6 g cement paste was placed in a 20 ml glass ampoule, which was sealed and placed in the calorimeter. The heat of hydration was recorded for 60 hours.

2.3.2 UV-spectroscopy

UV-spectroscopy allowed measuring the LSs concentration in the extracted pore solution from the cement paste samples.

After mixing according to section 2.2, about 35 ml paste was poured in 50 ml plastic centrifuge tubes and let to rest until the chosen analysis time. The pore solution was extracted from the cement paste by centrifuging the samples in a Heraeus Megafuge 8 centrifuge by Thermo Scientific for 3 minutes at the speed of 4500 rpm. The supernatant pore solution was extracted and filtered with 0.45 µm syringe filters. The pore solution was analysed with a Genesys 10S UV-spectrophotometer by Thermo Scientific. Wavelengths in the range 280-284 nm had been reported in literature to study the adsorption of lignosulfonate on cement particles [18, 30-33]. After scanning at several wavelengths, 281 nm was chosen as the most suitable wavelength to analyse the samples in this study.

Initially, the free plasticizer in the pore solution extracted from the cement paste was measured by UV-spectroscopy at increasing hydration time (from 5 to 120 minutes hydration). It was found that at 10 minutes hydration the LSs uptake reached an equilibrium value. All the samples were then analysed at 30 minutes hydration.

With the help of a calibration curve, obtained measuring the absorbance of solutions of different concentrations of LSs in deionised water, the amount of free plasticizer (g LS/100 g solution) could be determined. This amount was related to the amount of binder in the sample (g LS/100 g binder). The LSs consumed by the investigated systems was then calculated by subtracting the amount of free LSs from the total amount of LSs added to the sample, as displayed in equation 1:

$$LSs_{consumed} = LSs_{total} - LSs_{free} \quad (1)$$

Polymer adsorption by a solid is usually described using isotherms, in which the amount of polymer adsorbed is plotted against the total amount of polymer added to the system [34]. The shape of an isotherm is largely determined by the adsorption mechanism. In this study, the isotherms were drawn relating the amount of LSs consumed by the cement paste to the amount of total LSs added to the sample.

2.3.3 Solvent exchange

A solvent exchange procedure with isopropanol was used to stop the hydration of the cement paste after 30 minutes of hydration.

About 5 ml of cement paste was transferred in a 50 ml centrifuge tube and centrifuged for 1 minute at 2000 rpm. The supernatant was removed. About 40 ml of isopropanol was poured in the centrifuge tube. The tube was shaken for 30 seconds and let to rest for 5 minutes. The sample was centrifuged again for 1 minute at 2000 rpm and the supernatant liquid was removed. The solvent exchange procedure with isopropanol was repeated once, followed by a final solvent exchange with 10 ml of petroleum ether. The resulting paste was let to dry for 2 days in a desiccator over silica gel, and soda lime to minimize carbonation. After drying, the samples were ground to powder and homogenized in a porcelain mortar and stored in sealed containers in a desiccator over silica gel and soda lime until analysis.

2.3.4 BET of hydrated cement pastes

The BET measurements were performed using a Tristar II Plus by Micromeritics on cement paste samples of which the hydration was stopped with the solvent exchange procedure. The measurements were performed purging the samples with nitrogen. The samples were degassed in vacuum before the measurement, and the measurement was performed at 20 ºC.

2.3.5 ICP-MS of pore solution

ICP–MS (inductively-coupled plasma mass spectrometry) was used to determine the elemental concentration of Al, Ca, Fe, K, Na, S and Si in the pore solution extracted from the cement paste. The pore solution was extracted from ANL and CX cement pastes with 0, 0.8, 1.5 mass % LSs mixed both with IA and DA. The solution was filtered with the same procedure used for UV-spectroscopy (paragraph 2.3.2) and acidified prior to analysis by adding 1:1 by volume of 1:10 diluted HNO_3.

3 RESULTS

3.3 Rheological properties

The rheology of ANL and CX cement pastes was measured at 10 (12), 20 and 30 minutes of hydration with increasing dosages of LSs (0/0.4/0.8/1.5 mass % binder LSs for IA and 0/0.1/0.2/0.4 mass % binder for DA). The results at 10 (12 for DA) and 30 minutes hydration are shown in Figure 1 and in Figure 2, respectively, displaying the variation of normalized yield stress and plastic viscosity as the dosage of LSs increases, both for IA and DA. The normalized yield stress was obtained by dividing the yield stress of samples with increasing LSs dosage by the yield stress of the reference sample (without LSs). The normalized viscosity was calculated according to the same principle.

Increasing LSs dosage reduced both the yield stress and the viscosity of both cements both at 10 and 30 minutes of hydration, except for CX cement for IA after 30 minutes of hydration. The reduction was achieved for considerably lower LSs dosages for DA compared to IA. Less than one third LSs dosage was needed to reach the same drop in yield stress and viscosity for DA compared to IA. Regarding CX cement, a nearly constant yield stress and a remarkable increase in viscosity were measured for IA after 30 minutes of hydration with increasing LSs dosages.

Generally, a drop in yield stress would indicate LSs saturation in the cementitious system. In this study, a clear drop in yield stress was detected for DA for a LSs dosage between 0.10 and 0.25 mass % for ANL cement, and between 0.25 and 0.50 mass % for CX cement. No clear drop in yield stress was measured for IA. After 10 minutes of hydration, the yield stress decreased gradually for both cements. After 30 minutes of hydration, the yield stress showed a gradual decrease for ANL cement, while it remained nearly constant for CX cement.

The results from the rheological measurements are also presented in terms of flow resistance, as defined by Vikan et al. in [35]. This value is calculated as the area under the entire flow curve (shear rate from 1 to 60 s^{-1}), and it represents the power necessary to make a certain volume of sample flow at a chosen shear rate range (W/m^3 or kPa/s). The smaller the area under the flow curve is, the less power is required to make the sample flow. The results are shown in Figure 3. The results presented in Figure 3 seem to agree with the ones presented in Figure 1 and in Figure 2, considering that slightly different regions of the flow curves were used to calculate the parameters.

Surprisingly, the yield stress of CX cement with 0.25 mass % LSs mixed with DA was higher than in the sample without LSs. However, with the same LSs dosage, the viscosity was found to decrease, and all the other conditions in the cement paste system were similar. Additionally, the flow resistance obtained for the same data point did not show the same increase as the yield stress did. Therefore, the authors assume that the higher yield stress for this data point was most likely due to an error of measurement or to an artifact of the fitting method.

3.4 Setting time

The effect of the LSs dosage and of its addition time on the rate of hydration and setting time of ANL and CX cement pastes can be observed in the calorimetric curves in Figure 4 for IA, and in Figure 5 for DA. Based on the definition given by the ASTM standard C1679-14 [36], the setting time was identified as the time to reach half of the average maximum power of the main hydration peak in the calorimetric curve. The silicates and aluminates peaks are marked with different symbols in corresponding grey shade of the respective calorimetric curve.

In the reference samples without LSs, after the initial peak of hydration, which takes place almost immediately after the contact of cement with water, two peaks could be observed: first, the peak corresponding to hydration reaction of the silicate phases (mainly C_3S), followed by a peak related to sulfate depletion and hydration reactions of the aluminate phases. Both the silicates and the aluminates peak were delayed by LSs addition in both cement pastes both when mixed with IA and with DA. In general, increasing LSs dosages caused a larger retardation of the silicates peak compared to the aluminates one. The two peaks even merged in most samples with the higher LSs dosages analyzed.

Moreover, for the same LSs dosage, DA resulted in a larger retardation of both peaks compared to IA. CX cement paste showed a lower retardation than ANL cement paste both for IA and DA. The doubling of the LSs dosage led to a setting retardation between 1.5 and 2.5 times higher for CX cement, and between 4 and 5 times higher for ANL cement.

3.5 Concentration of aluminum ions in the pore solution

The elemental concentration of Al, Ca, Fe, Si and S in the pore solution extracted from ANL and CX cement pastes after 30 minutes of hydration was determined with ICP-MS. The LSs dosages tested were 0.8 and 1.5 mass % LSs both for IA and DA. Additionally, a reference sample without LSs was measured. Moreover, the content in Al, Ca, Fe, Si and S was also measured for two LSs solutions in artificial pore solution. The two solutions, containing 2.0 and 3.7 mass % LSs, were the ones used in the cement samples with 0.8 and 1.5 mass % LSs, respectively. The artificial pore solution was a solution of NaOH and KOH with K/Na molar ratio equal to 2 and measured pH of 12.9. The results from ICP-MS are shown in Figure 6 and reported in Table 7.

The samples mixed with DA showed an increase in Al, Fe and Si concentration in the pore solution as the LSs dosage increased. The increase was considerably larger for ANL cement than for CX cement. On the contrary, only a minor increase was measured for the samples mixed with IA.

3.6 Adsorption isotherms

The adsorption isotherms obtained for ANL and CX cement pastes were achieved by plotting the amount of consumed LSs after 30 minutes of hydration versus the total amount of LSs added. The tested dosages are given in Table 6. For CX cement it was not possible to extract pore solution at LSs dosages over 1.0 mass % due to paste hardening after 30 minutes hydration. The LSs was added to the cement paste either immediately together with the mixing water (IA), or after 10 minutes hydration (DA). The results per mass % binder and their fitting according to the Langmuir model [34] are presented in Figure 7.

Figure 7 shows that the cement pastes displayed similar LSs consumption at low LSs dosage (up to about 0.25 mass % LSs) independent of the time of LSs addition. At higher dosage, the curves obtained for IA differ from those obtained for DA.

For IA, no adsorption plateau could be detected within the tested range, neither for ANL nor for CX cement. The isotherms' shape indicated an increasing LSs consumption as more LSs was added to the mix.

For DA, an adsorption plateau was found for both cements. The DA isotherms displayed a considerably lower amount of LSs consumed by the cement pastes compared to the IA isotherms. The adsorption plateau was reached for a total LSs amount between 0.8 and 1.2 mass % for ANL cement, and between 1.2 and 1.5 mass % for CX cement. The authors assume the plateau to be due to the achievement of full monolayer surface coverage [27].

3.7 BET of hydrated cement pastes

The BET surface area was measured on ANL and CX cement pastes with varying LSs amounts after 30 minutes of hydration. The hydration was stopped by solvent exchange, as described in paragraph 2.3.3. The results are shown in Figure 8.

For both cements the surface area was found to increase as the dosage of plasticizer added to the cement paste increased. The increase in surface area was remarkably larger for IA compared to DA, and, for IA, for CX cement compared to ANL cement.

4 DISCUSSION

4.1 LSs consumption and changes in surface area

The adsorption isotherms shown in Figure 7 display a higher LSs consumption for IA than for DA.

In a previous article [27], the authors investigated the interactions between LSs and two Portland cements (the same as those used in the present paper). It was found that the LSs consumption mechanisms were different for the two cements used and for the two addition methods.

For DA, both cements' adsorption isotherms showed a plateau. According to the theory reported in [34], the achievement of a plateau in an adsorption isotherm corresponds to saturation of the available surface for adsorption. Therefore, the LSs consumption was considered to be mainly due to monolayer surface adsorption on the surface of cement particles and hydrates.

For IA, an increase in LSs dosage was found to cause additional ettringite formation and an increase in surface area of both cements after 30 minutes of hydration, to a larger extent for CX cement compared to ANL cement. On the contrary, this was not observed when the cements were mixed with DA [27].

The two cements displayed different LSs consumption mechanisms for IA. For CX cement, a large increase in ettringite formation and surface area (see Figure 8) led to a high LSs

consumption [27]. No surface saturation plateau was reached, which was explained by the continuous increase in surface available for adsorption for the LSs dosages investigated. Monolayer surface adsorption on the surface of cement particles and hydrates was identified as the dominating LSs consumption mechanism for CX cement [27]. For ANL cement, the adsorption isotherm also showed a high LSs consumption without reaching an adsorption plateau. Since the amount of formed ettringite and the surface area increased only moderately compared to CX cement (see Figure 8), other polymer consumption mechanisms might have played a role for ANL cement in addition to surface adsorption.

Finally, in the same paper [27], no AFm could be detected by TGA for the investigated materials. Therefore, intercalation in AFm, as proposed, amongst others, by Flatt and Houst [17], does not appear as a feasible LSs consumption mechanism for the investigated materials and dosages.

4.2 Rheological properties

The obtained rheological results indicate that the addition of lignosulfonate generally improved the workability of cement paste after 10, 20 and 30 minutes of hydration, decreasing both the yield stress and the viscosity. As an exception to this general trend, after 30 minutes of hydration, CX cement mixed with IA did not show changes in the yield stress with increasing LSs dosage, while its viscosity increased about 50 %. In general, the improvement in workability was remarkably larger when the samples were mixed with DA compared to IA.

When evaluating the rheological results in light of the adsorption isotherms shown in Figure 7, it appears that a clear drop in yield stress was observed solely for the samples which reached an adsorption plateau. The samples that did not reach an adsorption plateau showed a more gradual decrease in yield stress, as for ANL cement, or no decrease at all, as for CX cement. A correlation between the achievement of surface coverage and a drop in yield stress seems to exist. Indeed, as shown in Figure 7, the isotherms obtained for DA started differing from those obtained for IA, and showing the tendency to reach an adsorption plateau, for LSs dosages over about 0.25 mass %. As shown in Figure 1 and in Figure 2, for DA, a drop in yield stress was measured for LSs dosages between 0.10 and 0.25 mass % LSs for ANL cement, and between 0.25 and 0.40 mass % LSs for CX cement. Thus, the rheological behavior seems to relate to the degree of LSs coverage of the available surface.

As shown in [27], the TGA measurements performed on ANL and CX cements displayed that 1.5 mass % LSs added with IA led to an increase in the amount of bound water after 30 minutes of hydration, compared to the respective samples without LSs. This was explained by an increased amount of ettringite, which also is reflected in a higher surface area, as measured with BET (see Figure 8). For CX cement, the unexpected lack of any decrease in yield stress and the increase in viscosity at 30 minutes of hydration, as displayed in Figure 2 b, are therefore most likely due to the high amount of ettringite formed. A production of large amounts of ettringite was found to cause slump loss by, amongst others, Hanehara and Yamada [37]. The increase in amount of ettringite was larger for CX than for ANL cement.

Accordingly, CX cement displayed a larger reduction in workability compared to ANL cement.

Moreover, the initial yield stress (without LSs) was remarkably higher for CX than for ANL cement paste. This is most likely due both to the higher content of C_3A in CX cement and to the smaller particle size of the CX cement, leading to higher surface area available to interact with water and plasticizer, and thus higher reactivity.

4.3 Setting time

The setting retardation was calculated as the setting time measured with calorimetry, from which the setting time of the sample without LSs was subtracted. In Figure 9 a and b the setting retardation is related to the amount of total and free LSs, respectively.

For DA, total LSs dosages higher than about 0.25 mass % led to a major setting retardation (see Figure 9a). For IA, a more gradual increase in setting time was measured as the LSs added increased. Both for IA and for DA, the setting retardation was higher for ANL than for CX cement.

The results shown in Figure 9b indicate correlations between the setting retardation and the amount of free LSs in the pore solution. For LSs dosages over about 0.25 mass %, any increase in free LSs corresponded to a large increase in setting retardation, especially for samples mixed with DA. Over this dosage, the samples mixed with DA also displayed a drop in yield stress, as discussed in paragraph 4.2 and showed in Figure 1 and in Figure 2. These results seem to agree with the conclusions of Yamada et al. [38], who stated a progressive increase in setting time with a higher concentration of free sulfonic and carboxylic groups in the aqueous phase.

At equal amount of free LSs in the pore solution, a higher setting retardation was measured for ANL cement than for CX cement. The setting retardation was higher for DA than for IA. This might be due to several reasons:

First, in a previous paper [27], increasing LSs dosages added with IA were found to increase the amount of ettringite formed in cement paste. The increase as measured with TGA was larger for CX cement compared to ANL cement, and for IA compared to DA. An increased initial ettringite formation due to LSs addition with IA was also reported by Danner et al. [39]. In another paper, Danner et al. [40] found that Ca-LSs added with IA to a C_3A-gypsum system led to changes in the ettringite morphology, which appeared as wider, shorter and more rounded crystals. According to Zingg et al. [41], the smaller cubic ettringite crystals can be finely dispersed by the plasticizer, providing additional nucleation surface. In the present paper, the possible formation of a larger amount of smaller and more compact ettringite crystals could lead to the lower setting retardation measured for CX cement compared to ANL cement, and for IA compared to DA because of the additional nucleation surface.

As shown in Figure 4 and Figure 5, increasing LSs dosages led to larger retardation of the silicate peak compared to the aluminate one, causing the two peaks to merge in most samples with the higher LSs dosages analyzed. Similar observations were made in several studies [42-

45], in which it was even observed that the aluminate peak could occur earlier than the silicate one upon high plasticizer dosages. This might lead to poison of C_3S hydration and uncontrolled delay of setting. This is a commonly known phenomenon leading to incompatibility issues between plasticizer and cement. In light of the results reported in the present article, the smaller retardation of the C_3A peak compared to the C_3S one, or even the occurrence of the aluminate peak before the silicate one, might be partially explained by the enhanced precipitation of ettringite within the first 30 minutes of hydration, which could lead to a faster consumption of sulfates, thus to an earlier sulfate depletion point.

Regarding the difference in setting retardation between the two cements, Pourchet et al. [46] found that the sulfate type used modified the early C_3A-$CaSO_4$ hydrates and their rate of formation. The substitution of gypsum with hemihydrate increased the rate of ettringite formation during the first five hours of hydration. The difference in sulfate type between ANL and CX cements (gypsum and hemihydrate for ANL cement, hemihydrate and anhydrite for CX cement) could then be one of the reasons why more ettringite was formed in CX cement than in ANL cement. Moreover, the higher content in C_3A of CX cement and its smaller particle size could allow a higher amount of C_3A to enter in contact with water, favouring the production of ettringite compared to ANL cement.

Finally, aluminum ions dissolved in the pore solution appeared to negatively impact the C_3S hydration, both by increasing its induction period [47, 48], and by reducing the extent of its hydration [49]. The results from ICP-MS, displayed in Figure 6, showed that an increased concentration of Al was measured in the pore solution of both cements solely when mixed with DA. The Al concentration was higher for ANL than for CX cement. One of the hypothesized explanations for the retarding effect of Al on C_3S reaction is the substitution of some silicates by the Al ions with consequent formation of C-A-S-H instead of C-S-H. Since the first C-A-S-H nuclei do not grow nor support hydrates nucleation as C-S-H does, the C_3S induction period is extended [50]. Another possible explanation was given by Nicoleau et al. [51], who found that Al ions covalently bind to the silicates on the C_3S surface, strongly inhibiting C_3S dissolution. The poisoning of C_3S by Al ions, with consequent delay in C_3S hydration, appears then to be a feasible explanation for the increased setting retardation measured for DA compared to IA.

5 CONCLUSIONS

The aim of this paper was to obtain a better understanding of the effects of calcium lignosulfonate (LSs) on the rheology and setting time of Portland cement pastes. Two Portland cements mainly differing in surface area and C_3A content were used. The LSs was either added immediately with the mixing water (IA), or delayed after 10 minutes of hydration (DA). The following conclusions were drawn:

- The rheological behavior relates to the degree of LSs coverage of the available surface for adsorption. A drop in yield stress and viscosity was measured for the cement pastes that reached an adsorption plateau, as observed for DA. Samples which did not reach

surface saturation showed a more gradual improvement in workability, as observed for IA.

- An increased formation of ettringite, which was observed with elevated LSs dosages for IA, might lead to early hardening of the cement paste.
- The setting behavior appears to relate to the amount of free LSs in the pore solution.
- The difference in setting retardation between IA and DA might be related to the amount of ettringite formed in the system. Indeed:
    - The ettringite might supply additional surface area, which increase the amount of LSs consumed by monolayer adsorption. The consequent reduced amount of free LSs in the pore solution was reflected in a lower setting retardation.
    - Enhanced ettringite formation might supply additional nucleation surface, thus reducing the setting retardation when compared to a reference sample without LSs.
    - Increased ettringite precipitation could lead to a faster consumption of sulfates, thus to an earlier sulfate depletion.
    - Increased ettringite formation resulted in less Al dissolved in the pore solution and available to interact and retard the C_3S hydration.

6 FUTURE RESEARCH

In a follow-up study, the effect of LSs on the amount and morphology of ettringite and other early cement hydrates produced both for IA and DA will be investigated. The effect of LSs on the hydrates formed in the hardened cement paste will also be considered for future research.

7 ACKNOWLEDGEMENTS

The authors wish to acknowledge the Norwegian Research Council (NFR 225358/O30) and Borregaard AS, Norway, for financing this research work. Gwenn Le Saoût and Nathalie Azéma, Ecole des Mines d'Alès, France, are also acknowledged for the helpful discussions. Irene Bragstad, SINTEF, Norway, is acknowledged for performing the BET measurements. Syverin Lierhagen, NTNU, Norway, is acknowledged for performing the ICP-MS analysis.

8 REFERENCES

[1] C. Jolicoeur, M.-A. Simard, Chemical admixture-cement interactions: Phenomenology and physico-chemical concepts, Cement and Concrete Composites 20(2–3) (1998) 87-101.
[2] M. Bishop, S.G. Bott, A.R. Barron, A New Mechanism for Cement Hydration Inhibition: Solid-State Chemistry of Calcium Nitrilotris(methylene)triphosphonate, Chemistry of Materials 15(16) (2003) 3074-3088.
[3] J. Cheung, A. Jeknavorian, L. Roberts, D. Silva, Impact of admixtures on the hydration kinetics of Portland cement, Cement and Concrete Research 41(12) (2011) 1289-1309.
[4] D. Marchon, R.J. Flatt, 12 - Impact of chemical admixtures on cement hydration, Science and Technology of Concrete Admixtures, Woodhead Publishing2016, pp. 279-304.

[5] D. Jansen, J. Neubauer, F. Goetz-Neunhoeffer, R. Haerzschel, W.D. Hergeth, Change in reaction kinetics of a Portland cement caused by a superplasticizer — Calculation of heat flow curves from XRD data, Cement and Concrete Research 42(2) (2012) 327-332.
[6] N.L. Thomas, J.D. Birchall, The retarding action of sugars on cement hydration, Cement and Concrete Research 13(6) (1983) 830-842.
[7] P. Juilland, E. Gallucci, R. Flatt, K. Scrivener, Dissolution theory applied to the induction period in alite hydration, Cement and Concrete Research 40(6) (2010) 831-844.
[8] M. Collepardi, The influence of admixtures on concrete rheological properties, Il cemento1982.
[9] V.S. Ramachandran, R.F. Feldman, Adsorption of calcium lignosulfonate on tricalcium aluminate and its hydrates in a non-aqueous medium, Cement technology1971, pp. 121-129.
[10] V. Lorprayoon, D.R. Rossington, Early hydration of cement constituents with organic admixtures, Cement and Concrete Research 11(2) (1981) 267-277.
[11] V.S. Ramachandran, Interaction of calcium lignosulfonate with tricalcium silicate, hydrated tricalcium silicate, and calcium hydroxide, Cement and Concrete Research 2(2) (1972) 179-194.
[12] S. Monosi, G. Moriconi, M. Collepardi, Combined effect of lignosulfonate and carbonate on pure portland clinker compounds hydration. III. Hydration of tricalcium silicate alone and in the presence of tricalcium aluminate, Cement and Concrete Research 12(4) (1982) 425-435.
[13] M. Collepardi, A. Marcialis, V. Solinas, The influence of calcium lignosulfonate on the hydration of cements, Il cemento1973.
[14] V.S. Ramachandran, Interaction of admixtures in the cement-water system, Application of admixtures in concrete, CRC Press1994.
[15] J.F. Young, Hydration of tricalcium aluminate with lignosulphonate additives, Magazine of Concrete Research 14(42) (1962) 137-142.
[16] S. Monosi, G. Moriconi, M. Pauri, M. Collepardi, Influence of lignosulphonate, glucose and gluconate on the C3A hydration, Cement and Concrete Research 13(4) (1983) 568-574.
[17] R.J. Flatt, Y.F. Houst, A simplified view on chemical effects perturbing the action of superplasticizers, Cement and Concrete Research 31 (2001) 1169-1176.
[18] H. Uchikawa, S. Hanehara, T. Shirasaka, D. Sawaki, Effect of admixture on hydration of cement, adsorptive behaviour of admixture and fluidity and setting of fresh cement paste, Cement and Concrete Research 22(6) (1992) 1115-1129.
[19] G. Chiocchio, A.E. Paolini, Optimum time for adding superplasticizer to Portland cement pastes, Cement and Concrete Research 15(5) (1985) 901-908.
[20] I. Aiad, S. Abd El-Aleem, H. El-Didamony, Effect of delaying addition of some concrete admixtures on the rheological properties of cement pastes, Cement and Concrete Research 32(11) (2002) 1839-1843.
[21] J. Hot, Influence des polymères de type superplastifiants et agents entraineurs d'air sur la viscosité macroscopique des matériaux cimentaires, Université Paris-Est, Paris, 2013.
[22] K.-C. Hsu, J.-J. Chiu, S.-D. Chen, Y.-C. Tseng, Effect of addition time of a superplasticizer on cement adsorption and on concrete workability, Cement and Concrete Composites 21(5–6) (1999) 425-430.

[23] I. Aiad, Influence of time addition of superplasticizers on the rheological properties of fresh cement pastes, Cement and Concrete Research 33 (2003) 1229-1234.
[24] N. Roussel, A. Lemaître, R.J. Flatt, P. Coussot, Steady state flow of cement suspensions: A micromechanical state of the art, Cement and Concrete Research 40(1) (2010) 77-84.
[25] N. Roussel, Rheology of fresh concrete: from measurements to predictions of casting processes, Materials and Structures 40(10) (2007) 1001-1012.
[26] J. Hot, H. Bessaies-Bey, C. Brumaud, M. Duc, C. Castella, N. Roussel, Adsorbing polymers and viscosity of cement pastes, Cement and Concrete Research 63 (2014) 12-19.
[27] A. Colombo, M. Geiker, H. Justnes, R.A. Lauten, K. De Weerdt, On the mechanisms of consumption of calcium lignosulfonate by cement paste, Cement and Concrete Research (In review).
[28] G. Le Saoût, V. Kocaba, K. Scrivener, Application of the Rietveld method to the analysis of anhydrous cement, Cement and Concrete Research 41(2) (2011) 133-148.
[29] R.G. Gilbert, M. Hess, A.D. Jenkins, R.G. Jones, P. Kratochvil, R.F.T. Stepto, Dispesity in polymer science, Pure applied chemistry 81(2) (2009) 351-353.
[30] H. Vikan, Rheology and reactivity of cementitious binders with plasticizers, Department of Materials Science and Engineering, NTNU Trondheim, 2005.
[31] F. Perche, Adsorption de Polycarboxylates et de Lignosulfonates sur Poudre modele et Ciments, École Polytechnique Federale de Lausanne, 2004.
[32] K.R. Ratinac, O.C. Standard, P.J. Bryant, Lignosulfonate adsorption and stabilization of lead zirconate titanate in aqueous suspension, Journal of Colloid and Interface Science 273 (2004) 442-454.
[33] Y.F. Houst, P. Bowen, F. Perche, A. Kauppi, P. Borget, L. Galmiche, J.-F. Le Meins, F. Lafuma, R.J. Flatt, I. Schober, P.F.G. Banfill, D.S. Swift, B.O. Myrvold, B.G. Petersen, K. Reknes, Design and function of novel superplasticizers for more durable high performance concrete (superplast project), Cement and Concrete Research 38 (2008) 1197-1209.
[34] P.C. Hiemenz, R. Rajagopalan, Principles of colloid and surface chemistry, Taylor & Francis Group1997.
[35] H. Vikan, H. Justnes, F. Winnefeld, R. Figi, Correlating cement characteristics with rheology of paste, Cement and Concrete Research 37(11) (2007) 1502-1511.
[36] ASTM, Standard Practice for Measuring Hydration Kinetics of Hydraulic Cementitious Mixtures Using Isothermal Calorimetry, 2014.
[37] S. Hanehara, K. Yamada, Interaction between cement and chemical admixture from the point of cement hydration, absorption behaviour of admixture, and paste rheology, Cement and Concrete Research 29(8) (1999) 1159-1165.
[38] K. Yamada, T. Takahashi, S. Hanehara, M. Matsuhisa, Effects of the chemical structure on the properties of polycarboxylate-type superplasticizer, Cement and Concrete Research 30(2) (2000) 197-207.
[39] T. Danner, H. Justnes, M. Geiker, R.A. Lauten, Phase changes during the early hydration of Portland cement with Ca-lignosulfonates, Cement and Concrete Research 69(0) (2015) 50-60.
[40] T. Danner, H. Justnes, M. Geiker, R.A. Lauten, Early hydration of C3A–gypsum pastes with Ca- and Na-lignosulfonate, Cement and Concrete Research 79 (2016) 333-343.

[41] A. Zingg, F. Winnefeld, L. Holzer, J. Pakush, S. Becker, L. Gauckler, Adsorption of polyelectrolytes and its influence on the rheology, zeta potential, and microstructure of various cement and hydrate phases, Journal of Colloid and Interface Science 323 (2008) 301-312.
[42] P. Sandberg, L.R. Roberts, Studies of cement-admixture interactions related to use of chemical admixtures, 7th CANMET/ACI International Conference on Superplasticizers and other chemical Admixtures in concrete, 2003, pp. 529-542.
[43] D. Marchon, M. Jachiet, R.J. Flatt, P. Juilland, Impact of polycarboxylate superplasticizers on polyphased clinker hydration, 34th cement and concrete science conference, Sheffield, UK, 2014, pp. 79-82.
[44] L.H. Tuthill, R.F. Adams, S.N. Bailey, R.W. Smith, A case of abnormally slow hardening concrete for tunnel lining, ACI Journal 57(3) (1961) 1091-1109.
[45] L.R. Roberts, P.C. Taylor, Understanding cement-SCM-admixture interaction issues, Concrete international (2007) 33-41.
[46] S. Pourchet, L. Regnaud, J.P. Perez, A. Nonat, Early C3A hydration in the presence of different kinds of calcium sulfate, Cement and Concrete Research 39(11) (2009) 989-996.
[47] I. Odler, J. Schüppstuhl, Early hydration of tricalcium silicate III. Control of the induction period, Cement and Concrete Research 11(5–6) (1981) 765-774.
[48] G.L. Valenti, V. Sabatelli, B. Marchese, Hydration kinetics of tricalcium silicate solid solutions at early ages, Cement and Concrete Research 8(1) (1978) 61-72.
[49] A. Quennoz, Hydration of C3A with Calcium Sulfate Alone and in the Presence of Calcium Silicate, EPFL, 2011.
[50] F. Begarin, S. Garrault, A. Nonat, L. Nicoleau, Hydration of alite containing alumimium, 29 th Cement and Concrete Science Congress, Leeds, 2009, pp. 9-12.
[51] L. Nicoleau, E. Schreiner, A. Nonat, Ion-specific effects influencing the dissolution of tricalcium silicate, Cement and Concrete Research 59 (2014) 118-138.

Notation

ANL	Anlegg cement (CEM I 52.5 N)
CX	Cemex cement (CEM I 52.5 R)
DA	delayed addition of plasticizer (10 min)
IA	immediate addition of plasticizer
LSs	softwood low-sugar Ca-lignosulfonate
OPC	ordinary Portland cement
w/b	water-binder ratio
$\dot{\gamma}$	shear rate
τ	shear stress
μ	viscosity

-COOH carboxyl group

φ-OH phenolic OH-group

List of tables

List of figures

Table 1 – *Main phases in cement ANL and CX from XRD-Rietveld analysis [a]: results obtained with TGA analysis*

Phase composition (mass %)	**ANL**	**CX**
Alite	60.5	54.3
Belite	14.2	18.8
Aluminate cubic	1.3	4.7
Aluminate orthorhombic	0.9	2.4
Ferrite	14.0	6.5
Periclase	0.4	1.1
Quartz	0.3	-
Calcite	3.2/ 3.8 [a]	3.6/ 3.7 [a]
Portlandite	1.1/ 1.4 [a]	2.6/ 2.5 [a]
Anhydrite	-	2.1
Hemihydrate	2.6	1.8
Gypsum	1.0	-
Arcanite		0.6
Aphthitalite	0.4	0.7
Thenardite	-	0.8

Table 2 – *Chemical composition of the cements given by the producers*

Chemical compound (mass %)	**ANL**	**CX**
CaO	62.7	64.0
SiO_2	20.6	20.0
Al_2O_3	4.4	4.6
Fe_2O_3	3.5	2.6
SO_3	3.3	3.6
MgO	1.6	2.4
K_2O	0.4	1.0

Na_2O	0.3	0.2
TiO_2	0.2	0.2
P_2O_5	0.2	0.2
LOI (%) 1000 °C	1.6	1.7
Sum	97.2	98.9

Table 3 - *Physical properties of ANL and CX cements*

	ANL	**CX**
Surface area (BET) (m^2/kg)	890	1330
Blaine surface (m^2/kg)	360	540
Density (g/cm^3)	3.1	3.1
d_{10} (µm)	2.0	2.0
d_{50} (µm)	12.0	10.0
d_{90} (µm)	34.0	26.0

Table 4 - *Chemical and physical properties of LSs*

Mw	g/mol	29000
Mn	g/mol	2100
Organic S ($\propto SO_3$)	mass %	4.6
SO_4^{2-}	mass %	0.9
Ca^{2+}	mass %	4.6
Na^+	mass %	0.9
-COOH	mass %	7.1
φ-OH	mass %	1.4
Total sugar	mass %	8.3

Table 5 – *Sequence for rheology measurements*

		Duration (s)	**Cumulative duration** (min)
1	Stir up at $\dot{\gamma}$ = 60 1/s	30	0.5
2	Rest	30	1.0
3	Flow curve up, linear sweep $\dot{\gamma}$ from 0 to 60 1/s in 20 steps lasting 5 sec. each	100	2.7
4	Flow curve down, linear sweep $\dot{\gamma}$ from 60 to 0 1/s in 20 steps lasting 5 sec. each	100	4.3
5	Rest	340	10.0
6	Stir up at $\dot{\gamma}$ = 60 1/s	30	10.5
7	Rest	30	11.0
8	Flow curve up, linear sweep $\dot{\gamma}$ from 0 to 60 1/s in 20 steps lasting 5 sec. each	100	12.7
9	Flow curve down, linear sweep $\dot{\gamma}$ from 60 to 0 1/s in 20 steps lasting 5 sec. each	100	14.3
10	Rest	340	20.0
11	Stir up at $\dot{\gamma}$ = 60 1/s	30	20.5
12	rest	30	21.0
13	Flow curve up, linear sweep $\dot{\gamma}$ from 0 to 60 1/s in 20 steps lasting 5 sec. each	100	22.7
14	Flow curve down, linear sweep $\dot{\gamma}$ from 60 to 0 1/s in 20 steps lasting 5 sec. each	100	24.3

Table 6 – *Analysed samples to obtain adsorption isotherms*

Material	**LSs addition procedure**	**LSs dosage (mass % binder)**
ANL cement	IA	0.1; 0.2; 0.4; 0.6; 0.8; 1.2; 1.5
	DA	0.05; 0.1; 0.25; 0.4; 0.8; 1.2; 1.5
CX cement	IA	0.1; 0.2; 0.4; 0.6; 0.8; 1.0
	DA	0.05; 0.1; 0.2; 0.4; 0.8; 1.2; 1.5

Table 7 – *Elemental concentration of Al, Fe, Ca, Si, and S in ANL and CX cements with 0, 0.8 or 1.5 mass % LSs after 30 minutes hydration, and in two LSs solutions (mmol/L): the 2.0 and 3.7 % LSs solutions were used for the cement samples with 0.8 and 1.5 mass % LSs respectively*

Sample	LSs dosage	Al	Ca	Fe	S	Si
	Mass % binder			Mass %		
ANL IA	0	0.05	236	0.03	767	0.86
	0.8	0.07	260	0.09	963	1.1
	1.5	0.15	445	0.69	1390	1.2
ANL DA	0.8	11.2	375	5.5	1003	8.5
	1.5	35.7	523	14.3	715	26.0
CX IA	0	0.05	239	0.02	1759	0.90
	0.8	0.06	103	0.2	1691	3.0
	1.5	0.11	53.7	1.1	1414	3.6
CX DA	0.8	0.96	282	1.1	1762	2.3
	1.5	7.9	499	4.5	1929	5.6
2.0 % LSs sol.		0.18	183	0.19	370	3.1
3.7 % LSs sol.		0.26	324	0.31	659	2.7

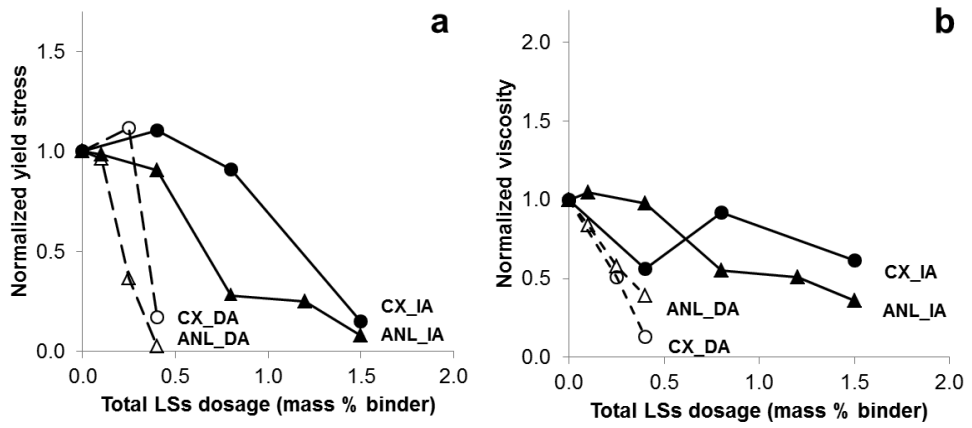

Figure 1 – *a) Normalized yield stress and b) normalized viscosity vs. total LSs (mass % binder) of ANL and CX cements mixed with IA or DA of LSs at 10 min of hydration (12 min of hydration for samples prepared with DA)*

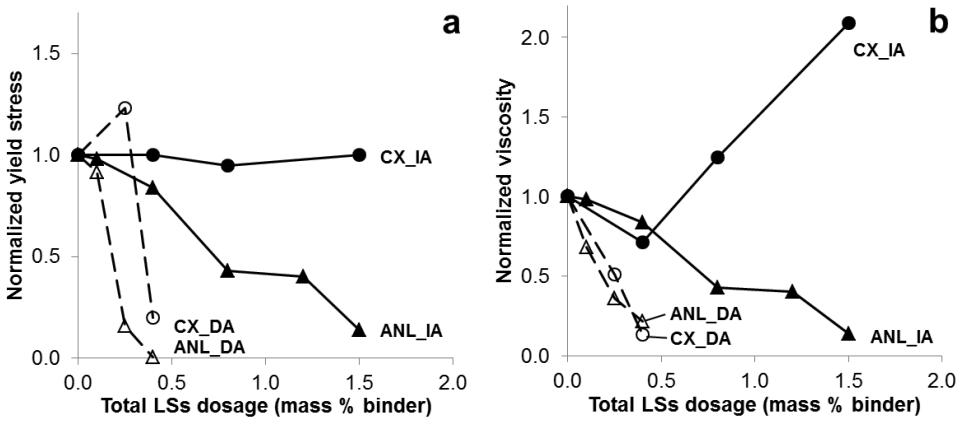

Figure 2– *a) Normalized yield stress and b) normalized viscosity vs. total LSs (mass % binder) of ANL and CX cements mixed with IA or DA of LSs at 30 min of hydration*

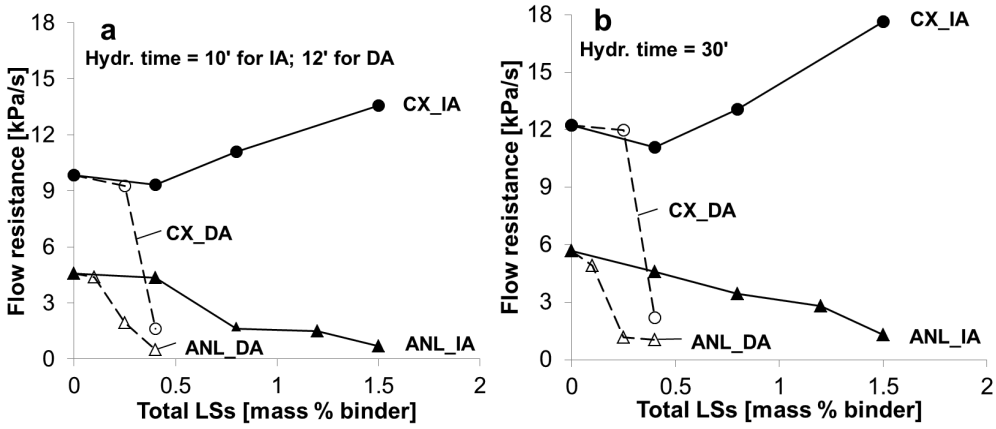

Figure 3 - *Flow resistance at 10 min. of hydration (12 min of hydration for samples prepared with DA) in fig. a and at 30 min. of hydration in fig. b vs. total LSs(mass % binder) of ANL and CX cements with IA or DA of LSs*

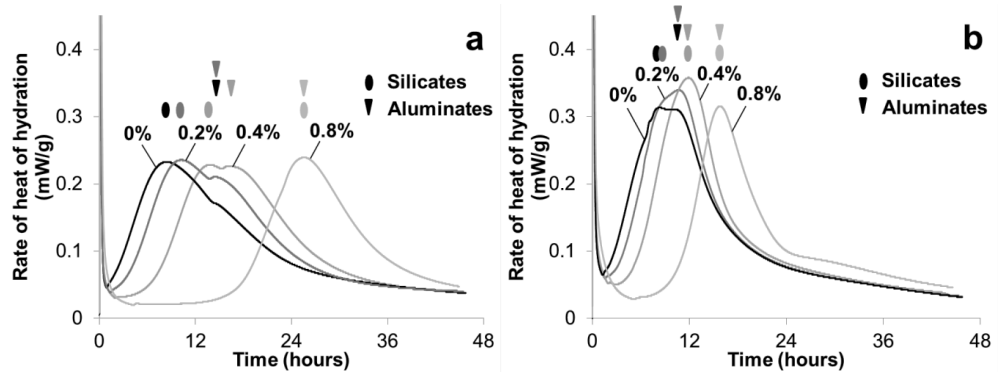

Figure 4 – *Rate of heat of hydration in time for a) ANL and b) CX cement pastes with increasing dosage of LSs mixed with IA (0, 0.2, 0.4, 0.8 mass % LSs). The silicates and aluminates peaks are marked with different symbols in corresponding colour of the respective calorimetric curve.*

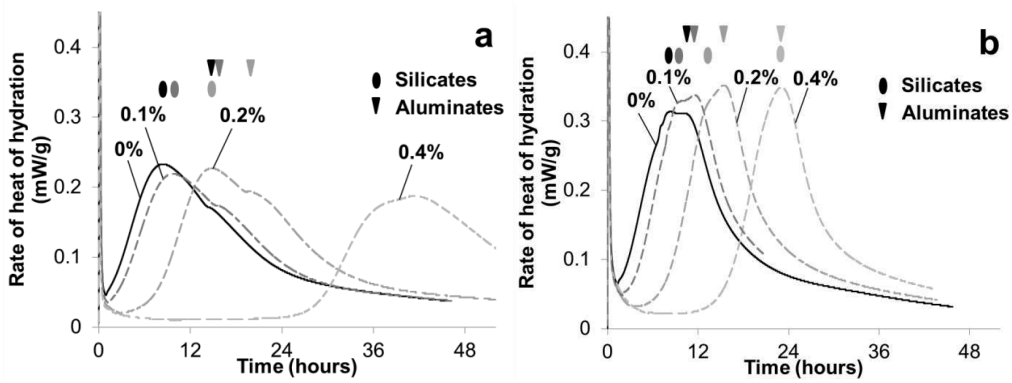

Figure 5 - *Rate of heat of hydration vs. time for a) ANL and b) CX cement pastes with increasing dosage of LSs mixed with DA (0, 0.1, 0.2, 0.4 mass % LSs). The silicates and aluminates peaks are marked with different symbols in corresponding colour of the respective calorimetric curve.*

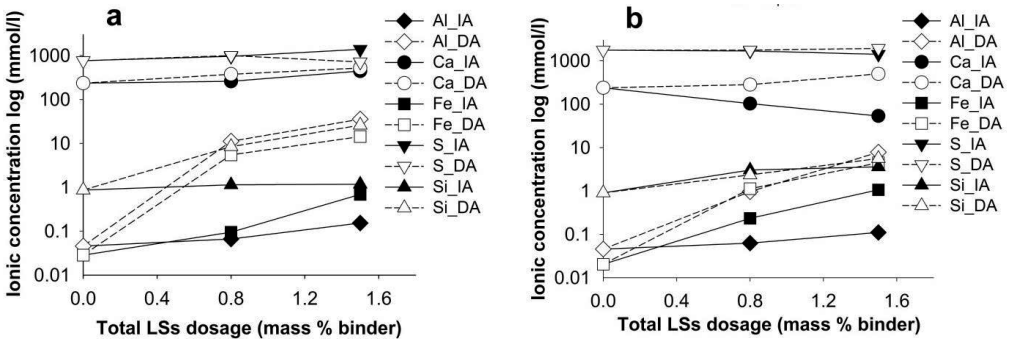

Figure 6 – *Concentration of Al, Fe, Ca, Si, and S ions in the pore solution (mmol/L) expressed in logarithmic scale vs. total LSs added (mass % binder) to a) ANL and b) CX cement pastes at 30 min of hydration both for IA and DA*

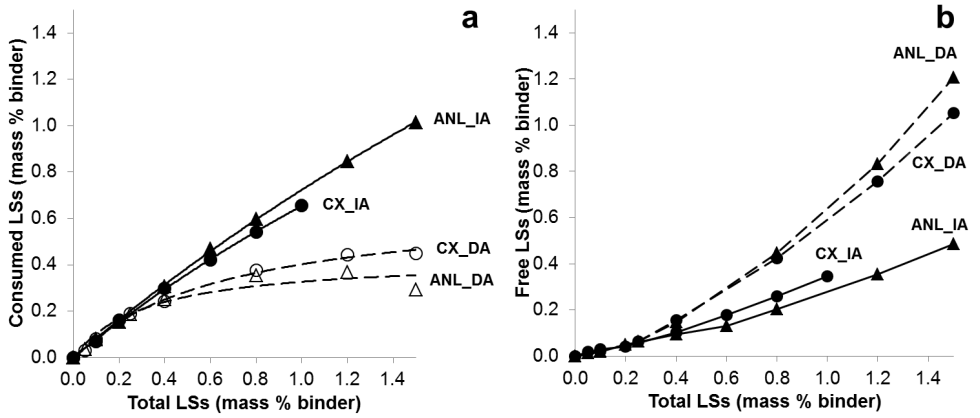

Figure 7 - *Amount of a) consumed LSs and of b) free LSs at 30 min of hydration vs. amount of LSs added to ANL and CX cements for IA and DA, after [27]. The results are calculated per mass % of binder*

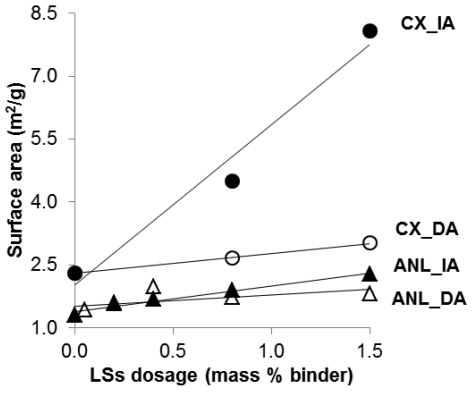

Figure 8 - *Surface area of ANL and CX cement particles hydrated for 30 min vs. total dosage of LSs added (mass % binder) both for IA and DA, after [27]*

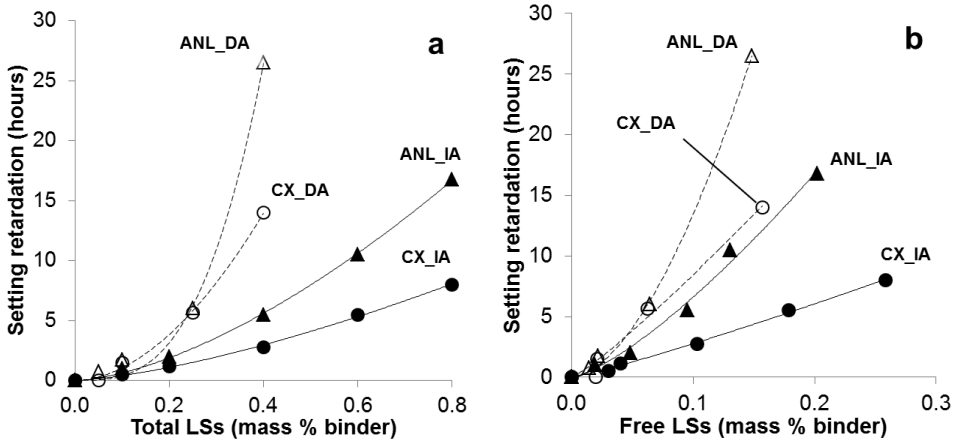

Figure 9 – *Setting time retardation vs. amount of a) total LSs and b) free LSs for ANL and CX cement pastes containing increasing dosage of LSs both for IA and DA. NB. The figures' scales are different*

Paper III

On the effect of calcium lignosulfonate on ettringite formation in cement paste

Submitted to Cement and Concrete Research (September 2016)

Colombo, A.; Geiker, M.R.; Justnes, H.; Lauten, R.A.; De Weerdt, K.

THE EFFECT OF CALCIUM LIGNOSULFONATE ON ETTRINGITE FORMATION IN CEMENT PASTE

A. Colombo (1), M. Geiker (1), H. Justnes (2, 3), R. A. Lauten (4), K. De Weerdt (1)

(1) Department of Structural Engineering, Norwegian University of Science and Technology, NTNU, Norway

(2) SINTEF Building and Infrastructure, Trondheim, Norway

(3) Department of Materials Science and Engineering, Norwegian University of Science and Technology, NTNU, Trondheim, Norway

(4) Borregaard, Sarpsborg, Norway

ABSTRACT

The effect of a softwood calcium lignosulfonate, LSs, on the ettringite formed in cement paste was investigated. Two Portland cements, mainly differing in surface area and C_3A content, were used. The effect of LSs addition time was studied, by adding either the LSs immediately with the mixing water or after 10 minutes of hydration. After 30 minutes of hydration of both cement pastes, the immediate addition of LSs caused the formation of numerous small ettringite crystals. The ettringite crystals had similar shape in pastes with and without LSs addition: cubic or cuboidal shape with length between 0.1 and 0.4 μm. These small particles caused an increase in surface area, which in turn increased the LSs adsorption by the cement paste. This could potentially lead to incompatibility issues between cement and plasticizer.

KEYWORDS

Ettringite; Hydrated surface area; Adsorption; Fresh cement paste; Lignosulfonate

1. INTRODUCTION

Water-reducers, or plasticizers, allow obtaining highly fluid concrete with low water-to-binder ratios, additionally improving the mechanical properties and the durability of the hardened concrete.

In this paper, a low-sugar softwood calcium lignosulfonate (LSs) is investigated. LSs is commonly used in concrete in the dosage of 0.25-0.40 mass % of binder. Lignosulfonates are polyelectrolytes derived from lignins in the pulping industry. Lignin can be derived from various sources of biomass, which allows producing lignosulfonates with different molecular weight and amount of functional groups.

Amongst the clinker phases, C_3A is the one with the highest hydraulic reactivity, reacting immediately upon water contact. In the presence of gypsum, the first stable hydration product from C_3A is ettringite (AFt). Ettringite forms as long as there are enough sulfate ions in solution. When gypsum is depleted, ettringite will start further reacting with the residual C_3A, forming monosulfoaluminate hydrate (AFm) [1].

The dispersing effectiveness of a superplasticizer on cementitious materials is, amongst others, a function of its degree of adsorption on the surface of cement grains and hydrates. The adsorbed plasticizer layer renders the particle surface of cement grains and hydrates negatively charged. As negatively charged particles approach each other, their repulsion prevents them from forming agglomerates. This is referred to as electrostatic repulsion. Additionally, when two surfaces approach enough for their adsorbed layers to overlap, a steric force develops. This will contribute in hindering particles to get close enough to form agglomerates [2]. Side chains stretching out from the polymer backbone also contribute to disperse the cement particles by steric hindrance.

The polymer is not adsorbed equally on the four main cement phases. According to Yoshioka et al. [3], a much higher adsorption occurs on aluminate and ferrite than on the silicate phases. According to Zingg et al. [4] and Plank et al. [5], the plasticizer will be adsorbed also on the cement hydrates, ettringite being the hydrate adsorbing the most.

It is known that plasticizers can cause changes in hydrates morphology, especially for ettringite. Prince et al. [6] studied a system of calcined kaolin, lime and anhydrite and found that sodium polynaphthalene sulfonate blocks the development of needle-like ettringite crystals. Instead, ettringite formed in small massive clusters. Hekal and Kishar [7] found that the size of the ettringite crystals formed in a C_3A-$CaSO_4$ system decreased as the dosage of a sodium naphthalene sulfonate-formaldehyde polycondensate increased. Cody et al. [8] synthesized ettringite in presence of a commercial lignosulfonate. They found that a large amount of ettringite formed in the form of small spherical crystals. Danner et al. [9] observed that the addition of calcium and sodium lignosulfonate led to the formation of small ettringite crystals with rounded oval shape. On the other hand, Kerui et al. [10] investigated a fly ash cement, reporting that a mixture of calcium lignosulfonate and sodium bicarbonate caused a change in ettringite formation from a large number of tiny crystals into a limited number of large needle-like crystal particles. In conclusion, plasticizers seem to generally cause the ettringite crystals to be smaller in size and to deviate from the typical needle-shape, taking a spherical or cubic morphology. This is contradictory to what was observed by Kerui et al. [10], who found that ettringite formed in few large needle-like crystals. However, it should be kept in mind that the results might have been influenced by the fact that lignosulfonate was combined with $NaHCO_3$.

Several studies reported that also the amount of formed hydrates might change upon plasticizer addition. Zingg [11] found that some polycarboxylate-type superplasticizers (PCE) had a limited influence on the amount of ettringite formed in Portland cements. This was confirmed by Dalas et al. [12], who found only a slight decrease in the amount of ettringite precipitated in a C_3A-$CaSO_4$ system, though its specific area was strongly increased. Hekal and Kishar [7] investigated a similar system of C_3A and $CaSO_4$ reporting that the ettringite formation was increasingly retarded in the first 24 hours of hydration as the dosage of a sodium naphthalene sulfonate-formaldehyde polycondensate increased. Lignosulfonate was, on the other hand, found to accelerate ettringite formation in cement by Bishop and Barron [13]. The amount of ettringite formed by a fly ash cement was found to increase in presence of a mixture of calcium lignosulfonate and sodium bicarbonate by Kerui et al. [10]. Danner et

al. [14] investigated three different cements in combination with a calcium-lignosulfonate and reported that the initial formation of ettringite was accelerated. In conclusion, the amount of ettringite formed has both been observed to increase and decrease depending on the plasticizers used.

The aim of this paper is to understand the effect of a calcium lignosulfonate (LSs) on the formation of ettringite in Portland cement paste. Two Portland cements mainly differing in surface area and C_3A content were chosen. The effects were studied both by adding the lignosulfonate immediately with the mixing water (IA), and by adding it after 10 minutes of hydration (DA). Changes in composition and amount of cement hydrates after 30 minutes of hydration caused by the addition of the LSs were investigated with thermogravimetric analysis (TGA) and X-ray powder diffraction (XRD). The effect of LSs on the hydrates of hardened cement was also studied with TGA after 28 days of hydration. The hydrates morphology was observed with scanning electron microscopy (SEM) after 30 minutes of hydration, and their chemical composition was analyzed with energy dispersive spectroscopy (EDS). The elemental composition of the pore solution extracted from the cement paste samples after 30 minutes of hydration was analysed with inductive coupled plasma – mass spectroscopy (ICP-MS). In addition, the effect of LSs on the solubility of the different calcium sulfates, i.e. anhydrite, hemihydrate and gypsum, was investigated by determining the soluble Ca and S by ICP-MS in calcium sulfate suspensions containing increasing LSs dosages. The adsorption isotherms and BET measurement presented in a previous paper by the same authors [15] were combined with the new results reported in the present paper. In the present paper, the authors succeeded in observing the morphology of ettringite in real cement paste with and without the LSs, and not as a pure synthesized phase. The results of this paper give further insight on the effect of LSs on the formation of cement hydrates, and thus contribute to a deeper understanding of the mechanisms behind the interactions between lignosulfonate and cement paste.

2. EXPERIMENTAL

2.1 Materials

The experiments were performed on two different cements: a CEM I 52.5 N (ANL) and a CEM I 52.5 R (CX), as defined by the European Standard EN197-1. The content of the main clinker phases of the cements quantified by XRD Rietveld, according to Le Saoût et al. [16], are given in Table 1. The chemical composition of the cements determined by XRF and the loss of ignition at 950 ºC are reported in Table 2. The particle size distribution (d_{10}, d_{50}, d_{90}), Blaine surface area, density, and BET surface area are given in Table 3.

A sugar-reduced softwood calcium lignosulfonate (LSs) was used as plasticizer. Its mass weighted molecular weight (M_w), as measured with gel permeation chromatography (GPC), was 29000 g/mol and the number weighted molecular weight (M_n) was 2100 g/mol, giving broad molar-mass dispersity ($Đ_M$) equal to 13.8. The molar-mass dispersity, also called polydispersity index, is defined as the ratio between M_w and M_n [17]. Additional physical and chemical properties of the lignosulfonate are listed in Table 4. For the lignosulfonate used in

the present investigation, the sugars were removed from the product by fermentation and resulting alcohol by distillation. The LSs was dissolved in deionised water to concentrations varying from 1 to 45 % to ease dosing, and the water content was included in the calculation of the water-to-binder ratio (w/b).

In order to study the effect of LSs on the solubility of calcium sulfates, anhydrite ($CaSO_4$), hemihydrate ($CaSO_4 \cdot 0.5H_2O$) and dihydrate ($CaSO_4 \cdot 2H_2O$) were used. The anhydrite and the dihydrate were analytical grade, while the hemihydrate was technical grade. In order to mimic the pH of cement paste, the calcium sulfates samples were mixed with LSs solution diluted in artificial pore water. The artificial pore water was a solution of NaOH and KOH with K/Na molar ratio equal to 2 and measured pH of 12.9.

2.2 Sample preparation

About 300 g cement was mixed with deionised water and/or lignosulfonate solution in a high-shear mixer MR530 by Braun at intensity 6 obtaining a paste with w/b = 0.4. A volume of about 200 ml was obtained for all the cement pastes. In order to investigate the effect of the time of addition of lignosulfonate, two different mixing procedures were applied: immediate addition of LSs with the mixing water (IA) and delayed addition of LSs after 10 minutes of hydration (DA).

For IA, the binder was mixed with deionised water (and/or lignosulfonate diluted in deionised water) according to the procedure used by Vikan [18]: 30 seconds mixing, 5 minutes resting and scraping the mixer walls to homogenize the mix, and 1 minute mixing.

For DA, the binder and 85% of the water were mixed according to the following mixing procedure: 30 seconds mixing, 10 minutes resting and scraping the mixer walls to homogenize the paste. The delay time of 10 minutes was found to be included in the range of optimum delay times to obtain the maximum workability increase with a given plasticizer dosage [19-22]. LSs and the remaining 15% of the needed water were then added to the mix, which was mixed for 1 additional minute.

2.3 Methods

2.3.1 UV-spectroscopy

UV-spectroscopy allowed measuring the LSs concentration in the pore solution of the cement paste samples, which again allows the determination of the LSs uptake.

After mixing according to paragraph 2.2, about 35 ml paste was poured in 50 ml plastic centrifuge tubes and left to rest until the selected hydration time. The pore solution was extracted from the cement paste by centrifuging the samples in a Heraeus Megafuge 8 centrifuge by Thermo Scientific for 3 minutes at the speed of 4500 rpm. The supernatant pore solution was extracted and filtered with 0.45 µm cellulose syringe filters. The pore water was analysed with a Genesys 10S UV-spectrophotometer by Thermo Scientific. Wavelengths in the range 280-284 nm had been reported in literature to study the adsorption of lignosulfonate on cement particles [2, 18, 23-25]. After scanning at several wavelengths, 281 nm was chosen as the most suitable wavelength to analyse the samples in this study.

After centrifugation plasticizer consumed by the cement paste was determined with UV-spectroscopy at increasing hydration times (from 5 to 120 minutes hydration). It was found that, after 10 minutes of hydration, the LSs uptake reached a plateau and did not change considerably with time. 30 minutes hydration was used for determination of the adsorption isotherms.

A calibration curve was obtained measuring the absorbance of pure LSs solutions dissolved in deionised water in different concentrations. Based on the absorbance value of the pore solution extracted from the samples of cement paste, the calibration curve allowed the calculation of the amount of free plasticizer (g LS/100 g solution) in the pore solution. This amount was then related to the amount of binder in the sample (g LS/100 g binder). The LSs consumed by the investigated systems was calculated by subtracting the amount of free LSs to the total amount of LSs initially added to the sample, as displayed in equation 1:

$$LSs_{consumed} = LSs_{total} - LSs_{free} \quad (1)$$

Polymer adsorption by a solid is usually described through isotherms, in which the amount of polymer adsorbed is plotted against the total amount of polymer added to the system [26]. The shape of an isotherm is largely determined by the adsorption mechanisms. In this study, the isotherms were drawn relating the amount of LSs consumed by the cement paste to the amount of total LSs added to the sample. When expressed as mass % of binder, the amount of LSs consumed was calculated considering the actual available water in the system, i.e. the mixing water was reduced by the bound water measured with TGA (paragraph 2.3.3).

2.3.2 Solvent exchange

A solvent exchange procedure with isopropanol and petroleum ether was used to stop the hydration of the cement paste.

About 5 ml of cement paste after 30 minutes of hydration was transferred in a 50 ml centrifuge tube and centrifuged for 1 minute at 2000 rpm. The supernatant water was removed. About 40 ml of isopropanol was poured in the centrifuge tube. The tube was shaken for 30 seconds and let to rest for 5 minutes. The sample was centrifuged again for 1 minute at 2000 rpm and the supernatant liquid was removed. The solvent exchange procedure with isopropanol was repeated once, followed by a final solvent exchange with 10 ml of petroleum ether. The resulting paste was let to dry in a ventilated oven for 15 minutes at 40 ºC, and then for 2 days in a desiccator over silica gel and soda lime to minimize carbonation. After drying, the samples were pulverized and homogenized in a porcelain mortar and stored in sealed containers in a desiccator over silica gel and soda lime until analysis.

After 6 hours of hydration, a slice of 6 mm was cut from the mid-section of the sample with an electric saw (the samples were not plastic anymore, but neither fully hardened). For this reason, the semi-hardened cement paste was crushed in a porcelain mortar and the hydration was stopped in equal manner as for the samples hydrated for 30 minutes.

A different set of samples of cement paste was let to hydrate for 28 days at 20 ºC in sealed conditions. After 28 days, a slice of 6 mm, equivalent to about 5 g of cement, was cut from

the mid-section of the sample with an electric saw. The sample was crushed in a porcelain mortar until the powder passed through a 1 mm sieve. The powder was then transferred into a 125 ml plastic bottle together with 50 ml isopropanol, which was shaken for 30 seconds and let to rest for 5 minutes until solids sedimented. The isopropanol was decanted and the procedure was repeated once more. The isopropanol was then filtered off with a filtration unit connected to a water pump, using Blauband filters by Schleicher & Schuell. The sample was then flushed with 10 ml petroleum ether while still in the filtration unit, and let to rest for 5 minutes, before removing the ether by filtration in the water pump. The sample was then transferred to a watch glass and let to dry in a ventilated oven for 15 minutes at 40 ºC. After drying, the samples were stored in sealed containers in a desiccator over silica gel and soda lime until analysis. Prior to analysis, the sample was pulverized and homogenized in a porcelain mortar.

2.3.3 TGA

The thermogravimetric analysis (TGA) was performed with a Mettler Toledo TGA DSC3+ on hydrated cement paste after stopping the hydration using solvent exchange. Approximately 200 mg of cement paste powder was loaded in 600 µl alumina crucibles. The samples were heated from 40 to 900 °C at a rate of 10 °C/min while purging with 50 ml/min N_2.

It was decided to present the results in terms of mass loss % of the mass of dry binder in different temperature intervals (see Figure 5 and Table 6). The intervals selected were: interval 1, from 50 to ca. 300 °C, interval 2 from ca. 300 to ca. 500 °C, and interval 3 from ca. 500 to 900 °C. The temperature ranges could slightly vary according to the actual peak boundaries in the derivative of the thermogravimetric curve (DTG). For the samples hydrated for 28 days, the intervals slightly changed in temperature ranges: interval 1, from 50 to ca. 420 °C, interval 2 from ca. 420 to ca. 540 °C, and interval 3 from ca. 540 to 900 °C.

Interval 1 includes the mass loss corresponding to the decomposition of ettringite, calcium sulfates, and C-S-H; interval 2 consists mainly of the mass loss corresponding to the decomposition of CH; interval 3 comprises the mass losses corresponding to the decomposition of carbonates. The sum of the mass loss in the interval 1 and 2 represents the release of bound water.

The mass losses are expressed relative to the dry mass of the sample as the dry weight is assumed to be constant during the hydration. Commonly the mass at 500 °C is used as the dry mass of hydrated cement paste containing limestone [27]. However, the addition of LSs to the cement paste led to an increase in mass loss in the temperature range between 500 and 800 °C due to the decomposition of LSs. Therefore, the dry weight was calculated as the sum of the sample weight at 800 °C and the mass loss due to the decomposition of limestone in the sample without LSs. For example, the mass loss in interval 1 was calculated as in equation 2:

$$\text{Mass loss Int. 1 (mass \%)} = \frac{w_{50} - w_{300}}{w_{800} + (w_{500} - w_{800})} * 100 \quad (2)$$

To calculate the amount of bound water in the cement paste, the mass loss in the interval from 50 to 500 ºC was considered. The amount of bound water was calculated as:

$$\text{Amount of bound water (mass \% dry weight of cement)} = \frac{w_{50}-w_{500}}{w_{800}+(w_{500}-w_{800})} * 100 \quad (3)$$

In order to have an approximate quantification of the maximum amount of ettringite formed in the cement pastes, the whole mass loss in the interval 1 (50 - ca. 300 ºC) was considered. This interval also includes the water loss due to the release of crystalline water from the remaining calcium sulfate components present. However, it was difficult to separate these mass losses corresponding to ettringite and sulfates as the TGA peaks overlap. The amount of ettringite (AFt) was calculated as:

$$\text{Amount of AFt (mass \% dry weight of cement)} = \frac{w_{50}-w_{300}}{w_{800}+(w_{500}-w_{800})} * \frac{M_m(AFt)}{M_m(H)} * 100 \quad (4)$$

2.3.4 XRD

The X-ray diffraction (XRD) analysis was performed using a Bruker AXS D8 Focus with a Lynxeye super speed detector operating at 40 kV and 40 mA. A CuKα source (λCuKα = 1.54 Å) with a 0.2 mm slit was used. The scan was performed between 7 and 55° 2θ with an increment of 0.02 and a scanning speed of 0.5 s/step. Front-loading sample holders were used. The scans are used qualitatively to detect changes in crystalline phases.

2.3.5 BET of hydrated particles

The BET measurements were performed using a Tristar II Plus by Micromeritics. The sample mass was about 2 g. The measurement was performed by first degassing the samples for about 5 minutes at room temperature and then purging them with nitrogen at room temperature. The sample preparation applied in this study, similar to the one described in [28], aimed to limit destruction of hydrates such as gypsum and ettringite. The hydration was stopped with the solvent exchange procedure described in paragraph 2.3.2. The solvent was removed by drying the samples in a ventilated oven at 40˚C for 15 minutes and subsequently leaving the sample to dry in a desiccator over silica gel and soda lime for 2 days. The samples were then sealed and stored in the same type of desiccator prior to the analysis.

2.3.6 SEM-EDS

An ultra-high-resolution in-lens cold field emission SEM S-5500 by Hitachi was used for the scanning electron microscopy (SEM). The cement powder was dried for 2 days in a desiccator over silica gel and soda lime prior to the analysis. The powder sample was placed on a sample holder with copper tape and the excess powder was removed with a N_2 gun. A voltage of 5 kV and a current varying between 1 and 7 µA were used to observe the samples with the scanning electron microscope in secondary electron-mode (SE). The chemical composition of the samples was analyzed with energy-dispersive X-ray spectroscopy (EDS) using a Bruker XFlash detector set on a voltage of 5 kV and a current of 20 µA. The samples were coated with a 4 nm-thick layer of a platinum-palladium alloy to avoid charging of the sample during the analysis.

2.3.7 ICP-MS

Inductively-coupled plasma mass spectrometry (ICP-MS) was used to determine the elemental concentration of Al, Ca, Fe, K, Na, S and Si in the pore solution extracted from the cement paste. A triple quad Agilent 8800 by Agilent Technologies was used. The samples

were filtered with the same procedure used for UV-spectroscopy (paragraph 2.3.1) and acidified by adding 1:1 by volume of 1:10 diluted HNO_3.

3 RESULTS

3.1 TGA after 30 minutes of hydration

The effect of the dosage of LSs on cement hydrates after 30 minutes of hydration was investigated with TGA. The analysis was performed on ANL and CX cement pastes with different dosages of LSs both for immediate addition (IA) and for delayed addition (DA). A maximum LSs dosage of 1.5 mass % of binder was used for the samples prepared with DA because of the extremely large setting retardation displayed by this sample, as showed in a previous paper [29]. Reference samples of neat ANL and CX without LSs were also measured. The hydration of the tested samples was stopped after 30 minutes with the solvent exchange procedure with isopropanol and petroleum ether, as described in paragraph 2.3.2. The results are displayed in Figure 1 and in Figure 2 for ANL cement and in Figure 3 and in Figure 4 for CX cement.

Several peaks could be observed: the peak at about 120 ºC and the smaller one at 240 ºC indicate the presence of AFt. The peak around 160 ºC represents the release of water from calcium sulfates (anhydrite, hemihydrate or gypsum) ($CaSO_4 \cdot xH_2O$). This peak might overlap with the one representing the decomposition of AFm, but, since no AFm was detected with XRD (see Figure 6 and Figure 7), it is assumed that this peak is only ascribable to the release of crystalline water from the calcium sulfates. The peak around 420 ºC relates to the release of crystalline water from portlandite (CH); the ones around 610 ºC and 780 ºC represent the decomposition of carbonates ($\underline{C}$) (release of CO_2). The peaks over 500 ºC can be attributed both to the decomposition of limestone included in the used cements and, for the samples containing LSs, to the decomposition of LSs.

The ANL cement contains gypsum and hemihydrate, while CX cement contains hemihydrate and anhydrate (see Table 1). Upon contact with water, normally both anhydrite and hemihydrate partially or completely convert to gypsum. For ANL cement, the peak at 160 ºC corresponds to the dehydration of gypsum and hemihydrate. The TGA data for CX cement do not show peaks at 160 ºC. This indicates that the hemihydrate in CX cement paste is consumed after 30 minutes of hydration and no anhydrite has converted to gypsum. The latter is also confirmed by the XRD data, as shown in Figure 6 and Figure 7.

The mass loss was quantified with the horizontal step method applied in three temperature intervals, as described in paragraph 2.3.3. The results are shown in Figure 5 and summarized in Table 6.

From the results showed in Figure 5 and reported in Table 6, it can be observed that, for IA, the increase in LSs dosage led for both cements to an increase in the intensity of the peak corresponding to the decomposition of ettringite and a reduction in the one corresponding to the decomposition of calcium sulfate hydrates up to a LSs dosage of 1.5 mass % of binder. Similar trends were observed for both cements, even though the ettringite peak was noticeably

more intense and the one of calcium sulfate hydrates less intense for CX cement compared to ANL cement. For higher LSs dosages, the increase in intensity of the ettringite peak was lower than that with 1.5 mass % of binder LSs for both cements.

The mass loss corresponding to the decomposition of CH did not noticeably change with increasing LSs amount.

The mass loss corresponding to carbonates decomposition was found to increase in intensity with the increase of the LSs amount, and may thus actually include a contribution from the LSs decomposition.

The amount of bound water (interval 1+2) followed a similar trend as interval 1. The increasing amount of bound water with increasing LSs dosages (up to 1.5 mass % of binder) shown by CX cement for IA agrees with the observation that, for IA, CX was found to set already after 30 minutes of hydration for LSs dosages over 1.0 mass % of binder.

In the sample of CX cement paste with 1.5 mass % of binder LSs (IA), the amount of bound water resulted to be about 5 mass % of dry weight of cement, which represented the 12 % of the initial mixing water (40 mass % of dry weight, since w/b = 0.4).

For DA, no noticeable changes in the ettringite, calcium sulfate hydrates, or CH amount were observed for any of the cements. Only an increased intensity of the carbonate peak was measured with increasing LSs amount.

3.2 XRD

The increase in the ettringite amount measured with TGA for IA was confirmed by x-ray diffraction (XRD) on ANL and CX cement pastes containing 0, 0.8, 1.5 mass % of binder LSs added with IA. The hydration of the cement pastes was stopped after 30 minutes with the solvent exchange procedure using isopropanol and petroleum ether, as described in paragraph 2.3.2. The results are shown in Figure 6 and Figure 7.

The main peaks displayed by the XRD curves are summarized in Table 7. The peak at 2θ = 9.1º, representing ettringite, increases in intensity with the increase of LSs for both cements, supporting the results found with TGA. For the ANL cement samples, clear peaks at 2θ = 11.6 º and 20.7 º are observed, representing gypsum. Whereas for CX cement samples, peaks at 2θ = 25.7 º and 31.2 º were detected and represent anhydrite. This is in line with the composition on the unhydrated cements (Table 1), where the sulfate source in CX cement is anhydrite and hemihydrate, and for ANL cement gypsum and hemihydrate, with the exception that hemihydrate was not detected in the XRD spectrum. For ANL and CX cement, the peak intensities of respectively gypsum and anhydrite noticeably decreased with the LSs dosage, indicating enhanced reaction of the calcium sulfate phases upon addition of LSs. The peaks at 2θ = 12.2 º and 2θ = 24.3 º indicates C_4AF, which appeared to slightly decrease with increasing LSs dosage. The peak at 2θ = 14.9 º represents C_3S and displayed an approximately constant intensity with increasing LSs dosage in both cement pastes. The peak at 2θ = 23.0 º indicates either ettringite or $CaCO_3$. This peak was found to slightly increase with the increase in LSs for both cements.

3.3 SEM

3.3.1 After 30 minutes of hydration

The morphology and size of early hydrates in presence of LSs was investigated with SEM. Pastes of both cements containing 1.5 mass % of binder LSs both for IA and DA were studied. The hydrates formed in these samples were compared to those formed in reference samples without LSs.

Figure 8 displays grains of left) ANL and right) CX cement after 30 min hydration without LSs. Both cements showed large areas of unhydrated surface and few initial hydrates. It was noted that the presence of hydrates was largest inside cavities and holes on the particles' surface.

Figure 9 and Figure 10 display a typical particle of ANL and CX cement after 30 minutes of hydration, respectively, with 1.5 mass % of binder LSs mixed with IA. Large portions of the particles' surface were covered with crystals. The crystals were cubic with size between 0.1 and 0.2 μm for ANL cement, and cuboidal with length between 0.2 and 0.4 μm for CX cement (aspect-ratio varying between 1.5:1 and 4:1). For CX cement, the crystals appeared to be larger in amount than in ANL cement, being located densely on top of each other on the cement grains' surface.

When the same LSs amount was added with DA, as shown in Figure 11 and in Figure 12 for ANL and CX cement, respectively, the surfaces of particles and hydrates appeared rough and irregular, with fewer well-defined crystals than when the LSs was added with IA (see Figure 9 and Figure 10).

SEM-EDS was performed in order to analyse the chemical composition of the crystals present on the surface of unhydrated cement grains. The results from the SEM-EDS analysis of two crystals are displayed in Figure 13 and in Figure 14. It has to be noticed that the crystals turned to more rounded shapes during the scanning due to dehydration.

The SEM-EDS line scans allowed a qualitative chemical analysis of a line of points which included both the crystals and the unhydrated cement grain below them. In both cements, the results showed that, in comparison to the cement grain on which the crystals lay, the crystals were richer in Al, S and Ca, while they contained less Si.

The chemical composition of the samples was analysed by performing SEM-EDS analysis on 4 points for each object analysed. The objects analysed were both the crystals and the underlying cement grains. The average content in Al, Si, S and Ca of 4 analysis points was calculated for both cement pastes. Al and S were used to identify the phase composing the crystals, as the crystals analysed were deposited on C_3S surfaces. The ratio between these two elements can indeed be used to identify the phase they belong to. The crystals were found to contain Al and S in ratio of about 1:3 in ANL cement and 1.8:3 in CX cement. The theoretical Al to S ratio in ettringite is 2:3. Considering the non-ideal conditions for SEM-EDS analysis (e.g. relief, small crystals, and charging material) and the limited number of data points, the

crystals were identified as ettringite, even though the observed ratio between Al and S was lower than the theoretical one for ettringite for both cement pastes.

3.3.2 After 6 hours of hydration

The ettringite formed by pastes of the two cements without LSs was observed with SEM at final setting. The aim was to verify whether the ettringite crystals formed by pastes of the two cements without the LSs at a later stage of hydration displayed a needle-like shape and to compare them to those formed after 30 minutes of hydration.

The analysis time was after 6 hours of hydration, which corresponded to a time right before the main hydration peak determined by isothermal calorimetry, as shown in a previous paper [29]. It was assumed that, at this time of hydration, a minor amount of AFm or no AFm was present. The results are shown in Figure 15 for ANL cement paste and in Figure 16 for CX cement paste.

The particles of both cement samples without LSs were completely covered by hydrates after 6 hours of hydration. C-S-H appeared as thin needles or fibres about 0.3 μm long and about 0.05 μm wide. The C-S-H fibres embedded some ettringite crystals varying in morphology. Some ettringite crystals appeared as parallelepipeds with dimensions about 0.10x0.15 μm, while other crystals appeared more needle-like, with dimensions about 0.4x0.1 μm. Some clinker grains displayed more ettringite crystals on their surface, others less. In general, there seems to be an indication of more ettringite crystals on the CX clinker grains compared to ANL ones, in agreement with the difference in cement composition and fineness.

The identification of ettringite and C-S-H was based on visual appearance and on the comparison to references in literature [30] and supported by SEM-EDS. Because of the high density of hydrates on the surface of unhydrated cement grains, it was difficult to analyse their chemical composition with SEM-EDS. However, the SEM-EDS analysis of the crystals visually identified as ettringite indicated that they contained Al and S, while the crystals identified as C-S-H appeared to be richer in Ca and Si.

3.4 BET

The BET surface area was measured for ANL and CX cement pastes with varying LSs amounts after 30 minutes of hydration. The hydration was stopped by solvent exchange after 30 minutes. The results are shown in Figure 17.

For both cements the surface area was found to increase as the dosage of plasticizer added to the cement paste increased. The increase in surface area was noticeably larger for CX than for ANL cement, and for IA compared to DA, corresponding to more AFt formed.

3.5 Adsorption isotherms

3.5.1 Cement pastes

The adsorption isotherms obtained for ANL and CX cement pastes were achieved by plotting the amount of consumed polymer versus the total amount of polymer added after 30 minutes of hydration. The tested dosages are given in Table 5. The LSs was added to the cement paste either immediately together with the mixing water (IA), or after 10 minutes of hydration

(DA). Note that the adsorption isotherm obtained for CX cement for IA could only be measured up to 1.0 mass % of binder LSs. At higher dosages it was not possible to extract pore water as the paste had hardened after 30 minutes of hydration. The results and their fits according to the Langmuir model [26] are presented as mass % of binder in Figure 18 a, and relative to the BET hydrated specific surface area (Table 3) available for adsorption in Figure 18 b.

Figure 18 a shows that, for DA, an adsorption plateau was found for both cements. At high LSs dosage the isotherms obtained for DA also displayed a considerably lower amount of LSs consumed by the cement pastes compared to the isotherms obtained for IA. According to the theory reported in [26], an adsorption plateau is achieved when full monolayer surface coverage is reached. Therefore, for DA, the LSs consumption was considered to be mainly due to monolayer surface adsorption on the cement particles and hydrates, as reported in a previous paper [15].

For IA, no adsorption plateau could be detected within the tested range, neither for ANL nor for CX cement. The isotherms' shape indicated a continuous LSs uptake as more LSs was added to the mix.

In Figure 18 b the consumed LSs was expressed relative to the available surface after 30 minutes of hydration. The adsorption isotherms of CX cement paste for IA and DA nearly coincided, both reaching and adsorption plateau. As found in [15], this indicates that the high LSs consumption by CX cement paste for IA was mainly due to monolayer surface adsorption on the large specific surface area caused by the additional ettringite formed.

For ANL cement, the amount of ettringite formed, and in turn the surface area, increased only moderately compared to CX cement (see Figure 17). Thus, as concluded in [15], surface adsorption could not entirely explain the measured LSs consumption. Therefore, for IA, other polymer consumption mechanisms, still to be determined, might have played a role in consuming the LSs in ANL cement paste.

3.5.2 Calcium sulfates

CX cement paste formed a larger amount of ettringite for IA compared to ANL cement paste. One of the differences between CX and ANL cement is the calcium sulfate source present, i.e. CX contains mainly anhydrite whereas ANL contains mainly gypsum (see Table 1). The difference in the amount of ettringite formed in both cement pastes might be related to the differences in the dissolution of the calcium sulfates i.e. enhanced dissolution of anhydrite compared to gypsum in the presence of LSs might have led to a higher amount of ettringite formed. In order to verify this, the interaction between the LSs and gypsum, hemihydrate and anhydrite was investigated. Adsorption isotherms were measured for anhydrite ($CaSO_4$), hemihydrate ($CaSO_4 \cdot 0.5H_2O$) and gypsum ($CaSO_4 \cdot 2H_2O$). The samples had water-to-powder ratio 1.0 and they were analysed 30 minutes after mixing. The results are displayed in Figure 19 with unit a) mass % of solid and b) g LSs / m^2 unhydrated surface. The isotherms of ANL for IA are also shown as reference.

Figure 19 a shows that the adsorption isotherms of the three different calcium sulfates reached a plateau, which corresponds to monolayer surface saturation. The influence of the surface area was eliminated by normalizing the adsorption isotherms obtained by the BET surface area of each calcium sulfate. The results shown in Figure 19 b display that the higher LSs consumption of anhydrite was due to its higher surface area. Hemihydrate still showed a LSs consumption slightly higher than gypsum and anhydrite. Even when taking into account a hypothetical 30 % error in the BET results, the trends shown in Figure 19 b did not noticeably change. The amount of LSs consumed by the calcium sulfates was, however, noticeably lower than the one of ANL cement for IA (which was similar to that of CX cement).

3.6 ICP-MS

The elemental concentration of Al, Ca, Fe, Si and S in the pore solutions extracted from ANL and CX cement pastes after 30 minutes of hydration was determined with ICP-MS. The cement pastes contained 0.8 and 1.5 mass % of binder LSs added either with IA and DA. Additionally, a reference sample without LSs was measured. Moreover, the content in Al, Ca, Fe, Si and S was also measured for two LSs solutions dissolved in artificial pore water at concentrations corresponding to those used in cement pastes (see Table 8). The artificial pore water composition is described in paragraph 2.1. The results from ICP-MS are shown in Figure 20 and reported in Table 8.

The samples mixed with DA showed an increase in Al, Fe and Si concentration dissolved in the pore solution as the LSs dosage increased. The increase was considerably larger for ANL cement than for CX cement. Only minor increases were measured for the samples mixed with IA. Moreover, except for CX cement for DA, the concentration of S and Ca appeared to be rather constant with increasing LSs dosage, in spite of the increased amount of these elements added by the increasing amount of LSs.

In order to investigate the effect of increasing LSs dosages on the solubility of the sulfates present in the cement pastes, the elemental concentration of Ca and S in the pore solution extracted from anhydrite, hemihydrate, and gypsum slurries after 30 minutes of hydration was determined with ICP-MS. The LSs dosages tested were 0.2, 0.4, 0.8 and 1.5 mass % of binder LSs added with IA. Additionally, a reference sample without LSs was measured. Moreover, the content in Ca and S was also measured for two LSs solutions dissolved in artificial pore water (see Table 9). The artificial pore water composition is described in paragraph 2.1.The results from ICP-MS are shown in Figure 21 and reported in Table 9.

The results, shown in Figure 21, highlight that, for LSs dosages between 0 and around 0.4 mass % of binder LSs, the trend of the content in Ca and S deviates from the one observed for higher LSs dosages. As shown by the isotherms in Figure 19, with LSs dosages under about 0.4 mass % of binder, all the samples were in a highly dynamic stage and far from reaching a constant level of surface adsorption. For this reason, the authors decided to focus on the values of Ca and S concentrations obtained for LSs dosages higher than about 0.4 mass % of binder. The content in Ca and S was found to be nearly independent of the LSs dosage for anhydrite and hemihydrate, while for gypsum it increased slightly as the LSs dosage increased. However, the increase was less than the Ca and S provided by the additional LSs.

3.7 TGA after 28 days of hydration

The effect of increasing the LSs dosage on the hydrates formed in hardened cement paste were investigated with TGA. The analysis was performed on ANL and CX cement pastes after 28 days of sealed curing at 20 ºC containing different dosages of LSs both for IA and DA. A reference sample of neat ANL and CX without LSs was also measured. The hydration of the tested samples was stopped after 28 days with the solvent exchange procedure with isopropanol and petroleum ether, as described in paragraph 2.3.2. The results are displayed in Figure 22.

The peak at about 125 ºC and the smaller one at 270 ºC indicate the presence of AFt. The peak around 170 ºC in this case represents most likely the decomposition of AFm, since it can be expected that, after 28 days of hydration, the sulfates are depleted. The peak around 480 ºC shows the decomposition of portlandite (CH). Note that C-S-H loses water over the entire temperature range from 50 to 600 ºC, with a main weight loss coinciding with the first ettringite peak just above 100 ºC. The peaks over 600 ºC represent the decomposition of carbonates (C$\underline{C}$). These can be attributed to the decomposition of limestone included in the used cements and, for the samples containing LSs, to the decomposition of LSs.

The peaks corresponding to ettringite and to, most likely, AFm strongly overlapped for most samples. It was therefore difficult to quantify the amount of these phases. Hence it was decided to present the results in terms of mass loss % of the mass of dry binder in different temperature intervals, as described in paragraph 2.3.3. The results are shown in Figure 23 and summarized in Table 10.

From the results shown in Figure 23 and reported in Table 10, it can be observed that, variations in the LSs dosage and time of addition (IA vs. DA), in general, led to little or no differences in mass loss % in the range comprising the AFt decomposition. For IA, there is an indication that the increase in LSs dosage for both cements led to a slight increase in the mass loss measured in interval 1 (AFt, AFm, C-S-H). As expected, the mass loss due to the decomposition of carbonates increased when more LSs was present in the mix. For ANL cement, the DA of 1.5 mass % of binder LSs caused the cement not to harden even after 28 days of hydration. For this reason the data of this sample is not showed in Figure 23 and is reported in brackets in Table 10.

4 DISCUSSION

4.1 Effect of LSs on ettringite formation in fresh cement paste

4.1.1 Ettringite amount

As displayed in Figure 1 and Figure 3, when LSs was added to the cement pastes with IA, a higher amount of ettringite was formed in both cements compared to the sample without LSs, up to a threshold LSs dosage of 1.5 mass % of binder. With equal LSs dosage, a larger amount of ettringite is observed in CX cement paste compared to ANL cement paste, which might have been influenced by the larger amount of C_3A and the higher fineness of CX cement compared to ANL cement.

A higher amount of ettringite crystals in CX cement paste when LSs was added with IA could also be observed with SEM, as shown in Figure 9 and Figure 10. The crystals observed in CX cement paste appeared to be located densely on top of each other on the cement grains' surface. The ettringite morphology will be discussed more in detail in paragraph 4.1.2.

With 1.5 mass % of binder LSs added with IA, the amount of ettringite calculated according to Equation 4 was about 8 and 14 mass % of the dry weight of cement for ANL and CX cement pastes, respectively, after 30 minutes of hydration. These amounts of ettringite appear feasible when compared to other references in literature [27, 31], taking into account possible differences due to the different materials used and time of analysis.

Theoretically, the maximum amount of ettringite that can form in a cementitious system is limited either by the amount of Al_2O_3 or by the amount of SO_3 available. The amount of ettringite that theoretically can form can be calculated with the following formulas, where M_m is the molar mass:

$$\text{Amount of AFt} = Al_2O_3 \text{ amount} \cdot \frac{\text{Mm (AFt)}}{\text{Mm } (Al_2O_3)} \quad (5)$$

$$\text{Amount of AFt} = SO_3 \text{ amount} \cdot \frac{\text{Mm (AFt)}}{\text{Mm } (SO_3)} \quad (6)$$

Knowing the amount of Al_2O_3 and SO_3 available, the theoretical amount of ettringite that was calculated. This amount was then compared to the amount of ettringite measured with TGA.

The Al_2O_3 amount was calculated only considering the aluminates contained in C_3A, since it was assumed that C_4AF only slightly reacted after 30 minutes of hydration. This resulted in 0.8 and 2.7 mass % Al_2O_3 in ANL and CX cement, respectively. The maximum amount of ettringite that could have formed with this amount of Al_2O_3 is 11 and 35 mass % of solid, respectively. These values are higher than those measured with TGA (8 and 14 mass % of solid for ANL and CX cement, respectively), therefore the alumina content appears not to be a limiting factor for the formation of ettringite.

The amount of SO_3, as measured with XRF (Table 2), was 3.3 and 3.6 mass % of solid in ANL and CX cements, respectively. The maximum amount of ettringite that could have formed with this amount of SO_3 is 18 and 20 mass % of solid, respectively. When these values are compared with the amount of ettringite formed in the system as measured with TGA (8 and 14 mass % of solid for ANL and CX cement, respectively), it can be noticed that neither the SO_3 content appears to be a limiting factor for the formation of ettringite.

On the other hand, the TGA curves and the XRD graphs indicated that not all the available calcium sulfates initially present in the system had reacted after 30 minutes of hydration, but about 1/3 were still unreacted. Additionally, some of the sulfates measured with XRF come from the clinker silicate phases, which can be expected to have reacted only in a limited manner after 30 minutes of hydration. Considering the possibility that only 2/3 of the sulfates measured with XRF had actually reacted after 30 minutes of hydration (based on the respective height of the peaks of the calcium sulfates with and without LSs in the XRD graph), the amount of ettringite that could have formed would be 12 and 13 mass % of solid

for ANL and CX cement paste, respectively. In this case, the amount of ettringite that could have formed, based on the amount of SO_3 available, was actually slightly lower than the one that was measured with TGA for CX cement. However, taking into account the variations in the results and the approximations made, the difference in the measured amount of ettringite by TGA and the calculated based on the SO_3 content available is negligible for the CX cement.

Finally, the LSs molecule contains sulfonate groups, which might replace the sulfates and enter in the ettringite structure. Indeed, the possible replacement of the sulfates coming from the calcium sulfates with the sulfonate groups contained in the LSs molecule, forming intercalated calcium aluminate hydrates, was highlighted by Stöber and Pöllmann [32, 33]. In the present paper, the highest amount of ettringite was formed in CX cement paste with 1.5 mass % of binder LSs for IA. This amount was found to be similar to the calculated amount of ettringite based on the amount of available sulfates (considering that 1/3 of the sulfates were left after 30 minutes of hydration). In addition, the inclusion of elements or molecules in the ettringite structure would have most likely caused a shift in the peaks representing ettringite in the XRD spectrum, which was not observed in the samples analysed. Therefore, the intercalation of the sulfonate groups of the LSs appeared to be a minor mechanism, if present at all.

In conclusion, the amount of ettringite measured by TGA was large, but feasible when compared with literature. In the sample where the largest amount of ettringite formed, enough aluminates and sulfates were available to form the entire amount of ettringite. Therefore, mechanisms such as intercalation of sulfonate groups from the LSs molecule in the ettringite structure seemed minor, if present at all.

4.1.2 Ettringite morphology

ANL and CX cement paste with 1.5 mass % of binder LSs added either with IA or with DA where hydration was stopped after 30 minutes were studied with SEM in order to investigate possible changes in hydrates morphology caused by the addition of LSs. The results were compared to those obtained for pastes of the two cements without LSs. After 30 minutes of hydration, ANL and CX cement grains appeared to be partially covered by crystals, identified as ettringite with EDS (Figure 13 and Figure 14). The degree of coverage and the crystals' size varied according to the presence of LSs and to its addition method: considerably fewer smaller crystals were found for the samples without LSs and for the ones where the LSs was added with DA compared to when the LSs was added with IA.

Several studies in literature found that plasticizers can change the morphology of ettringite from the typical needle-like structure, to a more round or cubic one [6-9]. In partial disagreement, Kerui et al. [10] found that the shape of the ettringite crystals was changed from numerous small needles to few large needle-like crystals. Indeed, as observed by Shi et al. [34] and hypothesized by Dalas et al. [12], superplasticizers can inhibit ettringite growth by adsorbing on their surface. The crystal shape will therefore depend on the preferred surface for adsorption. In the present study, the ettringite is visually observed in a real cement system and not as a pure synthesized phase. The crystals observed for the two cements appeared of

different size and shape: cubic with size between 0.1 and 0.2 μm for ANL cement (Figure 9), and with cuboidal shape with length between 0.2 and 0.4 μm for CX cement (aspect-ratio varying between 1.5:1 and 4:1) (Figure 10).

When comparing samples of the same cement containing no LSs or 1.5 mass % of binder LSs added with IA or with DA after 30 minutes of hydration, it can be noticed that the crystals of ettringite displayed a similar cubic or cuboidal shape for all samples. It can be therefore concluded that, after 30 minutes of hydration, the addition of LSs did not lead to changes in ettringite shape for the cements analysed in this study.

Finally, ANL and CX cement paste without LSs were investigated with SEM after 6 hours of hydration. The aim was to verify whether the ettringite crystals formed by pastes of the two cements without the LSs at a later stage of hydration displayed a needle-like shape. The time of analysis corresponded to a time right before the main hydration peak determined by isothermal calorimetry, as shown in a previous paper [29], when the ettringite crystals were expected to be fully developed. The results (Figure 15 and Figure 16) displayed no major difference in ettringite morphology between the samples with 1.5 mass % of binder LSs added with IA hydrated for 30 minutes and those without LSs hydrated for 6 hours, and between the two cements. Indeed, in both systems the ettringite crystals appeared with a compact and cuboidal shape instead of the expected needle-like shape.

In conclusion, for the system analysed in this paper, no changes in the morphology of the ettringite crystals appeared to be caused by the LSs addition. These results do not fully agree with what found by other studies in literature [6-10]. This might be connected to the analytical technique used and to potential difference in the behaviour of synthetic ettringite crystals and ettringite in a hydrating cement paste.

4.2 Effect of LSs on the solubility of cement phases and calcium sulfates

The LSs used for the experiments reported in this paper is particularly rich in Ca and S (see Table 8).

Increasing dosages of LSs led to an increased concentration of Al, Fe, and Si in the pore solution of ANL and CX cement pastes (Figure 21), as shown from the ICP-MS results (Table 8). The concentration of these elements was particularly pronounced for DA. For DA, the LSs addition did not change the amount nor the type of hydrates formed by the cement pastes. Therefore, the presence of more Al, Fe and Si indicates that the dissolution of all the cement phases was increased by the LSs addition after 30 minutes of hydration. A higher dispersion of the cement grains also might have played a role.

The higher amount of ettringite formed in the CX cement might be due to a higher dissolution of the anhydrite present in CX compared to the dissolution of gypsum present in ANL. In order to verify this or rule this out, the content in Ca and S of the pore solution extracted from gypsum, hemihydrate and anhydrite slurries containing increasing LSs dosages was measured. For LSs dosages higher than about 0.4 mass % of binder, the LSs adsorption by all the calcium sulfates was constant and reached a plateau, as shown by Figure 19. Therefore, when more LSs was added in the solution, one would expect the concentration in Ca and S to

increase, as LSs is rich in both elements. However, as the LSs dosage increased, the calcium sulfates showed a different behaviour: the content in Ca and S was found to be nearly constant in the pore solutions extracted from anhydrite and hemihydrate, while it increased in the pore solution of gypsum. However, the increase in Ca and S content was lower than it would be expected from the added LSs (Table 9). These results indicate that the LSs might even suppress the dissolution of gypsum, anhydrite and hemihydrate after 30 minutes of hydration.

In conclusion, for DA, the dissolution of all the cement phases was increased by the LSs addition after 30 minutes of hydration. As to the calcium sulfates, for IA, the dissolution of gypsum, hemihydrate and anhydrite was found not to be enhanced upon LSs addition. Therefore, it appears that the large increase in ettringite formed was not due to an increased dissolution of the calcium sulfates.

4.3 On the surface area and LSs consumption by cement paste

In a previous article [15], the increase in the amount of ettringite formed in cement paste after 30 minutes of hydration was found to correspond to an increase in the hydrated surface area, as shown in Figure 24. The increase in surface area was larger when the LSs was mixed with IA and for CX cement.

As shown in Figure 1 and in Figure 3, a difference in amount of ettringite formed was found between IA and DA with the same LSs dosage for pastes of both cements. This led to a difference in surface area between IA and DA, especially for CX cement (Figure 24). This caused, in turn, a difference in LSs consumption for monolayer adsorption between IA and DA (Figure 18 a).

The amount of LSs that could potentially adsorb in a monolayer on the additional amount of ettringite formed for IA was calculated. The following assumptions were made:

- The ettringite is characterized by a density of 1778 kg/m^3 [35], a cubic shape, and an average size of 0.15 μm for ANL cement and 0.3 μm for CX cement;
- The entire ettringite surface area is available for polymer adsorption;
- The molecular footprint of LSs is 27.5 nm^2 for both cements. This value is an average of the molecular footprints of the two cements, as calculated in a previous paper [15] based on the amount of LSs adsorbed on the cement surface at the plateau value in the adsorption isotherms.

The calculated amount of consumed LSs was compared to the difference in consumed LSs amount experimentally measured between the sample mixed with IA and the one mixed with DA at the LSs dosages of 0.8 and 1.5 mass % of binder (Table 11). The calculated ettringite amounts were found to be lower than the measured ones for all the samples. However, for CX cement, the calculated amount was relatively close to the measured amount, also taking into account the error connected to the approximations made.

These results confirm that, for CX cement, the difference in LSs consumption between IA and DA appears to mainly be due to the additional surface available for adsorption given by the increased ettringite amount formed for IA. On the contrary, for ANL cement, the difference in

LSs consumption between IA and DA cannot be due solely to the additional surface offered by the increased ettringite formed for IA.

4.4 Impact of the increased amount of ettringite on setting time and rheology of cement paste

As investigated in a previous paper [29], the increased formation of ettringite seems to have an impact on the properties of fresh cement paste, in particular on setting time and rheology. The following aspects will be separately discussed in the following paragraphs.

4.4.1 On the setting time of cement paste

In a previous paper [29] it was found that the setting retardation was directly correlated to the amount of free LSs in the pore solution. In the samples which formed the higher amounts of ettringite (IA), the increased LSs adsorption caused by the additional surface area reduced the amount of free LSs in the pore solution compared to DA for the same LSs dosage. This was reflected in a lower setting retardation for IA compared to DA for the same LSs dosage. In addition, the retardation appeared to be less sensitive to small variations in dosing for IA than for DA, i.e. the system was more robust for IA. Small variations in the dosing of the LSs with DA led to large differences in retardation: the same LSs dosage of 0.4 mass % of binder caused an increase in setting retardation of 21 and 11 hours for ANL and CX cement respectively, when compared to the setting retardation caused by the same LSs dosage added with IA. This severe delay of setting can be a source of incompatibility between cement and plasticizer.

4.4.2 On the rheology of cement paste

The presence of numerous ettringite crystals on the surface of unhydrated cement grains, as observed in the present paper, could change the workability of the cement paste. The increased formation of ettringite led to early stiffening of the cement paste, reduced workability until potential rapid set, as measured in a previous paper [29] for CX cement with 1.5 mass % of binder LSs added with IA. This is a form of incompatibility between cement and plasticizer.

4.5 Effect of LSs on the hydrates of hardened cement paste

In light of the differences in amount of ettringite in fresh cement paste caused by the addition of LSs, the effect of LSs on the hydrates of 28 days-old cement were also investigated.

From the TGA results shown in Figure 23 and reported in Table 10, it can be observed that, in all intervals, few or no differences in mass loss could be observed; neither between samples containing different LSs amounts, nor between the samples prepared with IA and those prepared with DA. The most noticeable change, even though still of limited entity in a general scale, was observed for IA, where the increase in LSs dosage led for both cements to a slight increase in the mass loss measured in interval 1 (AFt, AFm, C-S-H). In particular, the intensity of the peak corresponding to the decomposition of ettringite was found to increase slightly with the LSs dosage, especially for ANL cement.

In conclusion, the addition of LSs and its addition time seemed not to play a major role in type and amount of hydrates formed in ANL and CX cement pastes after 28 days of

hydration. For DA, the addition of a high LSs dosage (compared to the dosages normally used in practice), was found to cause lack of hardening in ANL cement even after 28 days of hydration.

5 CONCLUSIONS

The aim of this paper was to investigate the effect of varying dosages of a softwood calcium lignosulfonate (LSs) on the amount and morphology of ettringite formed in Portland cement paste. Two Portland cements, CX and ANL, mainly differing in surface area and C_3A content were chosen; CX had higher surface area and C_3A content than ANL. The influence of two different LSs addition methods was investigated. The LSs was either added immediately to the cement with the mixing water (IA), or after 10 minutes of hydration (DA). The following conclusions are drawn:

Immediate addition (IA) of LSs to the cement pastes led to a considerable increase in the amount of ettringite formed compared to pastes of the same cements without LSs. Delayed addition (DA) of LSs did not affect the amount of ettringite formed.

For the systems analyzed in this paper, no changes in the morphology of the ettringite crystals appeared to be caused by LSs addition.

SEM imaging allowed observing the finely dispersed ettringite crystals in the cement paste. In case of immediate addition (IA) of LSs, the ettringite shape was cubic with size between 0.1 and 0.2 μm for ANL cement, and cuboidal with length between 0.2 and 0.4 μm for CX cement (aspect-ratio varying between 1.5:1 and 4:1).

The study of pure calcium sulfate systems indicated that the large amount of ettringite formed upon LSs addition with IA was not due to an increased dissolution of the calcium sulfates.

The presence of numerous small ettringite crystals on the surface of unhydrated cement grains upon LSs addition with IA led to an increase in plasticizer adsorption. This renders the system more robust, i.e. less sensitive to variations in dosing, regarding retardation and slump loss compared to DA. However, the large amount of crystals might potentially cause incompatibility problems due to early stiffening.

After 28 days of hydration, no noticeable effect of LSs addition and of its addition time on the amount of hydrates formed was observed, despite the large differences in the amount of ettringite formed after 30 minutes.

6 ACKNOWLEDGEMENTS

The authors wish to acknowledge the Norwegian Research Council (NFR 225358/O30) and Borregaard AS, Norway, for financing this research work. Gwenn Le Saoût and Nathalie Azema, Ecole des Mines d'Ales, France, are also acknowledged for the helpful discussions. Verner Håkonsen, NTNU, Norway, is acknowledged for performing the SEM-EDS analysis. Syverin Lierhagen, NTNU, is acknowledged for performing the ICP-MS analysis. Irene

Bragstad, SINTEF, Norway, is acknowledged for performing the BET particle surface measurements.

7 REFERENCES

[1] J. Bensted, P. Barnes, Structure and performance of cements, Taylor & Francis2002.
[2] Y.F. Houst, P. Bowen, F. Perche, A. Kauppi, P. Borget, L. Galmiche, J.-F. Le Meins, F. Lafuma, R.J. Flatt, I. Schober, P.F.G. Banfill, D.S. Swift, B.O. Myrvold, B.G. Petersen, K. Reknes, Design and function of novel superplasticizers for more durable high performance concrete (superplast project), Cement and Concrete Research, 38 (2008) 1197-1209.
[3] K. Yoshioka, E.-i. Tazawa, K. Kawai, T. Enohata, Adsorption characteristics of superplasticizers on cement component minerals, Cement and Concrete Research, 32 (2002) 1507-1513.
[4] A. Zingg, F. Winnefeld, L. Holzer, J. Pakush, S. Becker, L. Gauckler, Adsorption of polyelectrolytes and its influence on the rheology, zeta potential, and microstructure of various cement and hydrate phases, Journal of Colloid and Interface Science, 323 (2008) 301-312.
[5] J. Plank, P. Chatziagorastou, C. Hirsch, New model describing distribution of adsorbed superplasticizer on the surface of hydrating cement grain, Jianzhu Cailiao Xuebao, 10 (2007) 7-13.
[6] W. Prince, M. Edwards-Lajnef, P.C. Aïtcin, Interaction between ettringite and a polynaphthalene sulfonate superplasticizer in a cementitious paste, Cement and Concrete Research, 32 (2002) 79-85.
[7] E.E. Hekal, E.A. Kishar, Effect of sodium salt of naphthalene-formaldehyde polycondensate on ettringite formation, Cement and Concrete Research, 29 (1999) 1535-1540.
[8] A.M. Cody, H. Lee, R.D. Cody, P.G. Spry, The effects of chemical environment on the nucleation, growth, and stability of ettringite [Ca3Al(OH)6]2(SO4)3·26H2O, Cement and Concrete Research, 34 (2004) 869-881.
[9] T. Danner, H. Justnes, M. Geiker, R.A. Lauten, Early hydration of C3A–gypsum pastes with Ca- and Na-lignosulfonate, Cement and Concrete Research, 79 (2016) 333-343.
[10] Y. Kerui, Z. Caiwen, L. Zhigang, The influence of calcium lignosulphonate–sodium bicarbonate on the status of ettringite crystallization in fly ash cement paste, Cement and Concrete Research, 32 (2002) 51-56.
[11] A. Zingg, Cement-superplasticizer interaction: link between macroscopic phenomena and microstructural data on the early cement hydration, Swiss Federal Institute of Technology Zurich, 2008.
[12] F. Dalas, S. Pourchet, D. Rinaldi, A. Nonat, S. Sabio, M. Mosquet, Modification of the rate of formation and surface area of ettringite by polycarboxylate ether superplasticizers during early C3A–CaSO4 hydration, Cement and Concrete Research, 69 (2015) 105-113.
[13] M. Bishop, B.A. R., Cement Hydration Inhibition with Sucrose, Tartaric Acid, and Lignosulfonate: Analytical and Spectroscopic Study, Industrial & Engineering Chemistry Research, 45 (2006) 7042-7049.

[14] T. Danner, H. Justnes, M. Geiker, R.A. Lauten, Phase changes during the early hydration of Portland cement with Ca-lignosulfonates, Cement and Concrete Research, 69 (2015) 50-60.
[15] A. Colombo, M. Geiker, H. Justnes, R.A. Lauten, K. De Weerdt, On the mechanisms of consumption of calcium lignosulfonate by cement paste, Cement and Concrete Research, (2016, In review).
[16] G. Le Saoût, V. Kocaba, K. Scrivener, Application of the Rietveld method to the analysis of anhydrous cement, Cement and Concrete Research, 41 (2011) 133-148.
[17] R.G. Gilbert, M. Hess, A.D. Jenkins, R.G. Jones, P. Kratochvil, R.F.T. Stepto, Dispesity in polymer science, Pure applied chemistry, 81 (2009) 351-353.
[18] H. Vikan, Rheology and reactivity of cementitious binders with plasticizers, Department of Materials Science and Engineering, NTNU Trondheim, 2005.
[19] J. Hot, Influence des polymères de type superplastifiants et agents entraineurs d'air sur la viscosité macroscopique des matériaux cimentaires, Université Paris-Est, Paris, 2013.
[20] I. Aiad, Influence of time addition of superplasticizers on the rheological properties of fresh cement pastes, Cement and Concrete Research, 33 (2003) 1229-1234.
[21] G. Chiocchio, A.E. Paolini, Optimum time for adding superplasticizer to Portland cement pastes, Cement and Concrete Research, 15 (1985) 901-908.
[22] K.-C. Hsu, J.-J. Chiu, S.-D. Chen, Y.-C. Tseng, Effect of addition time of a superplasticizer on cement adsorption and on concrete workability, Cement and Concrete Composites, 21 (1999) 425-430.
[23] F. Perche, Adsorption de Polycarboxylates et de Lignosulfonates sur Poudre modele et Ciments, École Polytechnique Federale de Lausanne, 2004.
[24] K.R. Ratinac, O.C. Standard, P.J. Bryant, Lignosulfonate adsorption and stabilization of lead zirconate titanate in aqueous suspension, Journal of Colloid and Interface Science, 273 (2004) 442-454.
[25] H. Uchikawa, S. Hanehara, T. Shirasaka, D. Sawaki, Effect of admixture on hydration of cement, adsorptive behaviour of admixture and fluidity and setting of fresh cement paste, Cement and Concrete Research, 22 (1992) 1115-1129.
[26] P.C. Hiemenz, R. Rajagopalan, Principles of colloid and surface chemistry, Taylor & Francis Group1997.
[27] K. De Weerdt, M.B. Haha, G. Le Saout, K.O. Kjellsen, H. Justnes, B. Lothenbach, Hydration mechanisms of ternary Portland cements containing limestone powder and fly ash, Cement and Concrete Research, 41 (2011) 279-291.
[28] S. Mantellato, M. Palacios, R.J. Flatt, Impact of sample preparation on the specific surface area of synthetic ettringite, Cement and Concrete Research, 86 (2016) 20-28.
[29] A. Colombo, M. Geiker, H. Justnes, R.A. Lauten, K. De Weerdt, On the effect of calcium lignosulfonate on the rheology and setting time of cement paste, Cement and Concrete Research, (2016, In review).
[30] A. Bazzoni, Study of early hydration mechanisms of cement by means of electron microscopy, École Polytechnique Fédérale de Lausanne, Lausanne, 2014.
[31] K.L. Scrivener, T. Füllmann, E. Gallucci, G. Walenta, E. Bermejo, Quantitative study of Portland cement hydration by X-ray diffraction/Rietveld analysis and independent methods, Cement and Concrete Research, 34 (2004) 1541-1547.

[32] S. Stöber, H. Pöllmann, Basic investigations on the crystal chemistry of sulfonate containing AFm-phases, 11th International Congress on the Chemistry of CementDurban, South Africa, 2003.
[33] S. Stöber, H. Pöllmann, Crystalchemistry of organic sulfonates used as cement additives, Materials Science Forum, 278-281 (1998) 904-908.
[34] C. Shi, G. Zhang, T. He, Y. Li, Effects of superplasticizers on the stability and morphology of ettringite, Construction and Building Materials, 112 (2016) 261-266.
[35] M. Balonis, F.P. Glasser, The density of cement phases, Cement and Concrete Research, 39 (2009) 733-739.

Notation

ANL	Anlegg cement (CEM I 52.5 N)
CX	Cemex cement (CEM I 52.5 R)
$C\underline{S}H_x$	Calcium sulfate hydrates
$\underline{C}$	Carbonates (contained in $CaCO_3$ and in the LSs)
DA	delayed addition of plasticizer (10 min)
IA	immediate addition of plasticizer
LSs	softwood low-sugar Ca-lignosulfonate
OPC	ordinary Portland cement
w/b	water-binder ratio
-COOH	carboxyl group
φ-OH	phenolic OH-group

List of tables

List of figures

Tables

Table 1 – *Main phases in cement ANL and CX from XRD-Rietveld analysis [a]: results obtained with TGA analysis*

Phase composition (mass % of powder)	**ANL**	**CX**
Alite	60.5	54.3
Belite	14.2	18.8
Aluminate cubic	1.3	4.7
Aluminate orthorhombic	0.9	2.4
Ferrite	14.0	6.5
Periclase	0.4	1.1
Quartz	0.3	-
Calcite	3.2/ 3.8 [a]	3.6/ 3.7 [a]
Portlandite	1.1/ 1.4 [a]	2.6/ 2.5 [a]
Anhydrite	-	2.1
Hemihydrate	2.6	1.8
Gypsum	1.0	-
Arcanite		0.6
Aphthitalite	0.4	0.7
Thenardite	-	0.8

Table 2 – *Chemical composition of the cements given by the producers*

Chemical compound (mass % of powder)	**ANL**	**CX**
CaO	62.7	64.0
SiO_2	20.6	20.0
Al_2O_3	4.4	4.6
Fe_2O_3	3.5	2.6
SO_3	3.3	3.6
MgO	1.6	2.4
K_2O	0.4	1.0
Na_2O	0.3	0.2

TiO_2	0.2	0.2
P_2O_5	0.2	0.2
LOI (%) 1000 °C	1.6	1.7
Sum	97.2	98.9

Table 3 - *Physical properties of the materials used*

	ANL	CX	Anhydrite	Hemihydrate	Gypsum
Surface area (BET) (m^2/kg)	890	1330	3000	550	580
Blaine surface (m^2/kg)	360	540			
Density (g/cm^3)	3.1	3.1			
d_{10} (µm)	2.0	2.0			
d_{50} (µm)	12.0	10.0			
d_{90} (µm)	34.0	26.0			

Table 4 - *Chemical and physical properties of LSs*

Mw	g/mol	29000
Mn	g/mol	2100
Organic S ($\propto SO_3$)	mass %	4.6
SO_4^{2-}	mass %	0.9
Ca^{2+}	mass %	4.6
Na^+	mass %	0.9
-COOH	mass %	7.1
φ-OH	mass %	1.4
Total sugar	mass %	8.3

Table 5 – *Analysed samples to obtain adsorption isotherms*

Material	LSs addition procedure	LSs dosage (mass % of binder)
ANL cement	IA	0.1; 0.2; 0.4; 0.6; 0.8; 1.2; 1.5; 2.0; 3.0
	DA	0.05; 0.1; 0.25; 0.4; 0.8; 1.2; 1.5
CX cement	IA	0.1; 0.2; 0.4; 0.6; 0.8; 1.0
	DA	0.05; 0.1; 0.2; 0.4; 0.8; 1.2; 1.5

Table 6 – *Mass loss (% dry binder) of ANL and CX cements with increasing amount of LSs added with IA and DA after 30 minutes of hydration. The mass loss is calculated in three temperature intervals: 1: ettringite, calcium sulfates, possibly C-S-H; 2: CH; 3: carbonates. The sum of the mass loss in interval 1 and 2 represents the amount of bound water. *:40-350 ºC for CX cement*

Cement type	LSs dosage	Addition procedure	Interval 1 40-300 ºC *	Interval 2 300-500 ºC	Interval 3 500-850 ºC	Bound water 40-500 ºC
			Mass % of dry binder			
ANL	0		2.8	0.6	2.1	3.3
	0.8		2.5	0.4	2.6	3.0
	1.5	IA	3.9	0.8	4.8	4.7
	2.0		2.5	0.6	3.9	3.1
	3.0		3.0	0.7	4.4	3.7
	0.8	DA	2.7	0.2	2.7	2.8
	1.5		2.7	0.7	3.9	3.4
CX	0		2.9	0.8	2.0	3.7
	0.8		4.7	0.9	3.4	5.6
	1.5	IA	6.7	1.0	4.4	7.7
	2.0		5.7	1.0	5.3	6.7
	3.0		4.9	1.0	5.8	5.8
	0.8	DA	2.4	0.8	3.0	3.1
	1.5		2.8	0.9	4.1	3.7

Table 7 – *Summary of the elements detected with XRD in ANL and CX cement pastes with 0/0.8/1.5 mass % of binder LSs (IA) which hydration was stopped after 30 minutes*

Angle 2θ	Element	Symbol in graph
9.1	Ettringite	AFt
11.6; 20.7	Gypsum	G
12.2; 24.3	C_4AF	F
14.9	C_3S	C_3S
23.0	$CaCO_3$/AFt	Cc/AFt
25.4	Anhydrite	A

Table 8 - *Elemental concentration of Al, Fe, Ca, Si, and S in ANL and CX cements with 0, 0.8 or 1.5 mass % of binder LSs after 30 minutes hydration, and in two LSs solutions (mmol/L): the 2.0 and 3.7 % LSs solutions were used for the cement samples with 0.8 and 1.5 mass % of binder LSs respectively*

Sample	**LSs dosage**	**Al**	**Ca**	**Fe**	**S**	**Si**
	Mass % of binder			Mass %		
ANL IA	0	0.01	24	0	77	0.09
	0.8	0.01	26	0.01	96	0.11
	1.5	0.02	45	0.07	139	0.12
ANL DA	0.8	1.1	38	0.55	100	0.85
	1.5	3.6	52	1.4	72	2.6
CX IA	0	0.01	24	0	176	0.09
	0.8	0.01	10	0.02	169	0.30
	1.5	0.01	54	0.11	141	0.36
CX DA	0.8	0.01	28	0.11	176	0.23
	1.5	0.79	50	0.45	193	0.56
2.0 % LSs sol.		0.02	18	0.02	37	0.31
3.7 % LSs sol.		0.03	32	0.03	66	0.27

Table 9 - *Elemental concentration of Ca and S in the pore solution (mmol/L) of calcium sulfate anhydrous, hemihydrate, and dihydrate, analysed after 30 minutes of hydration, and in two LSs solutions (mmol/L) (2.0 and 3.7 %)*

Sample	**LSs dosage**	**Ca**	**S**
	Mass % of binder	Mass %	
$CaSO_4$	0	34	68
	0.2	38	55
	0.4	36	55
	0.8	30	52
	1.5	30	57
$CaSO_4 \cdot 0.5H_2O$	0	28	74
	0.2	83	93

	0.4	75	86
	0.8	67	83
	1.5	66	85
$CaSO_4 \cdot 2H_2O$	0	20	57
	0.2	30	44
	0.4	42	53
	0.8	63	77
	1.5	72	89
2.0 % LSs sol.		18	37
3.7 % LSs sol.		32	66

Table 10 - *Mass loss (% dry binder) of ANL and CX cements with increasing amount of LSs added with IA and DA after 28 days of hydration. The mass loss is calculated in three temperature intervals: 1: AFt, calcium sulfates, AFm, possibly C-S-H, other hydrates; 2: CH; 3: carbonates. The sum of the mass loss in interval 1 and 2 represents the amount of bound water.*

Cement type	LSs dosage	Addition procedure	Interval 1	Interval 2	Interval 3
			40-420 ºC	420-540 ºC	540-850 ºC
			Mass % of solid		
ANL	0		19.3	5.6	3.8
	0.8	IA	21.0	5.7	4.7
	1.5		22.1	5.7	5.3
	0.8	DA	18.0	5.3	4.0
	1.5		-	-	-
CX	0		21.3	5.8	4.5
	0.8	IA	21.7	5.6	5.2
	1.5		22.4	5.5	5.6
	0.8	DA	21.8	6.0	4.6
	1.5		20.9	5.8	5.5

Table 11 – *Comparison between the amount of LSs that could potentially adsorb in a monolayer on the additional amount of ettringite formed for IA ("calculated Δ"), and the difference in consumed LSs amount experimentally measured between the sample mixed with IA and the one mixed with DA ("measured Δ")*

Cement	**LSs dosage**	**Calculated Δ consumed LSs IA-DA**	**Measured Δ consumed LSs IA-DA**
	mass % of binder	mass % of binder	mass % of binder
ANL	0.8	0.07	0.25
	1.5	0.17	0.72
CX	0.8	0.12	0.16
	1.5	0.18	n.a.

Figures

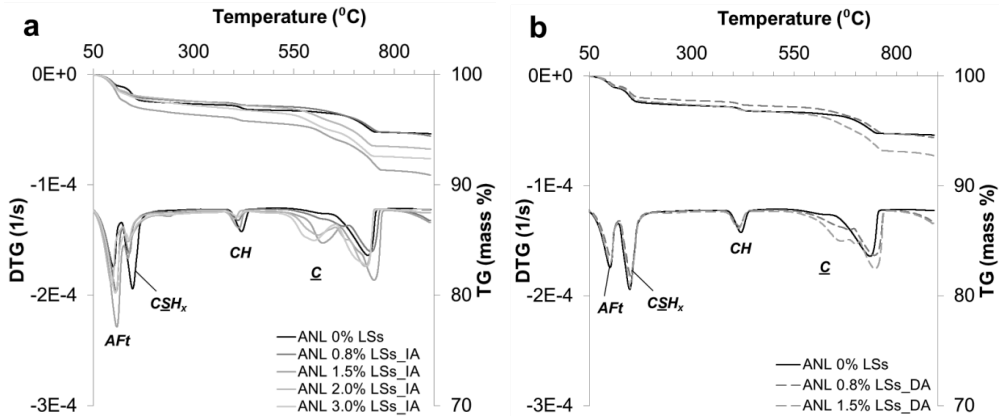

Figure 1 – *TG and DTG curves of ANL cement paste without LSs or a) with 0.8, 1.5, 2.0, 3.0 mass % of binder LSs mixed with IA, or b) with 0.8 and 1.5 mass % of binder LSs mixed with DA. Hydration was stopped after 30 minutes. The peaks corresponding to the decomposition of ettringite (AFt), calcium sulfates ($C\underline{S}H_x$), portlandite (CH) and carbonates ($\underline{C}$) are marked in the figures.*

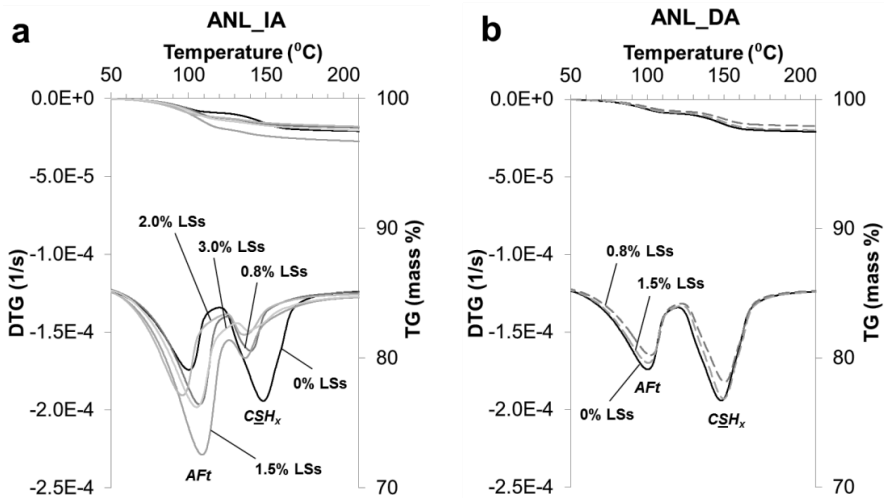

Figure 2 - *TG and DTG curves of ANL cement paste without LSs or with a) 0.8, 1.5, 2.0, 3.0 mass % of binder LSs mixed with IA and b) 0.8, 1.5 mass % of binder LSs mixed with DA , for which hydration was stopped after 30 minutes (Part of Figure 1; temperature range: 50-210 ºC). The peaks corresponding to the decomposition of ettringite (AFt) and calcium sulfates ($C\underline{S}H_x$) are marked in the figures.*

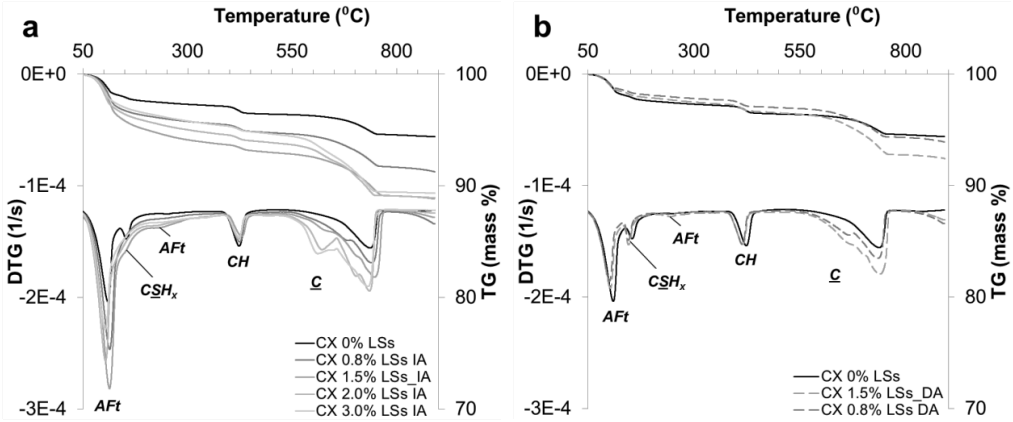

Figure 3 – *TG and DTG curves of CX cement paste without LSs or with 0.8, 1.5, 2.0, 3.0 mass % of binder LSs mixed with a) IA and b) DA, for which hydration was stopped after 30 minutes. The peaks corresponding to the decomposition of ettringite (AFt), anhydrite, hemihydrate or gypsum ($C\underline{S}H_x$), portlandite (CH) and carbonates ($\underline{C}$) are marked in the figures.*

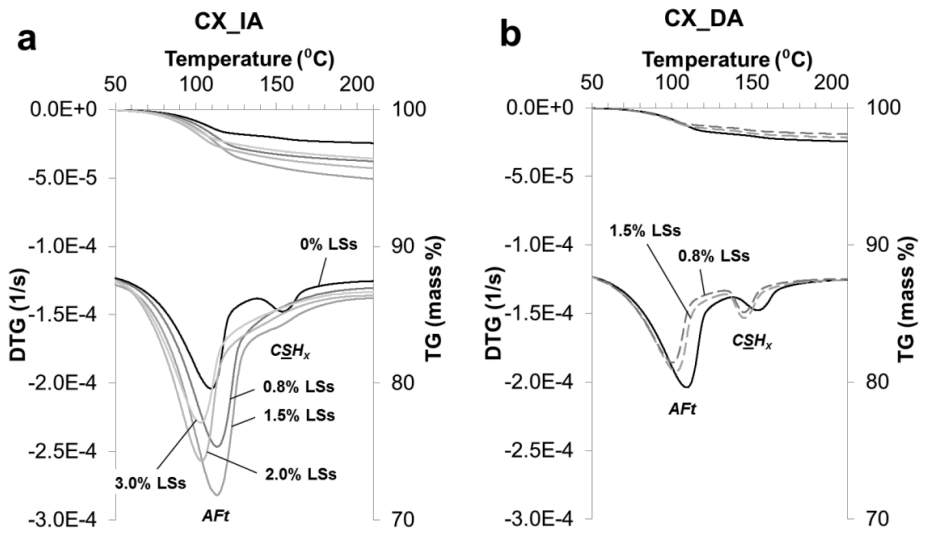

Figure 4 - *TG and DTG curves of CX cement paste without LSs or with a) 0.8, 1.5, 2.0, 3.0 mass % of binder LSs mixed with IA and b) 0.8, 1.5 mass % of binder LSs mixed with DA, for which hydration was stopped after 30 minutes (Part of Figure 3; temperature range: 50-210 ºC). The peaks corresponding to the decomposition of ettringite (AFt) and calcium sulfates (C$\underline{S}H_x$) are marked in the figures.*

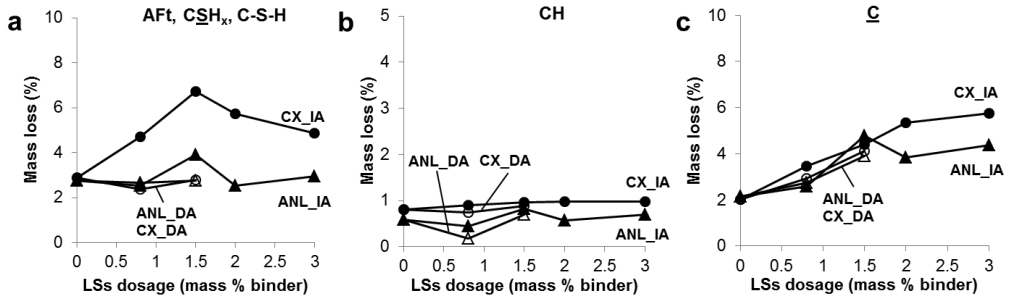

Figure 5 – *Mass loss (% of initial weight) due to a) ettringite (AFt), calcium sulfates (C$\underline{S}H_x$), possibly C-S-H; b) CH; c) carbonates (C) vs. LSs dosage (mass % of binder) for ANL and CX cements with increasing amount of LSs added with IA and with DA. NB. The scale of the y-axis of figure b is different from the one of the other figures.*

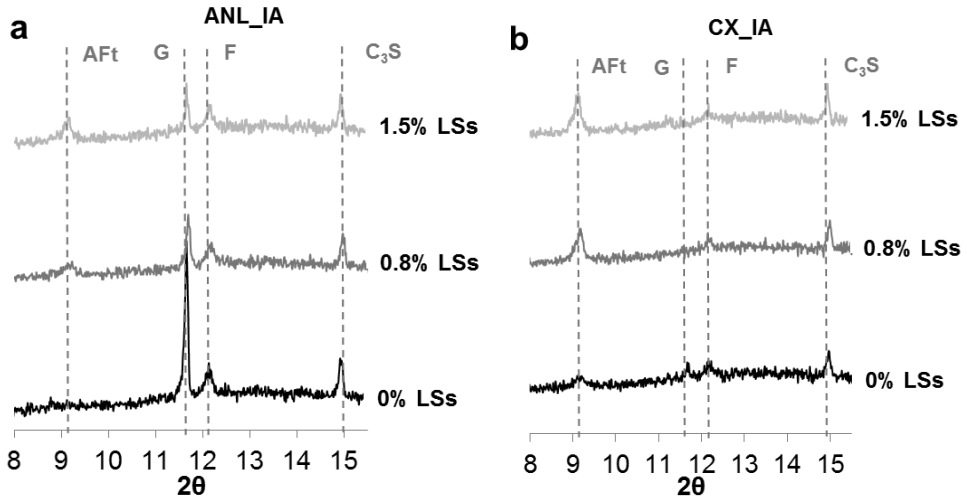

Figure 6 – *X-ray diffraction curves from 2θ = 9 º to 15.5 º for a) ANL and b) CX cement pastes with 0, 0.8, 1.5 mass % of binder LSs (IA) which hydration was stopped after 30 minutes. Several peaks are displayed in the figures: AFt: ettringite; G: gypsum; F: C_4AF; C_3S*

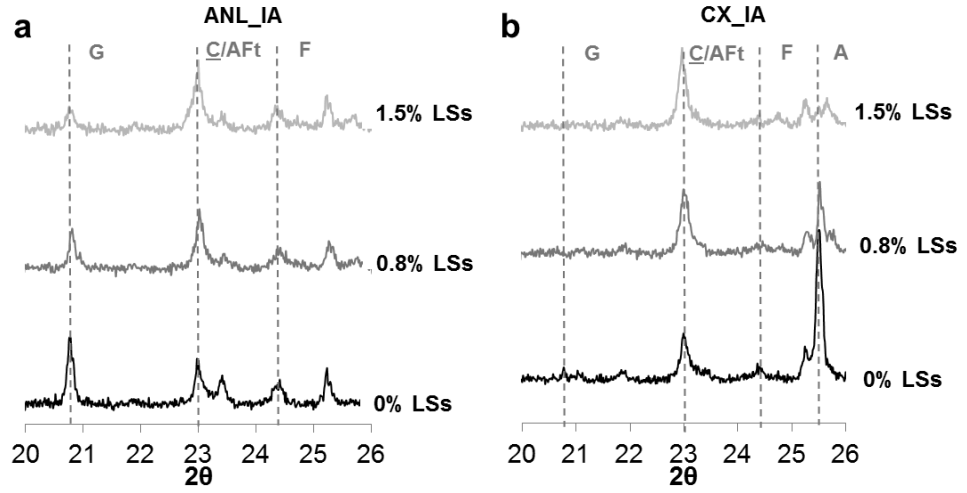

Figure 7 - *X-ray diffraction curves from 2θ = 20 º to 26 º for a) ANL and b) CX cement pastes with 0, 0.8, 1.5 mass % of binder LSs (IA) which hydration was stopped after 30 minutes. Several peaks are displayed in the figures: G: gypsum; C: $CaCO_3$; F: C_4AF; A: anhydrite*

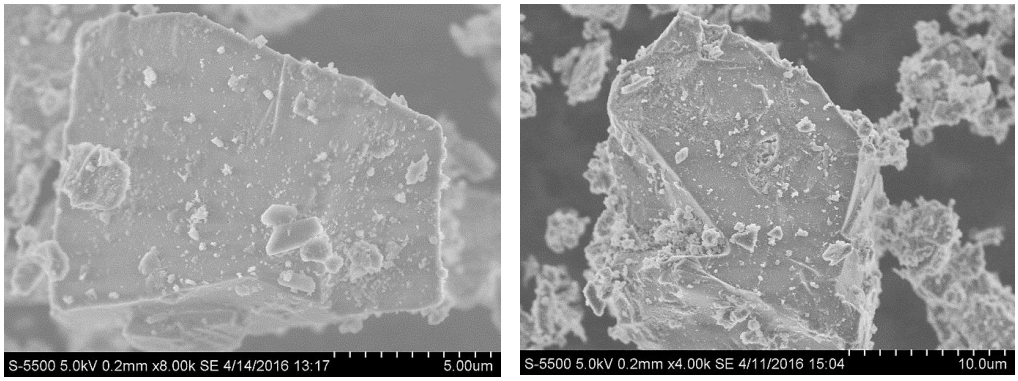

Figure 8 – *SEM images of cement grains of left) ANL and right) CX cement after 30 minutes of hydration without LSs. Width of micrograph: left) 16 µm, and right) 31 µm*

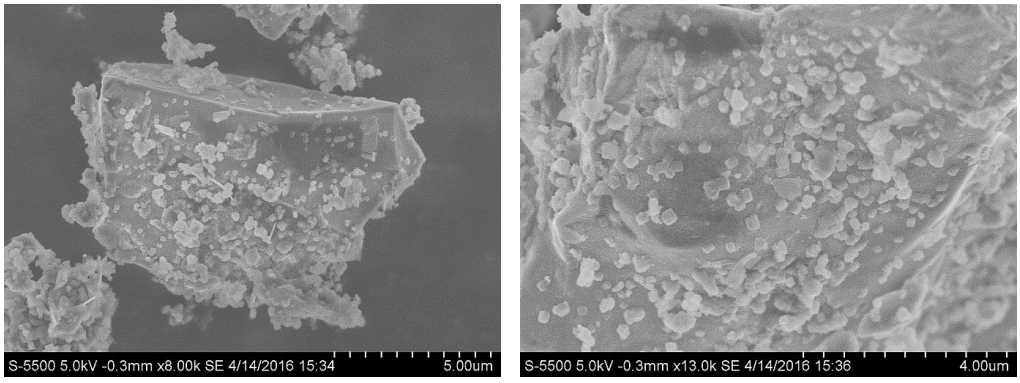

Figure 9 - *SEM images of ANL cement grains after 30 minutes of hydration with 1.5 mass % of binder LSs added with IA. Width of micrograph: left) 16 µm, and right) 10 µm*

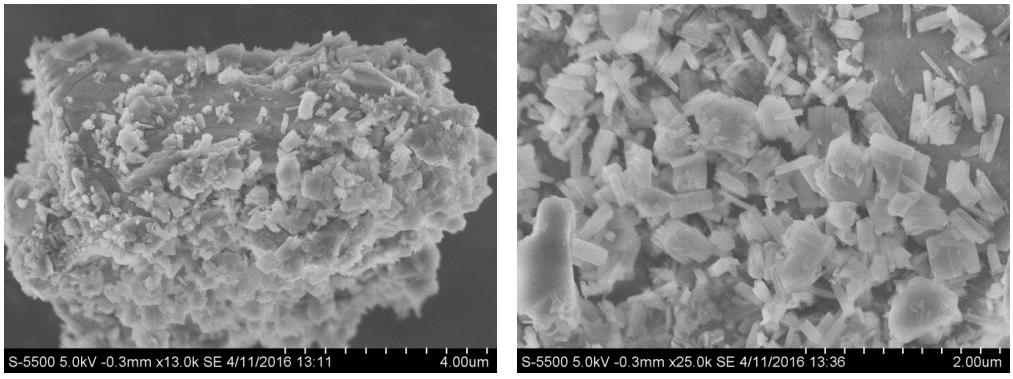

Figure 10 - *SEM images of CX cement grains with 1.5 mass % of binder LSs added with IA after 30 minutes of hydration. Width of micrograph: left) 10 µm, and right) 5 µm*

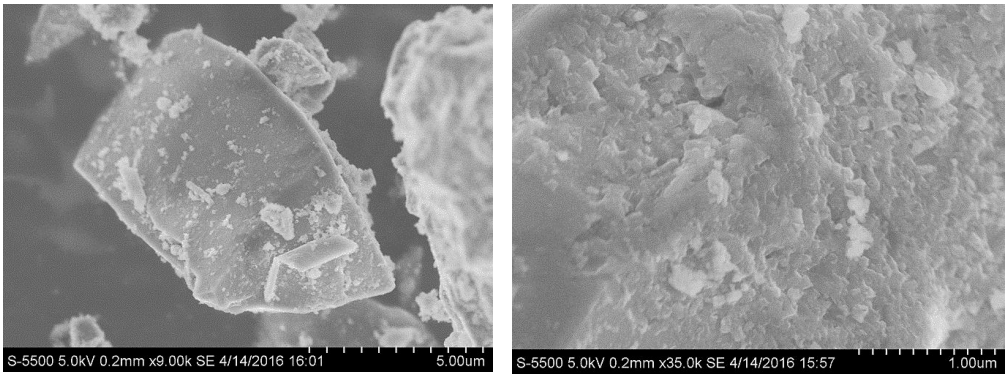

Figure 11 - *SEM images of ANL cement grains with 1.5 mass % of binder LSs added with DA after 30 minutes of hydration. Width of micrograph: left) 14 µm, and right) 4 µm*

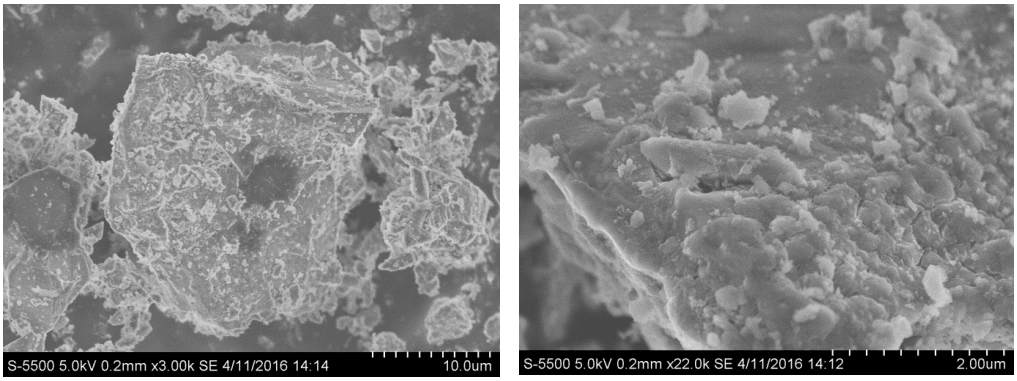

Figure 12 - *SEM images of CX cement grains with 1.5 mass % of binder LSs added with DA after 30 minutes of hydration. Width of micrograph: left) 42 µm, and right) 6 µm*

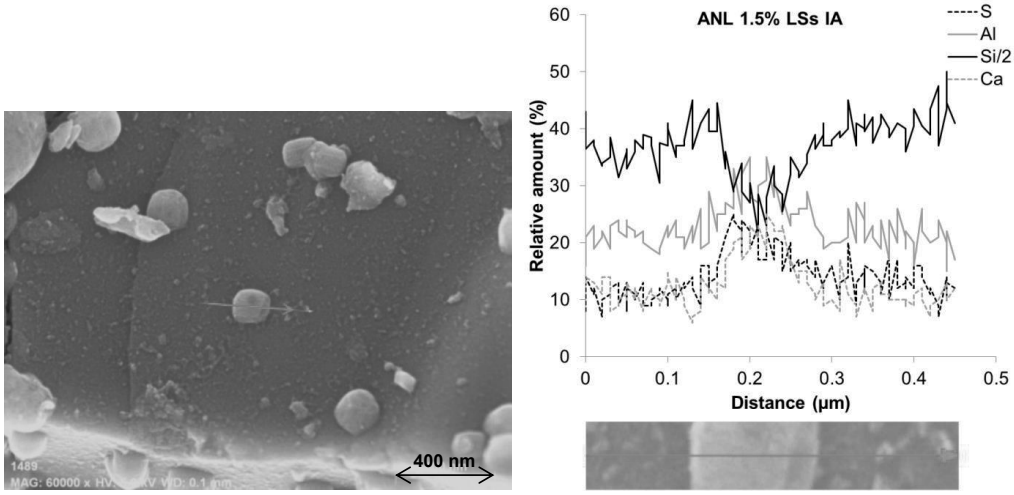

Figure 13 – *Linear SEM-EDS analysis of a crystal on the surface of an unhydrated grain of ANL cement with 1.5 mass % of binder LSs added with IA after 30 minutes of hydration. The crystal analysed is shown in the centre of the micrograph (left; width of micrograph: 2 µm). It has to be noticed that the crystals turned to more rounded shapes during the scanning due to dehydration. The curve representing Si was scaled down by multiplying it by 0.5 for better graphical representation.*

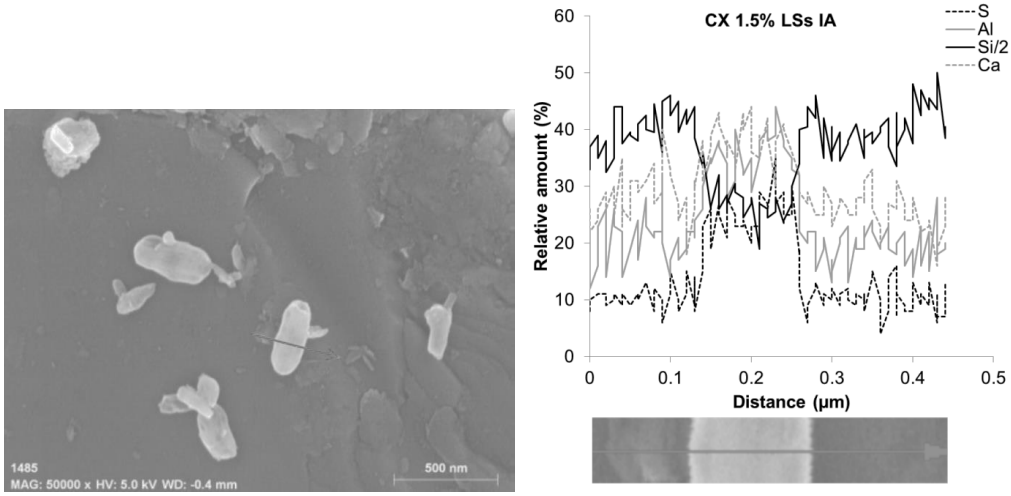

Figure 14 - *Linear SEM-EDS analysis of a crystal on the surface of an unhydrated grain of CX cement with 1.5 mass % of binder LSs added with IA after 30 minutes of hydration. The crystal analysed is shown in the centre of the micrograph (left; width of micrograph: 2.5 µm). It has to be noticed that the crystals turned to more rounded shapes during the scanning due to dehydration. The curve representing Si was scaled down by multiplying it by 0.5 for better graphical representation.*

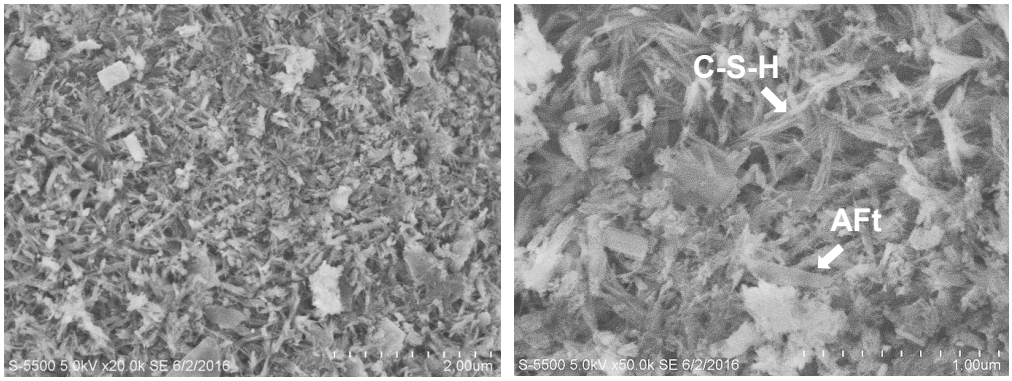

Figure 15 – *SEM images of ANL cement grains without LSs after 6 hours of hydration. Width of micrograph: left) 6 µm, and right) 2.5 µm. The identification of the hydrates (right) was based on visual appearance and comparison to literature, e.g.[30] .*

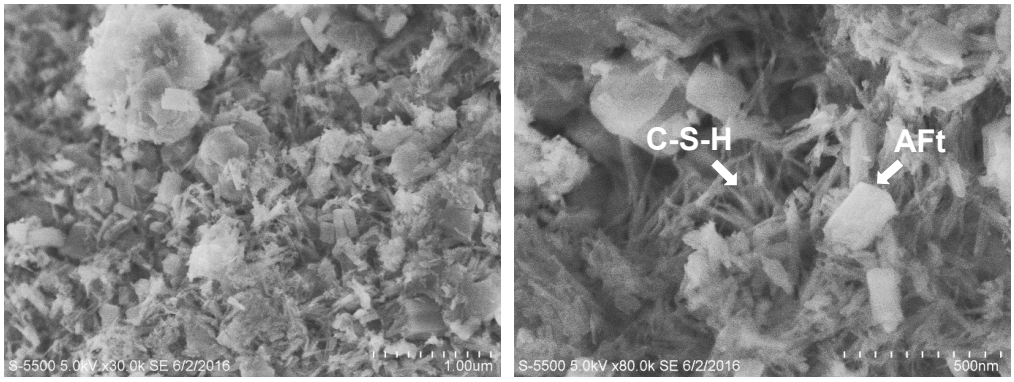

Figure 16 - *SEM images of CX cement grains without LSs after 6 hours of hydration. Width of micrograph: left) 4 µm, and right) 1.6 µm. The identification of the hydrates was based on visual appearance and comparison to literature, e.g. [30].*

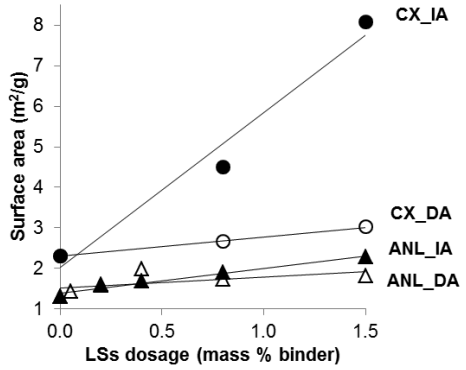

Figure 17 - *Surface area of pastes of ANL and CX cements after 30 minutes of hydration vs. LSs dosage added (mass % of binder) both for IA and DA, after [15]. The specific surface area comprehends the surface area of unhydrated cement grains and hydrates.*

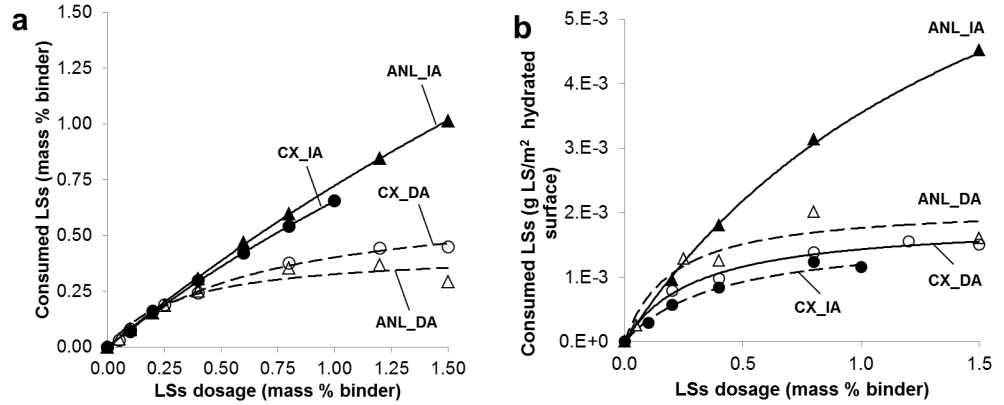

Figure 18 – *Amount of consumed LSs at 30 min. hydration vs. LSs dosage in neat ANL and CX cements for IA and DA, after [15]. The results are calculated as a) mass % of binder and as b) unit of surface area available for adsorption of hydrated pastes of ANL and CX cements*

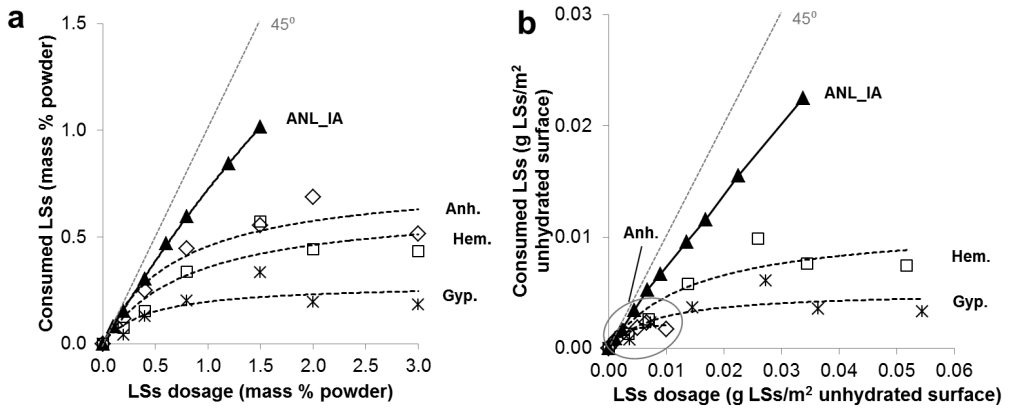

Figure 19 - *Amount of consumed LSs at 30 min. hydration vs. LSs dosage added to calcium sulfate anhydrous (anh.), hemihydrate (hem) and dihydrate (gyp.) for IA. The results are calculated as a) mass % of powder, and b) g LSs/m² unhydrated surface*

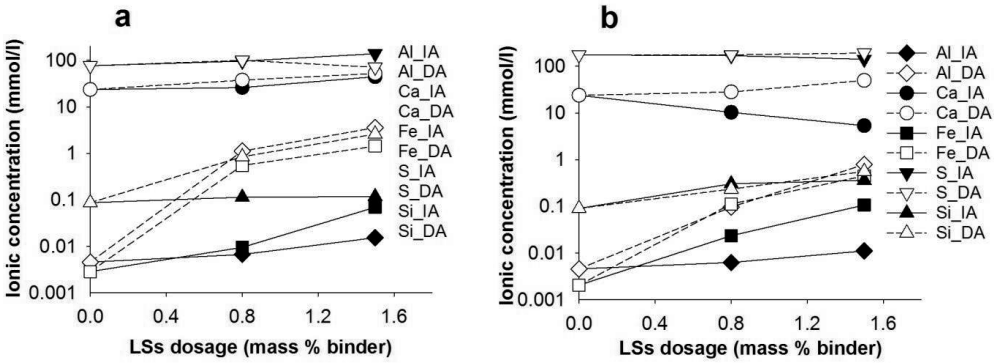

Figure 20 – *Concentration of Al, Fe, Ca, Si, and S in the pore solution (mmol/l) expressed in logarithmic scale vs. total LSs added (mass % of binder) to a) ANL and b) CX cement pastes analysed after 30 minutes of hydration both for IA and DA*

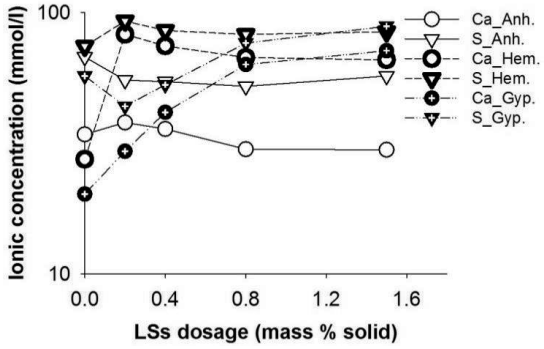

Figure 21 - *Concentration of Ca and S in the pore solution (mmol/l) expressed in logarithmic scale vs. total LSs added (mass % of powder) with IA to calcium sulfate anhydrous, hemihydrate, and dihydrate, analyzed after 30 minutes of hydration*

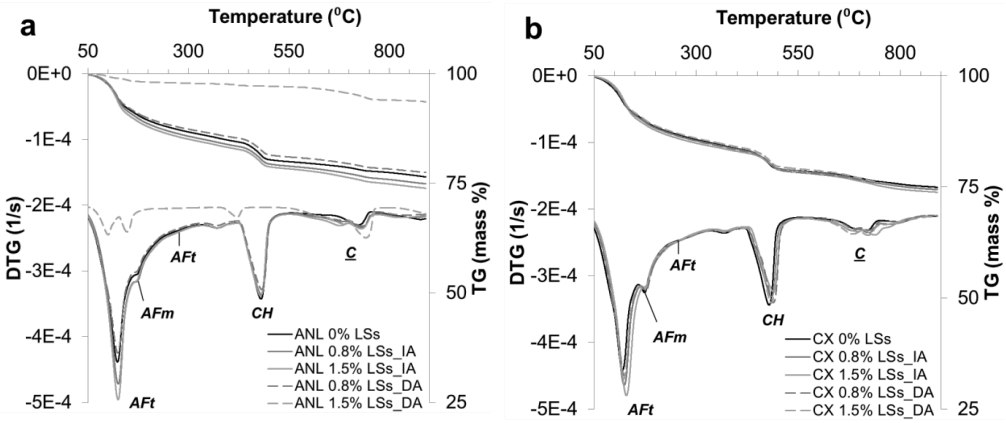

Figure 22 - *TG and DTG curves of a) ANL and b) CX cement paste without LSs or with 0.8, 1.5, 2.0, 3.0 mass % of binder LSs mixed with IA and DA, for which hydration was stopped after 28 days. The peaks corresponding to the decomposition of AFt, AFm, portlandite (CH) and carbonates (C) are marked in the figures.*

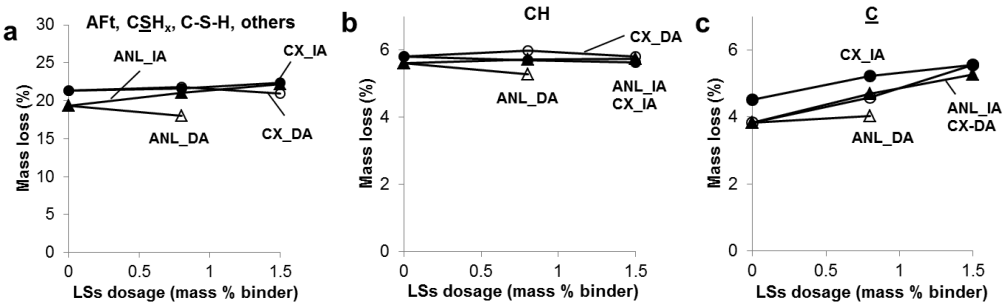

Figure 23 – M*ass loss (% of initial weight) of a) AFt, calcium sulfate hydrates (CSH$_x$), AFm, C-S-H; b) CH; c) carbonates (C)vs. LSs dosage (mass % of binder) for ANL and CX cements with increasing amount of LSs added with IA and with DA. NB. The scale of the y-axis of figure a) is different than the one of the other figures.*

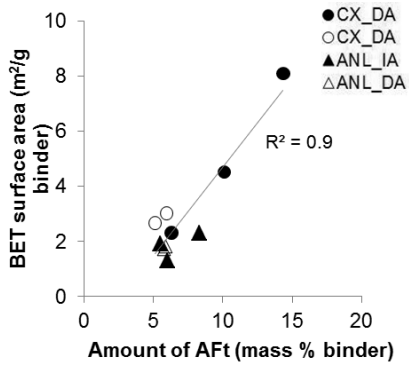

Figure 24 - *Correlation between the calculated amount of ettringite* and the particle surface area of solids in pastes of the two cements when LSs was added immediately with the mixing water (IA). *: Amount of ettringite calculated considering the mass loss in the whole interval 1 (50 - ca. 300 ºC)*

Part III - Appendix

Plastiserende stoffer til betong på nanonivå

Plastiserende stoffer forbedrer støpbarheten til fersk betong. Effekten av stoffet er sterkt avhengig av når man tilsetter det. Årsaken til den avhengigheten ble funnet på nanometernivå og skyldes dannelse av massevis av bitte små krystaller som øker vannbehovet. Oppdagelsen kan spare bruken av slike tilsetningsstoffer.

Alessia Colombo

Mette R. Geiker

Klaartje De Weerdt
Inst. for konstruksjonsteknikk

Hva er plastifiserende stoffer?
For å øke flyt eller støpbarhet til betong kan man tilsette mer vann. Minuset er bare den at økte vannmengden i betong fører til en svakere og mindre bestandig betong etter herding. Isteden tilsettes plastiserende stoffer til den ferske betongen. Bedre flyt oppnås ved at de plastiserende stoffene adsorberes på overflaten av sementpartiklene og sørger for at partiklene frastøter hverandre i stedet for å klumpe sammen.

Hvorfor blir plastiserende stoffer mere effektive når man tilsetter de senere?
Blant betongekspertene har det lenge vært klart at det utgjør en stor forskjell om man tilsetter det plastiserende stoffet i betongen samtidig med blandevannet, eller om man tilsetter det noen minutter etter vannet. Det siste gjør de plastiserende stoffene mer effektive, men årsaken til dette har derimot vært uklar.

Nanokrystaller forklarer
PhD kandidat Alessia Colombo har i tre år forsket på vekselvirkninger mellom sement og plastiserende stoffer. Veilederne hennes er Mette Geiker og Klaartje De Weerdt fra NTNU, Harald Justnes fra SINTEF og Rolf Andreas Lauten fra Borregaard. Alessia har i sin forskning fokusert på et bærekraftig plastiserende stoff, lignosulfonat. Lignosulfonat produseres i Norge av Borregaard og er basert på tre (biomasse). Lignosulfonater er et alternativ til plastiserende stoffer produsert fra olje.

Forskningen har oppdaget at man får en reaksjon mellom sementen og det plastiserende stoffet når man tilsetter det i blandevannet. Reaksjonen fører til dannelse av massevis av bitte små krystaller (ettringitt) som øker vannbehovet. Dannelse av de små krystallene skjer ikke når man tilsetter stoffet noen minutter etter man har tilsatt vann til betongen. Betingelsene for dannelsen av disse små krystallene (se mikroskopbildene) er dokumentert ved hjelp av elektronmikroskopet ved NTNUs Nanolab.

Dannelsen av de små krystallene fører til økt tilgjengelig overflate. Derfor er mer plastiseringsmiddel nødvendig for å dekke denne overflaten. Generelt sett gir høyere overflate et større vannbehov for samme flyt, eller mindre flyt med samme vannmengde. Det at man ikke finner de små krystallene, når man venter noen minutter med å tilsette plastiseringsmiddelet, forklarer den økte effektiviteten.

PhD kandidat Alessia Colombo måler betongens forbruk av plastifiserende stoffer. Foto: Giedrius Zirgulis.

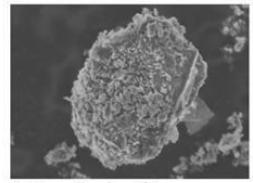

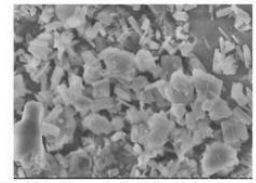

Elektronmikroskopbilder av en sementpartikkel (venstre) dekket til med små krystaller (høyre). Foto: Alessia Colombo.

Sparer tilsetningsstoff
Riktig tidspunkt for tilsetning av plastiserende stoffer er altså avgjørende for hvor effektive stoffene virker. Optimalt tilsetningstidspunkt fører dermed til at man kan redusere dosen av plastifiseringsmiddel. Her lønner det seg med andre ord ikke å være for tidlig ute.

Store doser av plastiserende stoffer, tilsatt samtidig med vannet til betongen, kan for øvrig gi så mange av de små krystallene at betongen stivner. Det gjelder å holde seg innenfor doseringsgrensene oppgitt av produsenten.

DEPARTMENT OF STRUCTURAL ENGINEERING
NORWEGIAN UNIVERSITY OF SCIENCE AND TECHNOLOGY

N–7491 TRONDHEIM, NORWAY
Telephone: +47 73 59 47 00 Telefax: +47 73 59 47 01

"Reliability Analysis of Structural Systems using Nonlinear Finite Element Methods",
C. A. Holm, 1990:23, ISBN 82-7119-178-0.

"Uniform Stratified Flow Interaction with a Submerged Horizontal Cylinder",
Ø. Arntsen, 1990:32, ISBN 82-7119-188-8.

"Large Displacement Analysis of Flexible and Rigid Systems Considering Displacement-Dependent Loads and Nonlinear Constraints",
K. M. Mathisen, 1990:33, ISBN 82-7119-189-6.

"Solid Mechanics and Material Models including Large Deformations",
E. Levold, 1990:56, ISBN 82-7119-214-0, ISSN 0802-3271.

"Inelastic Deformation Capacity of Flexurally-Loaded Aluminium Alloy Structures",
T. Welo, 1990:62, ISBN 82-7119-220-5, ISSN 0802-3271.

"Visualization of Results from Mechanical Engineering Analysis",
K. Aamnes, 1990:63, ISBN 82-7119-221-3, ISSN 0802-3271.

"Object-Oriented Product Modeling for Structural Design",
S. I. Dale, 1991:6, ISBN 82-7119-258-2, ISSN 0802-3271.

"Parallel Techniques for Solving Finite Element Problems on Transputer Networks",
T. H. Hansen, 1991:19, ISBN 82-7119-273-6, ISSN 0802-3271.

"Statistical Description and Estimation of Ocean Drift Ice Environments",
R. Korsnes, 1991:24, ISBN 82-7119-278-7, ISSN 0802-3271.

“Properties of concrete related to fatigue damage: with emphasis on high strength concrete”,
G. Petkovic, 1991:35, ISBN 82-7119-290-6, ISSN 0802-3271.

"Turbidity Current Modelling",
B. Brørs, 1991:38, ISBN 82-7119-293-0, ISSN 0802-3271.

"Zero-Slump Concrete: Rheology, Degree of Compaction and Strength. Effects of Fillers as Part Cement-Replacement",
C. Sørensen, 1992:8, ISBN 82-7119-357-0, ISSN 0802-3271.

"Nonlinear Analysis of Reinforced Concrete Structures Exposed to Transient Loading",
K. V. Høiseth, 1992:15, ISBN 82-7119-364-3, ISSN 0802-3271.

"Finite Element Formulations and Solution Algorithms for Buckling and Collapse Analysis of Thin Shells",
R. O. Bjærum, 1992:30, ISBN 82-7119-380-5, ISSN 0802-3271.

"Response Statistics of Nonlinear Dynamic Systems",
J. M. Johnsen, 1992:42, ISBN 82-7119-393-7, ISSN 0802-3271.

"Digital Models in Engineering. A Study on why and how engineers build and operate digital models for decisison support",
J. Høyte, 1992:75, ISBN 82-7119-429-1, ISSN 0802-3271.

"Sparse Solution of Finite Element Equations",
A. C. Damhaug, 1992:76, ISBN 82-7119-430-5, ISSN 0802-3271.

"Some Aspects of Floating Ice Related to Sea Surface Operations in the Barents Sea",
S. Løset, 1992:95, ISBN 82-7119-452-6, ISSN 0802-3271.

"Modelling of Cyclic Plasticity with Application to Steel and Aluminium Structures",
O. S. Hopperstad, 1993:7, ISBN 82-7119-461-5, ISSN 0802-3271.

"The Free Formulation: Linear Theory and Extensions with Applications to Tetrahedral Elements
with Rotational Freedoms",
G. Skeie, 1993:17, ISBN 82-7119-472-0, ISSN 0802-3271.

"Høyfast betongs motstand mot piggdekkslitasje. Analyse av resultater fra prøving i Veisliter'n",
T. Tveter, 1993:62, ISBN 82-7119-522-0, ISSN 0802-3271.

"A Nonlinear Finite Element Based on Free Formulation Theory for Analysis of Sandwich Structures",
O. Aamlid, 1993:72, ISBN 82-7119-534-4, ISSN 0802-3271.

"The Effect of Curing Temperature and Silica Fume on Chloride Migration and Pore Structure of High Strength Concrete",
C. J. Hauck, 1993:90, ISBN 82-7119-553-0, ISSN 0802-3271.

"Failure of Concrete under Compressive Strain Gradients",
G. Markeset, 1993:110, ISBN 82-7119-575-1, ISSN 0802-3271.

"An experimental study of internal tidal amphidromes in Vestfjorden",
J. H. Nilsen, 1994:39, ISBN 82-7119-640-5, ISSN 0802-3271.

"Structural analysis of oil wells with emphasis on conductor design",
H. Larsen, 1994:46, ISBN 82-7119-648-0, ISSN 0802-3271.

"Adaptive methods for non-linear finite element analysis of shell structures",
K. M. Okstad, 1994:66, ISBN 82-7119-670-7, ISSN 0802-3271.

"On constitutive modelling in nonlinear analysis of concrete structures",
O. Fyrileiv, 1994:115, ISBN 82-7119-725-8, ISSN 0802-3271.

"Fluctuating wind load and response of a line-like engineering structure with emphasis on motion-induced wind forces",
J. Bogunovic Jakobsen, 1995:62, ISBN 82-7119-809-2, ISSN 0802-3271.

"An experimental study of beam-columns subjected to combined torsion, bending and axial actions",
A. Aalberg, 1995:66, ISBN 82-7119-813-0, ISSN 0802-3271.

"Scaling and cracking in unsealed freeze/thaw testing of Portland cement and silica fume concretes",
S. Jacobsen, 1995:101, ISBN 82-7119-851-3, ISSN 0802-3271.

"Damping of water waves by submerged vegetation. A case study of laminaria hyperborea",
A. M. Dubi, 1995:108, ISBN 82-7119-859-9, ISSN 0802-3271.

"The dynamics of a slope current in the Barents Sea",
Sheng Li, 1995:109, ISBN 82-7119-860-2, ISSN 0802-3271.

"Modellering av delmaterialenes betydning for betongens konsistens",
Ernst Mørtsell, 1996:12, ISBN 82-7119-894-7, ISSN 0802-3271.

"Bending of thin-walled aluminium extrusions",
Birgit Søvik Opheim, 1996:60, ISBN 82-7119-947-1, ISSN 0802-3271.

"Material modelling of aluminium for crashworthiness analysis",
Torodd Berstad, 1996:89, ISBN 82-7119-980-3, ISSN 0802-3271.

"Estimation of structural parameters from response measurements on submerged floating tunnels",
Rolf Magne Larssen, 1996:119, ISBN 82-471-0014-2, ISSN 0802-3271.

“Numerical modelling of plain and reinforced concrete by damage mechanics”,
Mario A. Polanco-Loria, 1997:20, ISBN 82-471-0049-5, ISSN 0802-3271.

“Nonlinear random vibrations - numerical analysis by path integration methods”,
Vibeke Moe, 1997:26, ISBN 82-471-0056-8, ISSN 0802-3271.

"Numerical prediction of vortex-induced vibration by the finite element method",
Joar Martin Dalheim, 1997:63, ISBN 82-471-0096-7, ISSN 0802-3271.

"Time domain calculations of buffeting response for wind sensitive structures",
Ketil Aas-Jakobsen, 1997:148, ISBN 82-471-0189-0, ISSN 0802-3271.

"A numerical study of flow about fixed and flexibly mounted circular cylinders",
Trond Stokka Meling, 1998:48, ISBN 82-471-0244-7, ISSN 0802-3271.

"Estimation of chloride penetration into concrete bridges in coastal areas",
Per Egil Steen, 1998:89, ISBN 82-471-0290-0, ISSN 0802-3271.

"Stress-resultant material models for reinforced concrete plates and shells",
Jan Arve Øverli, 1998:95, ISBN 82-471-0297-8, ISSN 0802-3271.

"Chloride binding in concrete. Effect of surrounding environment and concrete composition",
Claus Kenneth Larsen, 1998:101, ISBN 82-471-0337-0, ISSN 0802-3271.

"Rotational capacity of aluminium alloy beams",
Lars A. Moen, 1999:1, ISBN 82-471-0365-6, ISSN 0802-3271.

"Stretch Bending of Aluminium Extrusions",
Arild H. Clausen, 1999:29, ISBN 82-471-0396-6, ISSN 0802-3271.

"Aluminium and Steel Beams under Concentrated Loading",
Tore Tryland, 1999:30, ISBN 82-471-0397-4, ISSN 0802-3271.

"Engineering Models of Elastoplasticity and Fracture for Aluminium Alloys",
Odd-Geir Lademo, 1999:39, ISBN 82-471-0406-7, ISSN 0802-3271.

"Kapasitet og duktilitet av dybelforbindelser i trekonstruksjoner",
Jan Siem, 1999:46, ISBN 82-471-0414-8, ISSN 0802-3271.

"Etablering av distribuert ingeniørarbeid; Teknologiske og organisatoriske erfaringer fra en norsk ingeniørbedrift",
Lars Line, 1999:52, ISBN 82-471-0420-2, ISSN 0802-3271.

"Estimation of Earthquake-Induced Response",
Símon Ólafsson, 1999:73, ISBN 82-471-0443-1, ISSN 0802-3271.

"Coastal Concrete Bridges: Moisture State, Chloride Permeability and Aging Effects"
Ragnhild Holen Relling, 1999:74, ISBN 82-471-0445-8, ISSN 0802-3271.

"Capacity Assessment of Titanium Pipes Subjected to Bending and External Pressure",
Arve Bjørset, 1999:100, ISBN 82-471-0473-3, ISSN 0802-3271.

“Validation of Numerical Collapse Behaviour of Thin-Walled Corrugated Panels”,
Håvar Ilstad, 1999:101, ISBN 82-471-0474-1, ISSN 0802-3271.

“Strength and Ductility of Welded Structures in Aluminium Alloys”,
Miroslaw Matusiak, 1999:113, ISBN 82-471-0487-3, ISSN 0802-3271.

“Thermal Dilation and Autogenous Deformation as Driving Forces to Self-Induced Stresses in High Performance Concrete”,
Øyvind Bjøntegaard, 1999:121, ISBN 82-7984-002-8, ISSN 0802-3271.

“Some Aspects of Ski Base Sliding Friction and Ski Base Structure”,
Dag Anders Moldestad, 1999:137, ISBN 82-7984-019-2, ISSN 0802-3271.

"Electrode reactions and corrosion resistance for steel in mortar and concrete",
Roy Antonsen, 2000:10, ISBN 82-7984-030-3, ISSN 0802-3271.

"Hydro-Physical Conditions in Kelp Forests and the Effect on Wave Damping and Dune Erosion. A case study on Laminaria Hyperborea",
Stig Magnar Løvås, 2000:28, ISBN 82-7984-050-8, ISSN 0802-3271.

"Random Vibration and the Path Integral Method",
Christian Skaug, 2000:39, ISBN 82-7984-061-3, ISSN 0802-3271.

"Buckling and geometrical nonlinear beam-type analyses of timber structures",
Trond Even Eggen, 2000:56, ISBN 82-7984-081-8, ISSN 0802-3271.

”Structural Crashworthiness of Aluminium Foam-Based Components”,
Arve Grønsund Hanssen, 2000:76, ISBN 82-7984-102-4, ISSN 0809-103X.

“Measurements and simulations of the consolidation in first-year sea ice ridges, and some aspects of mechanical behaviour”,
Knut V. Høyland, 2000:94, ISBN 82-7984-121-0, ISSN 0809-103X.

”Kinematics in Regular and Irregular Waves based on a Lagrangian Formulation”,
Svein Helge Gjøsund, 2000-86, ISBN 82-7984-112-1, ISSN 0809-103X.

”Self-Induced Cracking Problems in Hardening Concrete Structures”,
Daniela Bosnjak, 2000-121, ISBN 82-7984-151-2, ISSN 0809-103X.

"Ballistic Penetration and Perforation of Steel Plates",
Tore Børvik, 2000:124, ISBN 82-7984-154-7, ISSN 0809-103X.

"Freeze-Thaw resistance of Concrete. Effect of: Curing Conditions, Moisture Exchange and Materials",
Terje Finnerup Rønning, 2001:14, ISBN 82-7984-165-2, ISSN 0809-103X

"Structural behaviour of post tensioned concrete structures. Flat slab. Slabs on ground",
Steinar Trygstad, 2001:52, ISBN 82-471-5314-9, ISSN 0809-103X.

"Slipforming of Vertical Concrete Structures. Friction between concrete and slipform panel",
Kjell Tore Fosså, 2001:61, ISBN 82-471-5325-4, ISSN 0809-103X.

"Some numerical methods for the simulation of laminar and turbulent incompressible flows",
Jens Holmen, 2002:6, ISBN 82-471-5396-3, ISSN 0809-103X.

“Improved Fatigue Performance of Threaded Drillstring Connections by Cold Rolling”,
Steinar Kristoffersen, 2002:11, ISBN: 82-421-5402-1, ISSN 0809-103X.

"Deformations in Concrete Cantilever Bridges: Observations and Theoretical Modelling",
Peter F. Takâcs, 2002:23, ISBN 82-471-5415-3, ISSN 0809-103X.

"Stiffened aluminium plates subjected to impact loading",
Hilde Giæver Hildrum, 2002:69, ISBN 82-471-5467-6, ISSN 0809-103X.

"Full- and model scale study of wind effects on a medium-rise building in a built up area",
Jónas Thór Snæbjørnsson, 2002:95, ISBN82-471-5495-1, ISSN 0809-103X.

“Evaluation of Concepts for Loading of Hydrocarbons in Ice-infested water”,
Arnor Jensen, 2002:114, ISBN 82-417-5506-0, ISSN 0809-103X.

”Numerical and Physical Modelling of Oil Spreading in Broken Ice”,
Janne K. Økland Gjøsteen, 2002:130, ISBN 82-471-5523-0, ISSN 0809-103X.

”Diagnosis and protection of corroding steel in concrete”,
Franz Pruckner, 20002:140, ISBN 82-471-5555-4, ISSN 0809-103X.

“Tensile and Compressive Creep of Young Concrete: Testing and Modelling”,
Dawood Atrushi, 2003:17, ISBN 82-471-5565-6, ISSN 0809-103X.

“Rheology of Particle Suspensions. Fresh Concrete, Mortar and Cement Paste with Various Types of Lignosulfonates”,
Jon Elvar Wallevik, 2003:18, ISBN 82-471-5566-4, ISSN 0809-103X.

“Oblique Loading of Aluminium Crash Components”,
Aase Reyes, 2003:15, ISBN 82-471-5562-1, ISSN 0809-103X.

“Utilization of Ethiopian Natural Pozzolans”,
Surafel Ketema Desta, 2003:26, ISSN 82-471-5574-5, ISSN:0809-103X.

“Behaviour and strength prediction of reinforced concrete structures with discontinuity regions”, Helge Brå, 2004:11, ISBN 82-471-6222-9, ISSN 1503-8181.

“High-strength steel plates subjected to projectile impact. An experimental and numerical study”, Sumita Dey, 2004:38, ISBN 82-471-6282-2 (printed version), ISBN 82-471-6281-4 (electronic version), ISSN 1503-8181.

“Alkali-reactive and inert fillers in concrete. Rheology of fresh mixtures and expansive reactions.”
Bård M. Pedersen, 2004:92, ISBN 82-471-6401-9 (printed version), ISBN 82-471-6400-0 (electronic version), ISSN 1503-8181.

“On the Shear Capacity of Steel Girders with Large Web Openings”.
Nils Christian Hagen, 2005:9 ISBN 82-471-6878-2 (printed version), ISBN 82-471-6877-4 (electronic version), ISSN 1503-8181.

”Behaviour of aluminium extrusions subjected to axial loading”.
Østen Jensen, 2005:7, ISBN 82-471-6873-1 (printed version), ISBN 82-471-6872-3 (electronic version), ISSN 1503-8181.

”Thermal Aspects of corrosion of Steel in Concrete”.
Jan-Magnus Østvik, 2005:5, ISBN 82-471-6869-3 (printed version), ISBN 82-471-6868 (electronic version), ISSN 1503-8181.

”Mechanical and adaptive behaviour of bone in relation to hip replacement.” A study of bone remodelling and bone grafting.
Sébastien Muller, 2005:34, ISBN 82-471-6933-9 (printed version), ISBN 82-471-6932-0 (electronic version), ISSN 1503-8181.

“Analysis of geometrical nonlinearities with applications to timber structures”.
Lars Wollebæk, 2005:74, ISBN 82-471-7050-5 (printed version), ISBN 82-471-7019-1 (electronic version), ISSN 1503-8181.

“Pedestrian induced lateral vibrations of slender footbridges”,
Anders Rönnquist, 2005:102, ISBN 82-471-7082-5 (printed version), ISBN 82-471-7081-7 (electronic version), ISSN 1503-8181.

“Initial Strength Development of Fly Ash and Limestone Blended Cements at Various Temperatures Predicted by Ultrasonic Pulse Velocity”,
Tom Ivar Fredvik, 2005:112, ISBN 82-471-7105-8 (printed version), ISBN 82-471-7103-1 (electronic version), ISSN 1503-8181.

“Behaviour and modelling of thin-walled cast components”,
Cato Dørum, 2005:128, ISBN 82-471-7140-6 (printed version), ISBN 82-471-7139-2 (electronic version), ISSN 1503-8181.

“Behaviour and modelling of selfpiercing riveted connections”,
Raffaele Porcaro, 2005:165, ISBN 82-471-7219-4 (printed version), ISBN 82-471-7218-6 (electronic version), ISSN 1503-8181.

”Behaviour and Modelling og Aluminium Plates subjected to Compressive Load”,
Lars Rønning, 2005:154, ISBN 82-471-7169-1 (printed version), ISBN 82-471-7195-3 (electronic version), ISSN 1503-8181.

”Bumper beam-longitudinal system subjected to offset impact loading”,
Satyanarayana Kokkula, 2005:193, ISBN 82-471-7280-1 (printed version), ISBN 82-471-7279-8 (electronic version), ISSN 1503-8181.

“Control of Chloride Penetration into Concrete Structures at Early Age”,
Guofei Liu, 2006:46, ISBN 82-471-7838-9 (printed version), ISBN 82-471-7837-0 (electronic version), ISSN 1503-8181.

“Modelling of Welded Thin-Walled Aluminium Structures”,
Ting Wang, 2006:78, ISBN 82-471-7907-5 (printed version), ISBN 82-471-7906-7 (electronic version), ISSN 1503-8181.

”Time-variant reliability of dynamic systems by importance sampling and probabilistic analysis of ice loads”,
Anna Ivanova Olsen, 2006:139, ISBN 82-471-8041-3 (printed version), ISBN 82-471-8040-5 (electronic version), ISSN 1503-8181.

“Fatigue life prediction of an aluminium alloy automotive component using finite element analysis of surface topography”.
Sigmund Kyrre Ås, 2006:25, ISBN 82-471-7791-9 (printed version), ISBN 82-471-7791-9 (electronic version), ISSN 1503-8181.

”Constitutive models of elastoplasticity and fracture for aluminium alloys under strain path change”,
Dasharatha Achani, 2006:76, ISBN 82-471-7903-2 (printed version), ISBN 82-471-7902-4 (electronic version), ISSN 1503-8181.

“Simulations of 2D dynamic brittle fracture by the Element-free Galerkin method and linear fracture mechanics”,
Tommy Karlsson, 2006:125, ISBN 82-471-8011-1 (printed version), ISBN 82-471-8010-3 (electronic version), ISSN 1503-8181.

“Penetration and Perforation of Granite Targets by Hard Projectiles”,
Chong Chiang Seah, 2006:188, ISBN 82-471-8150-9 (printed version), ISBN 82-471-8149-5 (electronic version), ISSN 1503-8181.

"Deformations, strain capacity and cracking of concrete in plastic and early hardening phases",
Tor Arne Hammer, 2007:234, ISBN 978-82-471-5191-4 (printed version), ISBN 978-82-471-5207-2 (electronic version), ISSN 1503-8181.

"Crashworthiness of dual-phase high-strength steel: Material and Component behaviour", Venkatapathi Tarigopula, 2007:230, ISBN 82-471-5076-4 (printed version), ISBN 82-471-5093-1 (electronic version), ISSN 1503-8181.

"Fibre reinforcement in load carrying concrete structures",
Åse Lyslo Døssland, 2008:50, ISBN 978-82-471-6910-0 (printed version), ISBN 978-82-471-6924-7 (electronic version), ISSN 1503-8181.

"Low-velocity penetration of aluminium plates",
Frode Grytten, 2008:46, ISBN 978-82-471-6826-4 (printed version), ISBN 978-82-471-6843-1 (electronic version), ISSN 1503-8181.

"Robustness studies of structures subjected to large deformations",
Ørjan Fyllingen, 2008:24, ISBN 978-82-471-6339-9 (printed version), ISBN 978-82-471-6342-9 (electronic version), ISSN 1503-8181.

"Constitutive modelling of morsellised bone",
Knut Birger Lunde, 2008:92, ISBN 978-82-471-7829-4 (printed version), ISBN 978-82-471-7832-4 (electronic version), ISSN 1503-8181.

"Experimental Investigations of Wind Loading on a Suspension Bridge Girder",
Bjørn Isaksen, 2008:131, ISBN 978-82-471-8656-5 (printed version), ISBN 978-82-471-8673-2 (electronic version), ISSN 1503-8181.

"Cracking Risk of Concrete Structures in The Hardening Phase",
Guomin Ji, 2008:198, ISBN 978-82-471-1079-9 (printed version), ISBN 978-82-471-1080-5 (electronic version), ISSN 1503-8181.

"Modelling and numerical analysis of the porcine and human mitral apparatus",
Victorien Emile Prot, 2008:249, ISBN 978-82-471-1192-5 (printed version), ISBN 978-82-471-1193-2 (electronic version), ISSN 1503-8181.

"Strength analysis of net structures",
Heidi Moe, 2009:48, ISBN 978-82-471-1468-1 (printed version), ISBN 978-82-471-1469-8 (electronic version), ISSN1503-8181.

"Numerical analysis of ductile fracture in surface cracked shells",
Espen Berg, 2009:80, ISBN 978-82-471-1537-4 (printed version), ISBN 978-82-471-1538-1 (electronic version), ISSN 1503-8181.

"Subject specific finite element analysis of bone – for evaluation of the healing of a leg lengthening and evaluation of femoral stem design",
Sune Hansborg Pettersen, 2009:99, ISBN 978-82-471-1579-4 (printed version), ISBN 978-82-471-1580-0 (electronic version), ISSN 1503-8181.

"Evaluation of fracture parameters for notched multi-layered structures",
Lingyun Shang, 2009:137, ISBN 978-82-471-1662-3 (printed version), ISBN 978-82-471-1663-0 (electronic version), ISSN 1503-8181.

"Modelling of Dynamic Material Behaviour and Fracture of Aluminium Alloys for Structural Applications"
Yan Chen, 2009:69, ISBN 978-82-471-1515-2 (printed version), ISBN 978-82 471-1516-9 (electronic version), ISSN 1503-8181.

"Nanomechanics of polymer and composite particles"
Jianying He 2009:213, ISBN 978-82-471-1828-3 (printed version), ISBN 978-82-471-1829-0 (electronic version), ISSN 1503-8181.

"Mechanical properties of clear wood from Norway spruce"
Kristian Berbom Dahl 2009:250, ISBN 978-82-471-1911-2 (printed version) ISBN 978-82-471-1912-9 (electronic version), ISSN 1503-8181.

"Modeling of the degradation of TiB_2 mechanical properties by residual stresses and liquid Al penetration along grain boundaries"
Micol Pezzotta 2009:254, ISBN 978-82-471-1923-5 (printed version) ISBN 978-82-471-1924-2 (electronic version) ISSN 1503-8181.

"Effect of welding residual stress on fracture"
Xiabo Ren 2010:77, ISBN 978-82-471-2115-3 (printed version) ISBN 978-82-471-2116-0 (electronic version), ISSN 1503-8181.

"Pan-based carbon fiber as anode material in cathodic protection system for concrete structures"
Mahdi Chini 2010:122, ISBN 978-82-471-2210-5 (printed version) ISBN 978-82-471-2213-6 (electronic version), ISSN 1503-8181.

"Structural Behaviour of deteriorated and retrofitted concrete structures"
Irina Vasililjeva Sæther 2010:171, ISBN 978-82-471-2315-7 (printed version) ISBN 978-82-471-2316-4 (electronic version) ISSN 1503-8181.

"Prediction of local snow loads on roofs"
Vivian Meløysund 2010:247, ISBN 978-82-471-2490-1 (printed version) ISBN 978-82-471-2491-8 (electronic version) ISSN 1503-8181.

"Behaviour and modelling of polymers for crash applications"
Virgile Delhaye 2010:251, ISBN 978-82-471-2501-4 (printed version) ISBN 978-82-471-2502-1 (electronic version) ISSN 1503-8181.

"Blended cement with reducted CO_2 emission – Utilizing the Fly Ash-Limestone Synergy",
Klaartje De Weerdt 2011:32, ISBN 978-82-471-2584-7 (printed version) ISBN 978-82-471-2584-4 (electronic version) ISSN 1503-8181.

"Chloride induced reinforcement corrosion in concrete" Concept of critical chloride content – methods and mechanisms.
Ueli Angst 2011:113, ISBN 978-82-471-2769-9 (printed version) ISBN 978-82-471-2763-6 (electronic version) ISSN 1503-8181.

"A thermo-electric-Mechanical study of the carbon anode and contact interface for Energy savings in the production of aluminium".
Dag Herman Andersen 2011:157, ISBN 978-82-471-2859-6 (printed version) ISBN 978-82-471-2860-2 (electronic version) ISSN 1503-8181.

"Structural Capacity of Anchorage Ties in Masonry Veneer Walls Subjected to Earthquake". The implications of Eurocode 8 and Eurocode 6 on a typical Norwegain veneer wall.
Ahmed Mohamed Yousry Hamed 2011:181, ISBN 978-82-471-2911-1 (printed version) ISBN 978-82-471-2912-8 (electronic ver.) ISSN 1503-8181.

"Work-hardening behaviour in age-hardenable Al-Zn-Mg(-Cu) alloys".
Ida Westermann , 2011:247, ISBN 978-82-471-3056-8 (printed ver.) ISBN 978-82-471-3057-5 (electronic ver.) ISSN 1503-8181.

"Behaviour and modelling of selfpiercing riveted connections using aluminium rivets".
Nguyen-Hieu Hoang, 2011:266, ISBN 978-82-471-3097-1 (printed ver.) ISBN 978-82-471-3099-5 (electronic ver.) ISSN 1503-8181.

"Fibre reinforced concrete".
Sindre Sandbakk, 2011:297, ISBN 978-82-471-3167-1 (printed ver.) ISBN 978-82-471-3168-8 (electronic ver) ISSN 1503:8181.

"Dynamic behaviour of cablesupported bridges subjected to strong natural wind".
Ole Andre Øiseth, 2011:315, ISBN 978-82-471-3209-8 (printed ver.) ISBN 978-82-471-3210-4 (electronic ver.) ISSN 1503-8181.

"Constitutive modeling of solargrade silicon materials"
Julien Cochard, 2011:307, ISBN 978-82-471-3189-3 (printed ver). ISBN 978-82-471-3190-9 (electronic ver.) ISSN 1503-8181.

"Constitutive behavior and fracture of shape memory alloys"
Jim Stian Olsen, 2012:57, ISBN 978-82-471-3382-8 (printed ver.) ISBN 978-82-471-3383-5 (electronic ver.) ISSN 1503-8181.

“Field measurements in mechanical testing using close-range photogrammetry and digital image analysis”
Egil Fagerholt, 2012:95, ISBN 978-82-471-3466-5 (printed ver.) ISBN 978-82-471-3467-2 (electronic ver.) ISSN 1503-8181.

“Towards a better under standing of the ultimate behaviour of lightweight aggregate concrete in compression and bending”,
Håvard Nedrelid, 2012:123, ISBN 978-82-471-3527-3 (printed ver.) ISBN 978-82-471-3528-0 (electronic ver.) ISSN 1503-8181.

“Numerical simulations of blood flow in the left side of the heart”
Sigrid Kaarstad Dahl, 2012:135, ISBN 978-82-471-3553-2 (printed ver.) ISBN 978-82-471-3555-6 (electronic ver.) ISSN 1503-8181.

“Moisture induced stresses in glulam”
Vanessa Angst-Nicollier, 2012:139, ISBN 978-82-471-3562-4 (printed ver.) ISBN 978-82-471-3563-1 (electronic ver.) ISSN 1503-8181.

“Biomechanical aspects of distraction osteogensis”
Valentina La Russa, 2012:250, ISBN 978-82-471-3807-6 (printed ver.) ISBN 978-82-471-3808-3 (electronic ver.) ISSN 1503-8181.

“Ductile fracture in dual-phase steel. Theoretical, experimental and numerical study”
Gaute Gruben, 2012:257, ISBN 978-82-471-3822-9 (printed ver.) ISBN 978-82-471-3823-6 (electronic ver.) ISSN 1503-8181.

“Damping in Timber Structures”
Nathalie Labonnote, 2012:263, ISBN 978-82-471-3836-6 (printed ver.) ISBN 978-82-471-3837-3 (electronic ver.) ISSN 1503-8181.

“Biomechanical modeling of fetal veins: The umbilical vein and ductus venosus bifurcation”
Paul Roger Leinan, 2012:299, ISBN 978-82-471-3915-8 (printed ver.) ISBN 978-82-471-3916-5 (electronic ver.) ISSN 1503-8181.

“Large-Deformation behaviour of thermoplastics at various stress states”
Anne Serine Ognedal, 2012:298, ISBN 978-82-471-3913-4 (printed ver.) ISBN 978-82-471-3914-1 (electronic ver.) ISSN 1503-8181.

“Hardening accelerator for fly ash blended cement”
Kien Dinh Hoang, 2012:366, ISBN 978-82-471-4063-5 (printed ver.) ISBN 978-82-471-4064-2 (electronic ver.) ISSN 1503-8181.

“From molecular structure to mechanical properties”
Jianyang Wu, 2013:186, ISBN 978-82-471-4485-5 (printed ver.) ISBN 978-82-471-4486-2 (electronic ver.) ISSN 1503-8181.

"Experimental and numerical study of hybrid concrete structures"
Linn Grepstad Nes, 2013:259, ISBN 978-82-471-4644-6 (printed ver.) ISBN 978-82-471-4645-3 (electronic ver.) ISSN 1503-8181.

"Mechanics of ultra-thin multi crystalline silicon wafers"
Saber Saffar, 2013:199, ISBN 978-82-471-4511-1 (printed ver.) ISBN 978-82-471-4513-5 (electronic ver). ISSN 1503-8181.

"Through process modelling of welded aluminium structures"
Anizahyati Alisibramulisi, 2013:325, ISBN 978-82-471-4788-7 (printed ver.) ISBN 978-82-471-4789-4 (electronic ver.) ISSN 1503-8181.

"Combined blast and fragment loading on steel plates"
Knut Gaarder Rakvåg, 2013:361, ISBN978-82-471-4872-3 (printed ver.) ISBN 978-82-4873-0 (electronic ver.). ISSN 1503-8181.

"Characterization and modelling of the anisotropic behaviour of high-strength aluminium alloy"
Marion Fourmeau, 2014:37, ISBN 978-82-326-0008-3 (printed ver.) ISBN 978-82-326-0009-0 (electronic ver.) ISSN 1503-8181.

"Behaviour of threated steel fasteners at elevated deformation rates"
Henning Fransplass, 2014:65, ISBN 978-82-326-0054-0 (printed ver.) ISBN 978-82-326-0055-7 (electronic ver.) ISSN 1503-8181.

"Sedimentation and Bleeding"
Ya Peng, 2014:89, ISBN 978-82-326-0102-8 (printed ver.) ISBN 978-82-326-0103-5 (electric ver.) ISSN 1503-8181.

"Impact against X65 offshore pipelines"
Martin Kristoffersen, 2014:362, ISBN 978-82-326-0636-8 (printed ver.) ISBN 978-82-326-0637-5 (electronic ver.) ISSN 1503-8181.

"Formability of aluminium alloy subjected to prestrain by rolling"
Dmitry Vysochinskiy, 2014:363,, ISBN 978-82-326-0638-2 (printed ver.) ISBN 978-82-326-0639-9 (electronic ver.) ISSN 1503-8181.

"Experimental and numerical study of Yielding, Work-Hardening and anisotropy in textured AA6xxx alloys using crystal plasticity models"
Mikhail Khadyko, 2015:28, ISBN 978-82-326-0724-2 (printed ver.) ISBN 978-82-326-0725-9 (electronic ver.) ISSN 1503-8181.

"Behaviour and Modelling of AA6xxx Aluminium Alloys Under a Wide Range of Temperatures and Strain Rates"
Vincent Vilamosa, 2015:63, ISBN 978-82-326-0786-0 (printed ver.) ISBN 978-82-326-0787-7 (electronic ver.) ISSN 1503-8181.

“A Probabilistic Approach in Failure Modelling of Aluminium High Pressure Die-Castings”
Octavian Knoll, 2015:137, ISBN 978-82-326-0930-7 (printed ver.) ISBN 978-82-326-0931-4 (electronic ver.) ISSN 1503-8181.

“Ice Abrasion on Marine Concrete Structures”
Egil Møen, 2015:189, ISBN 978-82-326-1034-1 (printed ver.) ISBN 978-82-326-1035-8 (electronic ver.) ISSN 1503-8181.

“Fibre Orientation in Steel-Fibre-Reinforced Concrete”
Giedrius Zirgulis, 2015:229, ISBN 978-82-326-1114-0 (printed ver.) ISBN 978-82-326-1115-7 (electronic ver.) ISSN 1503-8181.

“Effect of spatial variation and possible interference of localised corrosion on the residual capacity of a reinforced concrete beam”
Mohammad Mahdi Kioumarsi, 2015:282, ISBN 978-82-326-1220-8 (printed ver.) ISBN 978-82-1221-5 (electronic ver.) ISSN 1503-8181.

“The role of concrete resistivity in chloride-induced macro-cell corrosion”
Karla Horbostel, 2015:324, ISBN 978-82-326-1304-5 (printed ver.) ISBN 978-82-326-1305-2 (electonic ver.) ISSN 1503-8181.

“Flowable fibre-reinforced concrete for structural applications”
Elena Vidal Sarmiento, 2015-335, ISBN 978-82-326-1324-3 (printed ver.) ISBN 978-82-326-1325-0 (electronic ver.) ISSN 1503-8181.

“Development of chushed sand for concrete production with microproportioning”
Rolands Cepuritis, 2016:19, ISBN 978-82-326-1382-3 (printed ver.) ISBN 978-82-326-1383-0 (electronic ver.) ISSN 1503-8181.

“Withdrawal properties of threaded rods embedded in glued-laminated timer elements”
Haris Stamatopoulos, 2016:48, ISBN 978-82-326-1436-3 (printed ver.) ISBN 978-82-326-1437-0 (electronic ver.) ISSN 1503-8181.

“An Experimental and numerical study of thermoplastics at large deformation”
Marius Andersen, 2016:191, ISBN 978-82-326-1720-3 (printed ver.) ISBN 978-82-326-1721-0 (electronic ver.) ISSN 1503-8181.

“Modeling and Simulation of Ballistic Impact”
Jens Kristian Holmen, 2016:240, ISBN 978-82-326-1818-7 (printed ver). ISBN 978-82-326-1819-4 (electronic ver.) ISSN 1503-8181.

“Early age crack assessment of concrete structures”
Anja B. Estensen Klausen, 2016:256, ISBN 978-82-326-1850-7 (printed ver). ISBN 978-82-326-1851-4 (electronic ver.) ISSN 1503-8181.

“Uncertainty quantification and sensitivity analysis for cardiovascular models”
Vinzenz Gregor Eck, 2016:234, ISBN 978-82-326-1806-4 (printed ver.) ISBN 978-82-326-1807-1 (electronic ver.) ISSN 1503-8181.

“Dynamic behaviour of existing and new railway catenary systems under Norwegain conditions”
Petter Røe Nåvik, 2016:298, ISBN 978-82-326-1935-1 (printed ver.) ISBN 978-82-326-1934-4 (electronic ver.) ISSN 1503-8181.

“Mechanical behaviour of particle-filled elastomers at various temperatures”
Arne Ilseng, 2016-295, ISBN978-82-326-1928-3 (printed ver.) ISBN 978-82-326-1929-0 (electronic ver.) ISSN 1503-8181.

“Nanotechnology for Anti-Icing Application”
Zhiwei He, 2016:348, ISBN 978-82-326-2038-8 (printed ver.) ISBN 978-82-326-2019-5 (electronic ver.) ISSN 1503-8181.

“Conduction Mechanisms in Conductive Adhesives with Metal-Coated Polyer Spheres”
Sigurd Rolland Pettersen, 2016:349, ISBN 978-326-2040-1 (printed ver,) ISBN 978-82-326-2041-8 (electronic ver.) ISSN 1503-8181.